Optimisation of the purification process of a zinc sulfate leach solution for zinc electrowinning

by

Bernard Josef Krause

Submitted in partial fulfillment of the requirements of the degree

Master of Engineering

in the

Department of Materials Science and Metallurgical Engineering, University of Pretoria, Pretoria, South Africa

July 2014

Optimisation of the purification process of a zinc sulfate leach solution for zinc electrowinning

by

Bernard Josef Krause

Supervisor:

Prof. RF Sandenbergh
Department of Materials Science and Metallurgical Engineering
University of Pretoria
Pretoria

Abstract

The leach solution obtained by leaching of zinc containing ores typically has to be highly purified before it can be used as electrolyte for the electrowinning of zinc. Cobalt is a troublesome impurity in the sense that not only has it even at relatively low concentrations a very significant negative impact on the zinc electrowinning process, but that is also difficult to remove by the zinc cementation process typically used for this purpose. The aim with the present work was to better understand the arsenic activated cementation of cobalt using zinc powder to enable the optimization of an industrial purification plant. Thermodynamic based calculations confirmed that the role of arsenic in the process is to allow for the precipitation of the cobalt at more positive potentials as cobalt arsenide and that it should be possible to remove the cobalt to very low concentrations with zinc cementation. The kinetics of cobalt cementation was studied using batch cementation experiments using different sizes and quantities of zinc dust and by varying the temperature. The nature of the cementation products was characterized using scanning electron microscopy and energy dispersive spectroscopy. It was found that the cobalt cementation could be described by a first order rate equation but with a faster initial stage with an activation energy of 43 kJ/mol followed by a much slower temperature insensitive second stage. Activating species such as copper, cadmium and arsenic cemented faster than the cobalt on the zinc. The rate of cobalt cementation was increased by using the same mass of finer zinc, increasing the temperature and recirculation of some of the cemented cobalt. It was shown that the zinc dust consumption and/or the minimum temperature required to achieve the required cobalt removal could be reduced by recirculation of the cobalt cement from the early stages of a train of backmix reactors or by using zinc dust with a finer size distribution.

Keywords: Hydrometallurgy, purification, cementation, zinc, cobalt, cobalt arsenide, surface area, activation

Acknowledgements

I am grateful to Exxaro Base Metals for providing me with an opportunity to study the purification process at the Zincor base metals refinery. It is with sadness that I think of the now defunct Zincor processing plant, which was finally shut down after years of deteriorating performance and escalating maintenance costs. The plant has been in operation for over 40 years and age and other factors finally caught up with it.

I am thankful for the support of my supervisor at Zincor, Joao Rodrigues. My thanks also extend to Glynnis Rawson and Joao Fernandez of the laboratory as well as their team for providing me with results for my samples.

I am grateful towards Dr Nanne Vegter who provided much of the literature referenced in this study. My heartfelt thanks goes to Professor Roelf Sandenbergh, my study leader, who continued to support my work with input and guidance through the period just prior to Zincor's closure, as this study lost a bit of momentum while I searched for alternative employment, and then through my subsequent relocation abroad, when no more testwork could be done despite some questions related to this study remaining unanswered.

I am most grateful towards my wife and children for their support over the time it took to complete this work.

TABLE OF CONTENTS

TABLE OF CONTENTS

TABLE OF FIGURES

LIST OF TABLES

LIST OF ABBREVIATIONS

- SEM: Scanning Electron Microscope
- EDS: Electron Dispersive Spectroscopy
- BET: After Brunauer, Emmett and Teller – developers of the procedure for determining surface area
- PSD: Particle Size Distribution
- CSTR: Continuously Stirred Tank Reactor

1. BACKGROUND

Zinc is produced most commonly by electrowinning from an acidic zinc sulfate solution, which in turn is produced by leaching zinc with dilute sulfuric acid from ores containing zinc oxide (calcine). This leach is relatively non-selective and a host of other elements are leached together with zinc including iron, arsenic, antimony, germanium, indium, gallium, selenium, copper, cadmium, silica, nickel and cobalt.

Metallic zinc is a reducing agent with a rather negative reversible potential of -0.76 V (SHE). It follows that plating of elements more noble than zinc are thermodynamically favoured at the potential applied during the electrowinning of zinc. Purification of the leachate is therefore required to prevent contamination of the final zinc product. Moreover, the plating of hydrogen gas from the acidic aqueous electrolyte is thermodynamically favoured above that of zinc and the economic electrowinning of zinc is only possible due to the sluggish kinetics of hydrogen ion reduction on zinc (Tozawa et al, 1992). However, many impurity metals, like germanium, arsenic, antimony, cobalt and nickel favour hydrogen ion reduction, such that even trace amounts of these metals, even in solution or once plated, will catalyze hydrogen evolution to reduce the efficiency of zinc electrowinning (Sinclair, 2005; Fugleberg and Rastas, 1976; Lawson and Nhan, 1981; Xiong and Richie, 1988; Raghavan et al, 1998; Yang et al, 2006). The effects of various impurities on zinc electrowinning were rated by Ohoyama and Morioka (1985) as quoted by Tozawa et al (1992) and grouped in terms of the volume of hydrogen evolved, as follows:

- Worst impurities: Ge, Sb, Te, Se
- Worse impurities: As, Ni, Sn, Co, Fe, Ag
- Bad impurities: Ga, Bi, Tl, Cd, Hg, In, Pb

Moreover, plated zinc can redissolve even during electrowinning underneath hydrogen bubbles where the potential may be more positive than the reversible

potential for zinc due to the increased resistance losses in the extended electrolyte path around the bubble (Wiart et al, 1999).

Iron plays an important role in the purification of leach solutions as it can not only be precipitated as an iron-3-hydroxide from zinc containing solutions, but the hydroxide then also aids in the removal of other impurities by co-precipitation or adsorption. The iron is leached as Fe(2+) during the initial stages of leaching, and then oxidized to Fe(3+) by the addition of oxidants such as oxygen or manganese dioxide and precipitated as $Fe(OH)_3$. Other metals like arsenic, antimony, aluminium, indium, gallium and germanium co-precipitates with iron or are adsorbed on iron hydroxide and removed in the solid/liquid separation step (Sinclair, 2005; Nelson et al, 2000). Ferrous iron that reports to the electrolyte may be oxidized at the anode to the trivalent state, but would not precipitate due to the highly acid nature of the electrolyte and may be transported to the cathode where it will be reduced to the divalent state, and further to iron metal. This will reduce the current available for zinc deposition and the current efficiency will be reduced accordingly (Sinclair, 2005).

Lead, cadmium and thallium do not affect electrolysis, but co-deposit with zinc, thereby contaminating the final zinc product. Copper too co-deposits with zinc, but has the added effect of lowering the hydrogen overpotential, thereby reducing the current efficiency (Sinclair, 2005; Raghavan et al, 1998; Fugleberg and Rastas, 1976). Lead is rather insoluble in the sulfate rich neutral leach solution and is also further removed by cementation on zinc dust. The primary source of lead contamination is corrosion of the lead anodes typically used in zinc electrowinning, with incorporation into the plated zinc as lead dioxide, lead sulfate or metallic lead (Sinclair, 2005).

Lead contamination may be controlled by:

- Reducing the release of lead from the anode by formation of a protective layer of manganese dioxide on the anode.

- Adding silver to the lead that catalyzes the oxidation of water to oxygen and so reduces the potential of the anode to potentials where lead corrosion is lower.

- Precipitation of the lead from the electrolyte using strontium additions to enhance co-precipitation of lead with strontium sulfate.

Metals like copper, cadmium, nickel and cobalt remain in solution after the neutral leach with iron precipitation and a separate process is required for their removal. Purifying of the leach solution to remove these metals is typically done using zinc dust cementation. Using zinc dust as reagent has the advantage of not introducing foreign ions into the sulfate solution. However, the zinc dust produced as reagent for purification purposes introduces a recirculating stream of zinc, which may be a significant fraction of the zinc electrowinning capacity. This, as well as the production of zinc dust from the cathode zinc adds significantly to the cost of electricity associated with the electrowinning of zinc. It is thus important to operate the purification process as efficiently as possible and to reduce this circulating load of zinc (Fugleberg et al, 1993).

This study focuses on the purification of a leach solution produced by neutral leaching of a roasted zinc sulfide concentrate and in particular on the effect of the operating conditions in the cementation process used for the removal of cobalt from the solution, using zinc dust as reagent and activation with arsenic, copper and high temperature. Cadmium is invariably removed during cobalt cementation, as will be discussed later. Brief references to the cementation of nickel are made, as nickel is removed together with cobalt. The level to which impurities may be removed, is limited by the reversible potential of zinc, the kinetics of the reactions involved and the design and operation of the purification circuit.

From a thermodynamic perspective the driving force for removal of cobalt, nickel, cadmium and copper are sufficient for effective removal with zinc as reagent, with the magnitude of that driving force increasing in the order of the elements listed. The kinetics of copper and cadmium are fast and the processes operate close to equilibrium with the required zinc dust addition rate slightly in excess of the stoichiometric requirement. Nickel and especially cobalt are difficult to remove, because of slow reaction kinetics and require higher temperatures and a greater excess of zinc dust for effective removal (Van der Pas and Dreisinger, 1996; Nelson

et al, 2000; Boyanov et al, 2004; Yang et al, 2006; Zeng et al, 2006; Ohgai et al, 1998).

Zinc electrowinning is favoured by maintaining a high zinc concentration in the feed to the cell house to minimize mass transfer limitations during electrowinning. Impurity concentrations, in contrast, are much lower and mass transfer will typically limit their reactions. As a result the purity of the plated zinc will be determined mostly by the rate at which zinc is plated, as the plating of the other species will not be significantly enhanced by the application of more negative potentials. Effective electrowinning and the maintenance of the water balance over the plant thus require that the spent electrolyte that is recycled back to the leach and purification stages has a rather high dissolved zinc content. The high concentration of recirculating residual zinc together with added new zinc from the neutral leach circuit inhibits the cementing of specifically cobalt and nickel, probably by the adsorption of zinc species onto the zinc dust. This is a problem mainly for reactions with kinetics limited by the chemical reaction rate i.e. activation controlled cobalt and nickel precipitation, whereas reactions with kinetics limited by mass transfer, such as those for copper and cadmium are not affected.

Addition of activators is required to improve kinetics of the cobalt and nickel removal reactions sufficiently for it to be used within the practical constraints of modern processing facilities (Dreher et al, 2001; Nelson et al, 2000). Activators like arsenic and antimony are used and added as arsenic trioxide, antimony trioxide, and antimony metal or potassium antimony tartrate (Singh, 1996; Yamashita et al, 1997). For cobalt that cannot be cemented with zinc dust without additives, chemical precipitation of an insoluble salt with α-nitroso-β-naphthol or xanthate is also used, followed by activated charcoal to remove the excess organic. In the latter case precipitation of cobalt depends on the requirement for cobalt(2+) to be oxidized to cobalt(3+) by the organic reagent where after insoluble cobalt(3+) tris 1-nitroso-2-naphtholate is formed (Fugleberg et al, 1980; Lawson and Nahn, 1981; Raghavan et al, 1998; Singh, 1996).

The typical removal sequence for conventional purification is to remove copper first (60 to 65 °C), then cobalt and nickel at high temperatures (70 to 100 °C) with addition

of activators, followed by a colder cadmium removal step (60 to 65 °C). In some cases a cold removal procedure is applied in order to remove copper, cadmium and nickel first, followed by hot cobalt removal with activators (Sinclair, 2005; Raghavan et al, 1998).

1.1 A typical zinc sulfate purification process

The process parameters applied to the purification process of the Zincor refinery in South Africa was used to prepare a base case laboratory test against which all other laboratory test results could be compared. The purification process used in this study is based on zinc cementation to sequentially remove copper (partially) at temperatures of 50 to 55 °C, then cobalt and nickel with arsenic and (remaining) copper activation at elevated temperatures (80 to 85°C) and finally cadmium with copper activation at temperatures of 60 to 65°C as indicated by Figure 1. In the plant the cemented solids are removed with filter presses and the remaining solution is transferred to the next process.

Reactor design information, such as rate constants, was not available for the industrial process. It was assumed that because of the similarity of the process to that used by Outokumpu's Kokkola plant in Finland, the same chemistry, kinetics, deposition mechanism and morphology would apply. However, the purification plant used in the case study performed poorly in terms of zinc dust consumption compared to Kokkola to achieve similar low levels of impurity concentrations in the purified solution. For example the stoichiometric excess zinc dust of up to 7.5 times consumed during cobalt removal and of up to 4 times consumed during cadmium removal do not compare well with values of 1.5 for cobalt and cadmium and 0.8 times for copper removal that have been reported for Kokkola (Fugleberg et al, 1993). At Kokkola the precipitation of cuprous chloride also contributes to copper removal and hence the sub-stoichiometric requirement.

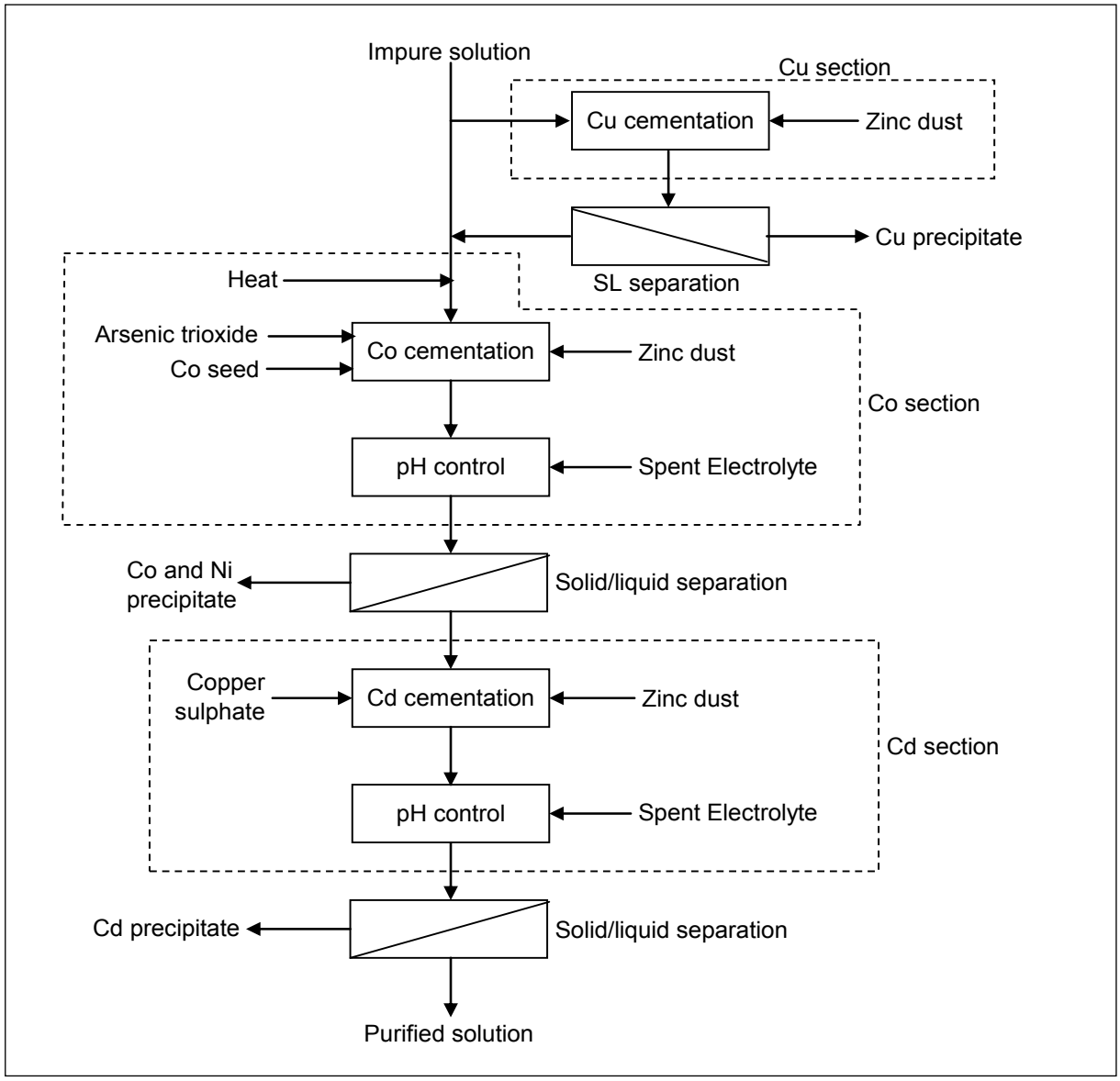

Figure 1: Flow sheet of the Zincor purification process.

1.2 Study objectives

This study has two objectives, namely:

- To characterize the industrial purification process in terms of the chemistry, thermodynamics, kinetics and cementation mechanism and morphology involved.

- To identify ways with which to improve cobalt removal efficiency based on the knowledge gained from investigations into the items listed above.

Ultimately it is the purpose of this study to establish ways and means to reduce zinc dust consumption, by providing operating conditions that increase the efficiency and robustness of the purification process, even with variable feed conditions, while maintaining the required levels of solution purity.

Efficient removal of cobalt, nickel and cadmium requires that excess zinc dust be present in solution, to prevent redissolution of the precipitated solids. This excess is quantified in terms of the number of times that the stoichiometric number of mols of reagent as defined in the balanced chemical reactions has to be exceeded for the reaction to be sustainable in the forward direction.

Some similarities have been observed between cobalt removal processes with arsenic trioxide and antimony trioxide. This study does not have as its aim a comparison between these two processes. Rather some results from tests with antimony trioxide are reported as confirmation of observations made from tests with arsenic trioxide or as reference to the application of relevant knowledge.

2. PURIFICATION OF ZINC LEACH SOLUTIONS

The metallurgy of zinc solution purification can be described in terms of the chemistry, thermodynamics, kinetics and the deposition mechanisms and morphology involved.

2.1 Chemistry of zinc sulfate solution purification reactions

Various chemical reactions have been proposed to describe the chemistry of solution purification for the arsenic process. This is discussed in terms of a conventional purification process i.e. cold copper removal, hot cobalt removal (hot arsenic process) and cadmium removal.

2.1.1 Copper precipitation chemistry

Whilst copper is partially removed in the copper section, a fraction of copper is retained in the impure solution to assist with activation of the cobalt cementation reaction (Fugleberg et al, 1980; Näsi, 2004). The chemical reactions in the copper removal section will therefore also occur in the cobalt removal reactions in addition to those that occur due to the presence of either arsenic or antimony.

Copper is precipitated whilst zinc dissolves according to the following half cell reactions:

Reduction: $CuSO_4\,(aq) + 2e = Cu^0 + SO_4^{2-}$ ……..…… (1)

Oxidation: $Zn^0 + SO_4^{2-} = ZnSO_4\,(aq) + 2e$ …… (2)

Giving the overall reaction:

$CuSO_4\,(aq) + Zn^0 = Cu^0 + ZnSO_4\,(aq)$ ……..…… (3)

Part of the deposited copper precipitates soluble copper as copper oxide according to the following half cell reactions:

Reduction: $2CuSO_4\,(aq) + H_2O + 2e = Cu_2O\,(s) + SO_4^{2-} + 2H^+$ … (4)

Oxidation: $2Cu^0 + H_2O = Cu_2O\,(s) + 2H^+ + 2e$ ……..….. (5)

Giving the overall reaction:

$CuSO_4\,(aq) + Cu^0 + H_2O = Cu_2O\,(s) + SO_4^{2-} + 2H^+$ …….. (6)

Some chloride is removed from the solution in reaction with copper as follows (Fugleberg et al, 1980):

$CuSO_4\,(aq) + Cu^0 + 2Cl^- = 2CuCl\,(s) + SO_4^{2-}$ …….. (7)

$2CuCl\,(s) + H_2O = Cu_2O\,(s) + 2H^+ + 2Cl^-$ …….. (8)

Näsi (2004) suggested that hydrogen is generated in addition to the above reactions during copper cementation according to the following half cell reactions:

Reduction: $2H^+ + 2e = H_2\,(g)$ …….. (9)

Oxidation: $Zn^0 + SO_4^{2-} = ZnSO_4\,(aq) + 2e$ …….. (2)

Giving the overall undesired reaction:

$Zn^0 + 2H^+ + SO_4^{2-} = ZnSO_4\,(aq) + H_2$ ……... (10)

Näsi further suggested that hydrogen evolves according to the following general reaction:

$Zn^0 + 2H_2O = Zn(OH)_2 + H_2$ ……..…. (11)

2.1.2 Cobalt precipitation chemistry

A number of other reactions in addition to copper cementation and copper hydrolysis (reactions 3 and 6) occur in the cobalt removal section in the presence of arsenic and cobalt (Fugleberg et al, 1993; Näsi, 2004; Sinclair, 2005).

Elemental cobalt precipitates in reaction with zinc dust according to the following half cell reactions:

Reduction: $CoSO_4\,(aq) + 2e = Co^0 + SO_4^{2-}$ …… (12)

Oxidation: $Zn^0 + SO_4^{2-} = ZnSO_4\,(aq) + 2e$ …… (2)

Giving the overall reaction:

$CoSO_4\,(aq) + Zn^0 = Co^0 + ZnSO_4\,(aq)$ ……..…….. (13)

However, this reaction is slow in solutions containing significant zinc in solution and cobalt cementation with zinc dust is activated by heat in the presence of copper and trivalent arsenic or antimony.

Copper is precipitated first as copper arsenide in the presence of arsenic and in reaction with zinc dust according to the following half cell reactions:

Reduction: $6CuSO_4\,(aq) + As_2O_3\,(s) + 6H^+ + 18e = 2Cu_3As\,(s) + 6SO_4^{2-} + 3H_2O$ …… (14)

Oxidation: $9Zn^0 + 9SO_4^{2-} = 9ZnSO_4\,(aq) + 18e$ …… (15)

Giving the overall reaction:

$6CuSO_4\,(aq) + As_2O_3\,(s) + 6H^+ + 3SO_4^{2-} + 9Zn^0 = 2Cu_3As\,(s) + 9ZnSO_4\,(aq) + 3H_2O$ ……... (16)

This is followed by precipitation of cobalt arsenide and elemental copper after reaction of precipitated copper arsenide and cobalt in solution with zinc dust in terms of the following half cell reactions:

Reduction: $Cu_3As\ (s) + CoSO_4\ (aq) + 2e = 3Cu^0 + CoAs\ (s) + SO_4^{2-}$ …. (17)

Oxidation: $Zn^0 + SO_4^{2-} = ZnSO_4\ (aq) + 2e$ …….. (2)

Giving the overall reaction:

$Cu_3As\ (s) + CoSO_4\ (aq) + Zn^0 = 3Cu^0 + CoAs\ (s) + ZnSO_4\ (aq)$ ……. (18)

In addition, cobalt and arsenic reacts with zinc dust where cobalt is cemented as cobalt arsenide in terms of half cell reactions as follows:

Reduction: $2CoSO_4\ (aq) + As_2O_3\ (s) + 6H^+ + 10e =$
$2CoAs\ (s) + 2SO_4^{2-} + 3H_2O$ ..…….. (19)

Oxidation: $5Zn^0 + 5SO_4^{2-} = 5ZnSO_4\ (aq) + 10e$ ……. (20)

Giving the overall reaction:

$2CoSO_4\ (aq) + As_2O_3\ (s) + 6H^+ + 3SO_4^{2-} + 5Zn^0 =$
$2CoAs\ (s) + 5ZnSO_4\ (aq) + 3H_2O$ ……..... (21)

Näsi (2004) suggested that copper precipitation dominates in the early stages of precipitation due to its more positive reversible potential, and also buffers the mixed potential at more positive values. Later, when the copper in solution is depleted the mixed potential moves more negative and nickel and cobalt starts to precipitate as the arsenides according to the following general reaction (Näsi, 2004; Fugleberg et al, 1993):

$2MeSO_4\ (aq) + As_2O_3\ (s) + 5Zn^0 + 3H_2O =$
$2MeAs(s) + 2ZnSO_4\ (aq) + 3Zn(OH)_2\ (s)$ ……. (22)

The addition of zinc should be limited to the minimum necessary to achieve the desired impurity metal removal not only from an economic point of view but also because higher zinc additions will favour less desirable mixed precipitates by depressing the mixed potential such that hydrogen, arsine and cadmium precipitation is favoured (Fugleberg et al, 1993; Näsi, 2004).

In addition to consuming zinc in a non-cementation related reaction, hydrogen gas evolution (equations 10 and 11) also presents a safety hazard and the accompanying alkalization of the solution favours metal precipitation as hydroxides and basic sulfates, which are generally undesirable as they redissolve easily and also tends to passify the anodic dissolution of zinc to inhibit further cementation. Hydrogen gas evolution cannot be avoided as the potentials required for impurity precipitation is more negative than its reversible potential, but may be controlled by limiting the hydrogen ion concentration, i.e. operating at higher pH levels, but not such that hydroxide precipitation occurs and by controlling the mixed potential by controlled zinc additions such that it is adequate for impurity removal, but do not unduly favour hydrogen precipitation (Fugleberg et al, 1980).

Arsenic reacts with zinc dust to form arsine gas according to the following half cell reactions:

Reduction: $As_2O_3\,(s) + 9H_2O + 12e = 2AsH_3\,(g) + 12OH^-$ ..... (23)

Oxidation: $6Zn^0 + 6SO_4^{2-} = 6ZnSO_4\,(aq) + 12e$ ..... (24)

Giving the overall reaction:

$As_2O_3\,(s) + 6Zn^0 + 9H_2O = 2AsH_3\,(g) + 6Zn(OH)_2\,(s)$ ..... (25)

Arsine evolution is controlled by limiting the zinc additions such that its rate is low at the mixed potential achieved during the cementation process.

Lawson and Nahn (1981) investigated arsenic activated cobalt precipitation using a rotating disc and found that for solution temperatures below 80 °C the overall reaction was:

$$2HAsO_2\,(aq) + CoSO_4\,(aq) + 6H^+ + 5Zn^0 = 2CoAs\,(s) + 5ZnSO_4\,(aq) + 4H_2O \quad \ldots\ldots\ldots\ldots \quad (26)$$

This is fundamentally the same equation as equation 21, but assuming hydrolysis of As_2O_3. For solution temperatures above 80 °C the equation was proposed to be:

$$2HAsO_2\,(aq) + CoSO_4\,(aq) + 6H^+ + 4Zn^0 = CoAs_2\,(s) + 4ZnSO_4\,(aq) + 4H_2O \quad \ldots\ldots\ldots\ldots\ldots \quad (27)$$

The reaction products CoAs and $CoAs_2$ were identified by the molar mass ratios of cobalt to arsenic (Co:As).

Although there is consensus in the literature (Fugleberg et al, 1993; Näsi, 2003; Sinclair, 2005) that cobalt is predominantly removed as a cobalt arsenide it has been reported too that a significant fraction of cobalt is precipitated as a basic salt under localized conditions of high pH and by reacting with zinc hydroxide (Bøckman and Østvold, 2000) according to the following reaction:

$$Zn(OH)_2\,(s) + CoSO_4\,(aq) = Co(OH)_2\,(s) + ZnSO_4\,(aq) \quad \ldots\ldots\ldots\ldots\ldots \quad (28)$$

The corrosion of zinc in the presence of dissolved oxygen is thermodynamically possible. The reaction with dissolved oxygen is undesirable as it represents a net consumption of zinc to the detriment of cementation reactions if the zinc content should decrease sufficiently to become rate limiting instead of the cobalt concentration. The rate of reaction with dissolved oxygen should be low however due to naturally low concentration of dissolved oxygen as the solubility of oxygen in water decreases with increasing temperature.

2.1.3 Cadmium precipitation chemistry

At Kokkola, cadmium present in the filtrate after cobalt removal is removed by passing the solution through fluidized bed reactors (Fugleberg et al, 1980). The solid fraction is separated from solution with hydrocyclones following cadmium deposition.

At the Zincor base metals refinery in Springs, South Africa, cadmium is removed by reaction with zinc dust in a series of conventional continuously stirred tank reactors according to the following reaction:

$$CdSO_4\,(aq) + Zn^0 = Cd^0 + ZnSO_4\,(aq) \quad \ldots\ldots\ldots\ldots\ldots\ldots\ldots\ldots\ldots\ldots\ldots\ldots \quad (29)$$

Although cadmium removal using zinc dust is ostensibly rather easy, activation by copper is also practiced to remove cadmium to low levels such as down to 1.5 mg/L at the Zincor plant.

2.2 Thermodynamics of zinc sulfate solution purification

The EMF series with standard half cell potentials predict that copper, cobalt, nickel and cadmium in solution will be reduced readily by the oxidation reaction of zinc as is indicated by positive cell potentials and negative free energies. These may be calculated by using either the cell potential or Gibbs Free Energy approaches:

$$E_{cell} = E_{cathode} - E_{anode} \quad \ldots\ldots\ldots\ldots\ldots\ldots\ldots\ldots\ldots\ldots\ldots\ldots\ldots\ldots \quad (30)$$

and

$$\Delta G = -n\,F\,E_{cell} \quad \ldots\ldots\ldots\ldots\ldots\ldots\ldots\ldots\ldots\ldots\ldots\ldots\ldots\ldots \quad (31)$$

and

$$\Delta G^o = -R\,T\,ln\,K \quad \ldots\ldots\ldots\ldots\ldots\ldots\ldots\ldots\ldots\ldots\ldots\ldots\ldots\ldots \quad (32)$$

With $E_{cathode}$ the half cell potential for the reduction reaction, E_{anode} the half cell potential for the oxidation reaction, n the number of electrons transferred, F Faraday's constant, R the universal gas constant and K the equilibrium constant.

Table 1: Standard half-cell and cell potentials and Gibbs Free Energy changes for the cementation of impurities with zinc.

Order	Element	E^0 (V)[1]	Half-reaction	E^0_{cell} (V)	ΔG^0 (J/mol)
1	Copper	0.34	$Cu^{2+}_{(aq)} + 2e^- \rightarrow Cu_{(s)}$	1.10	-212267
2	Nickel	-0.25	$Ni^{2+}_{(aq)} + 2e^- \rightarrow Ni_{(s)}$	0.51	-98415
3	Cobalt	−0.28	$Co^{2+}_{(aq)} + 2e \rightarrow Co_{(s)}$	0.48	-92626
4	Cadmium	-0.40	$Cd^{2+}_{(aq)} + 2e^- \rightarrow Cd_{(s)}$	0.36	-69469
	Zinc	-0.76	$Zn^{2+}_{(aq)} + 2e^- \rightarrow Zn_{(s)}$		

Note 1: All relative to the standard hydrogen electrode

The standard cell potentials for the cementation of the major impurities with zinc are significantly positive, as indicated in Table 1, indicating that their equilibrium concentrations in the presence of excess zinc will be low. This may be further illustrated by calculating the equilibrium constant for the cementation of cobalt with zinc to be:

$$K = \frac{[Zn^{2+}]}{[Co^{2+}]} = 2 \; x \; 10^{16} \qquad \ldots\ldots\ldots\ldots\ldots\ldots\ldots\ldots\ldots\ldots\ldots\ldots\ldots\ldots\ldots\ldots \quad (33)$$

Also note that for standard conditions the reaction between zinc metal and copper in solution has the greatest driving force (with copper being most noble), followed by nickel, cobalt and finally by cadmium. The equilibrium data suggest that removing the mentioned metal impurities from solution by zinc cementation should not be a problem.

However, only copper and cadmium behave according to thermodynamic predictions whereas the rates of cobalt and nickel cementation are too low for practical use, unless activated, as will be discussed in detail in the section on cobalt removal kinetics.

Of relevance to cobalt precipitation are the potentials of the half cell reactions described in the section on purification chemistry, in order to predict the reaction sequence and to possibly contribute to formulation of a precipitation mechanism. A set of associated thermodynamic data were conveniently provided by Yamashita et al (1997) for chemical reactions participating in cobalt precipitation and these are displayed in Table 2. The half cell potentials were determined for the industrially relevant conditions as indicated and illustrate that these may be significantly different than those for the standard conditions.

From Table 2 it is clear that the reaction between zinc, copper and arsenic to form copper arsenide has a greater thermodynamic driving force (ΔG^0 = 625 kJ per mol Cu_3As formed for an E_{cell} = 0.72 V and 9 electrons exchanged) compared to the reaction between zinc, cobalt and arsenic to form a cobalt arsenide (ΔG^0 = 227 kJ per mol CoAs formed for an E_{cell} = 0.47 V and 5 electrons exchanged).

Table 2: Standard and non-standard half cell potentials for relevant half cell reactions (after Yamashita et al, 1997).

Order	Reaction	$E^0(V)^1$	$E^*(V)^1$
1	$Cu^{2+} + 2e = Cu^0$	+0.34	+0.26
2	$HAsO_2$ (aq) + $3H^+ + 3e = As^0 + 2H_2O$	+0.25	-0.065
3	$HAsO_2$ (aq) + $3Cu^{2+} + 3H^+ + 9e = Cu_3As$ (s) + $2H_2O$	+0.19	-0.03
4	$2H^+ + 2e = H_2$	0	-0.25
5	$HAsO_2$ (aq) + $Co^{2+} + 3H^+ + 5e$ = CoAs (s) + $2H_2O$	-0.073	-0.29
6	$HAsO_2$ (aq) + $6H^+ + 6e = AsH_3$ (g) + $2H_2O$	-0.18	-0.44
7	$Co^{2+} + 2e = Co^0$	-0.28	-0.34
	$Zn^0 = Zn^{2+} + 2e$	-0.76	-0.75

Electrolyte conditions for E*(V): 60 °C, pH 4, concentrations of Zn: 2.3 mol/L or 150 g/L, Co: 3 x 10^{-4} mol/L or 18 mg/L and As: 5 x 10^{-4} mol/L or 37 mg/L
Note 1: All potentials relative to standard hydrogen electrode

These free energy values suggest that the formation of Cu_3As will be favoured relative to CoAs in support of the notion, discussed in the section on cobalt kinetics,

that Cu_3As plates first and then increases cobalt precipitation kinetics, through perhaps increasing the reaction surface area available for cobalt precipitation.

Moreover, it had been suggested that all metal arsenides are more stable than the metals at pH 3 to 5 (Tozawa et al, 1992). Tozawa et al used standard Gibbs Free Energy data from NBS tables of thermodynamic properties of organic and inorganic substances (Wagman et al, 1982) and standard Gibbs Free Energy data for metal arsenides from Kubaschewski et al (1979) and Barin et al (1977) to establish a Potential-pH (Pourbaix) diagram for the M-As-H_2O system. Standard free energies for the arsenides are displayed in Table 3.

Table 3: Standard Gibbs Free Energies for formation of arsenides (after Tozawa et al, 1992).

Arsenide	Standard Gibbs Free Energy - ΔG^0 (kJ/mol)
Cu_3As	-107.8
CoAs	-67.0

The potential-pH diagram in Figure 2 for the As-H_2O systems (Pourbaix, 1974) suggests that arsenic is dominant in the form $HAsO_2$ in the As(3+) oxidation state under conditions normally associated with zinc sulfate solution purification highlighted in yellow on blue. The diagram indicates that elemental arsenic too may form upon addition of zinc dust and that the formation of arsine will only be favoured at rather low pH values when coupled to zinc.

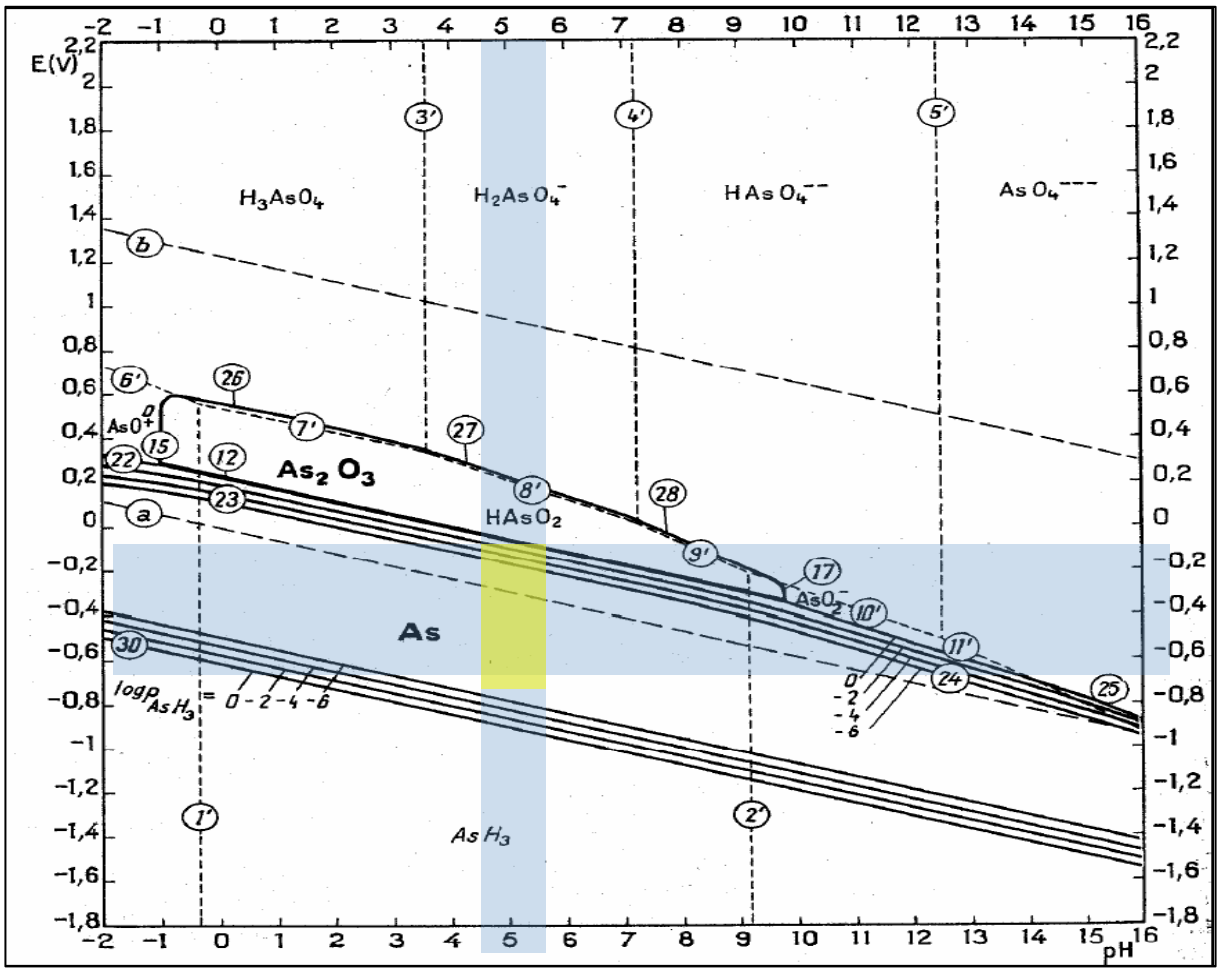

Figure 2: Potential-pH diagram for the As-H_2O System (Pourbaix, 1974).

From a study of impurity concentration as a function of electrochemical potential it can be concluded that the equilibrium levels achievable for cadmium, cobalt and copper are well below those typically accepted for electrowinning, if an excess of zinc dust is used, as displayed in Figure 3.

In practice, and as mentioned earlier, this of course applies to cadmium and copper only and cementation of cobalt is strongly inhibited in the presence of dissolved zinc, unless activated by arsenic or antimony in the presence of copper, using a high stoichiometric excess of zinc dust and increasing the temperature of the solution (Van der Pas and Dreisinger, 1996; Nelson et al, 2000; Boyanov et al, 2004; Yang et al, 2006; Zeng et al, 2006, Ohgai et al, 1998).

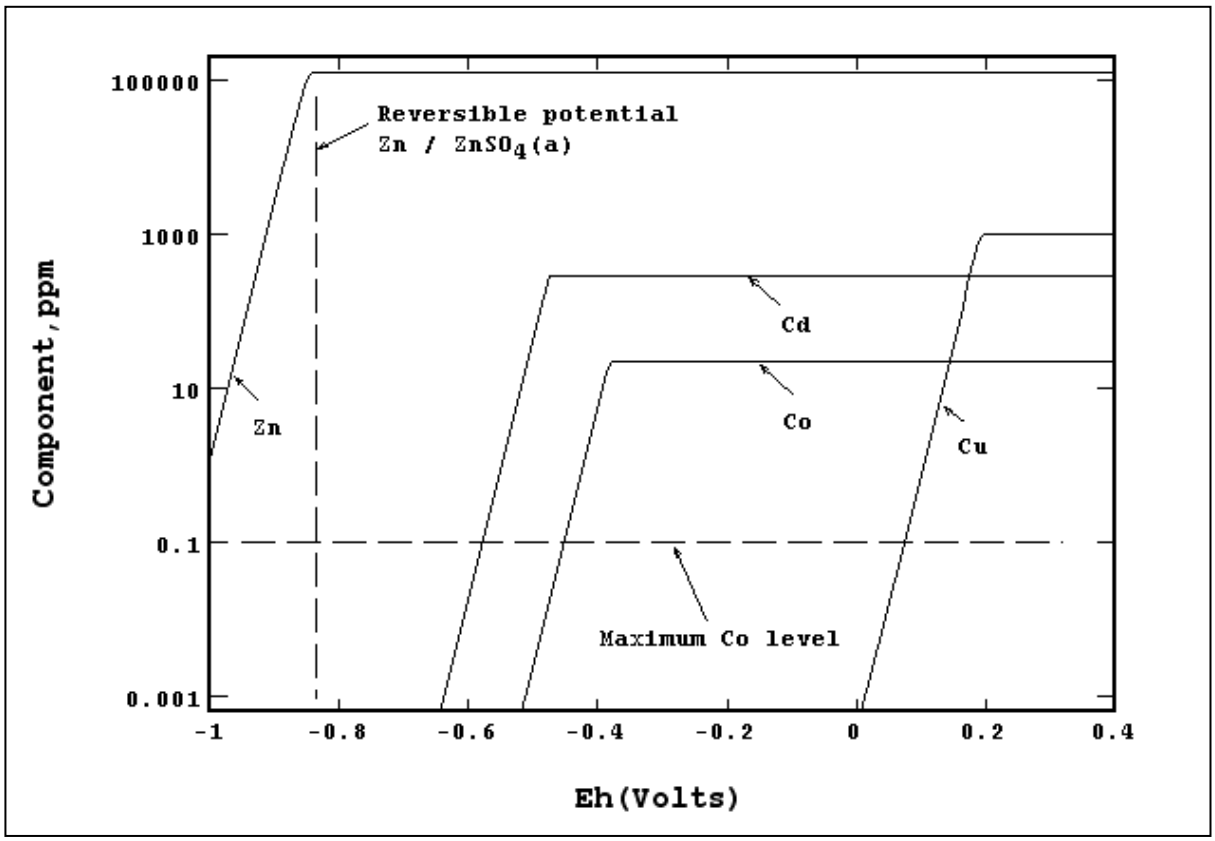

Figure 3: Calculated equilibrium concentrations of some metal impurities without arsenic in zinc sulfate solutions as a function of electrochemical potential with pH 4, temperature 25°C, initial concentrations (g/L) of Zn: 130, S(+6): 300, Cu: 1, Cd: 0.3, and Co: 0.05. Constructed with Stabcal using data from the NBS database.

Arsenic improves the driving force for copper cementation slightly and very significantly for cobalt cementation by forming, respectively, Cu3As and CoAs (Tozawa et al, 1992), as illustrated in Figure 4.

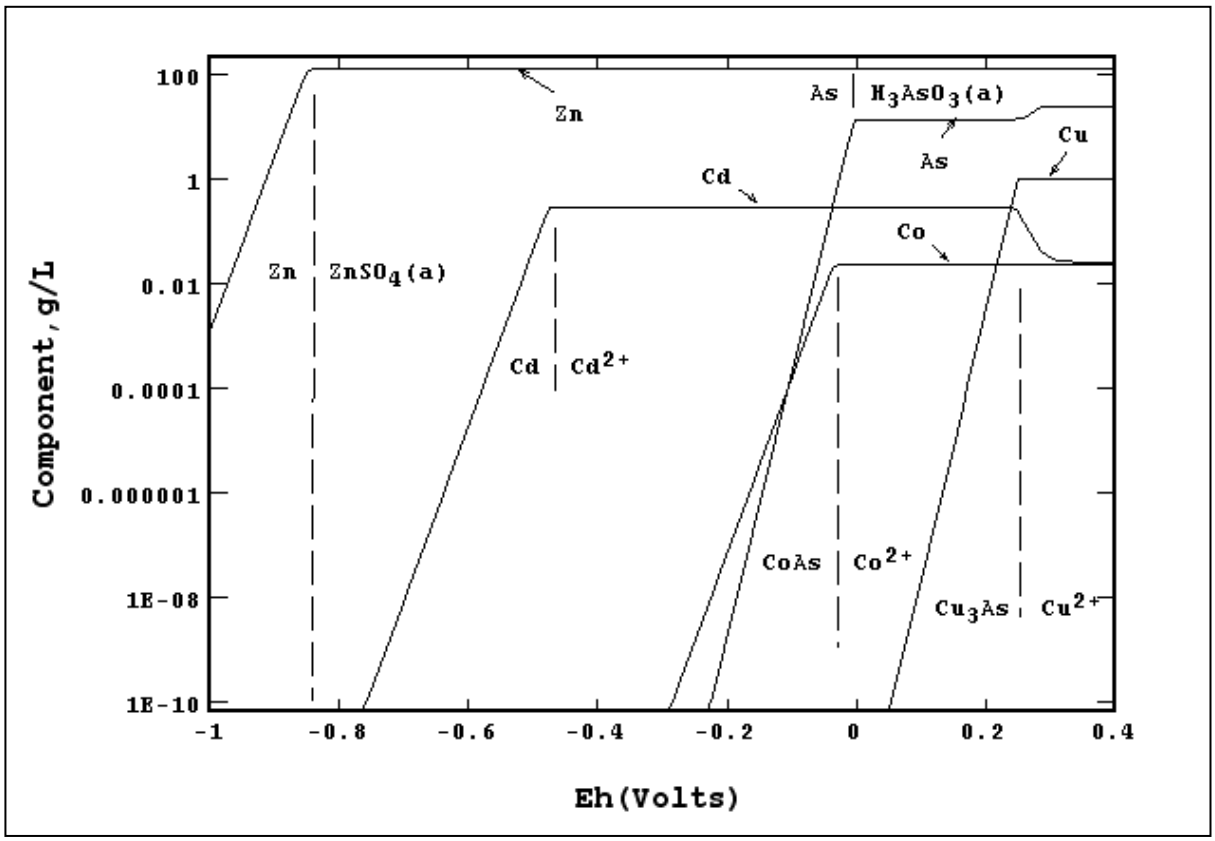

Figure 4: Equilibrium concentrations of some metal impurities and arsenic in zinc sulfate solutions as a function of the electrochemical potential with pH 4, temperature 25°C, initial concentrations (g/L) of Zn: 130, S(+6): 300, As: 24, Cu: 1, Cd: 0.3, Co: 0.05. Constructed with Stabcal using data from the NBS database and Tozawa et al (1992).

The more positive potentials at which cobalt can be plated in the presence of arsenic could contribute to its activating effect as the adsorption of inhibiting cationic species like $Zn(OH)^+$ should be less likely. The work of Fugleberg et al (1976) indicated that the arsenides are also less likely to stimulate hydrogen ion reduction and the resultant rise in the pH at the metal surface. This would limit the precipitation of basic cobalt sulfate, which becomes favourable at higher pH values, as illustrated in Figure 5, and which easily redissolves when the local pH decreases or the zinc metal is totally consumed (Bøckman and Østvold, 2000). It also follows from this diagram that CoAs is most stable at the more negative potentials expected in the presence of zinc.

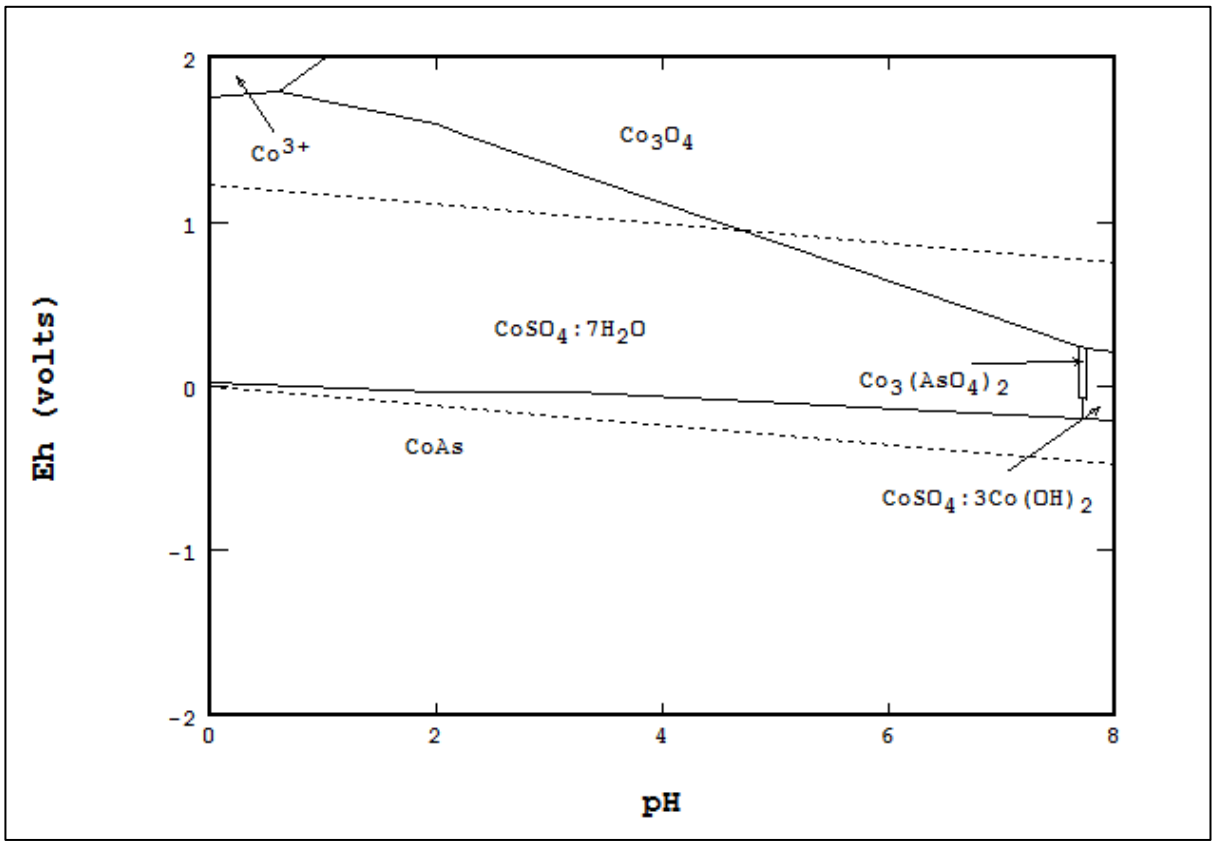

Figure 5: Potential-pH diagram for the Co-S(+6)-As-H_2O system with temperature 25°C and concentrations (g/L) of Co: 0.001, S(+6): 300, As: 0.001. Constructed with Stabcal using data from the NBS database and ΔG_f CoAs = -67 kJ/mol from Tozawa et al (1992).

2.3 Cobalt precipitation kinetics

The rate of cementation reactions for cobalt in a zinc sulfate solution with a high dissolved zinc concentration (typically 150 g/L) is slow without the presence of activators, as already indicated.

It is assumed that the inhibiting effects of a high zinc ion concentration on cobalt cementation kinetics at lower pH values may be due to adsorption of cations in high concentration in the electric double layer, even though the negative effects on cobalt cementation are typically rather ascribed to formation of basic zinc sulfate, which is formed at higher pH values. The slow rate of reaction between cobalt and zinc has generally been ascribed to the high deposition overpotential of cobalt reduction on

zinc (Lawson & Nahn, 1981; Yamashita et al, 1997). The possible mechanisms involved are discussed in detail in Section 2.3.4 on the effects of zinc ion on cobalt cementation.

Since cementation is an electrochemical process the actual deposition step (cathodic half cell) may occur at locations, which are separated from the sacrificial metal dissolution sites (anodic half cell). Galvanic cells are in effect created between reductants and oxidants and the slowest step in this coupled series process will determine the rate of the overall process.

These steps are typically:

- Transport of soluble reactant to and product species from the interface to the bulk solution via a mass transfer boundary layer and possibly also a product layer of cobalt and nickel or of basic metal sulfates caused by the local increase in pH at the reaction interface.

- Electrochemical reactions at the various sites comprising the exchange of electrons to and from the metal and to and from adsorbed species.

- Conduction of charge via electrons and ions between the anodic and cathodic sites.

It is generally agreed that the rate of cobalt precipitation is electrochemically controlled during cementation with zinc in acidic solutions. This is confirmed by the work of Lawson & Nahn (1981) using tests with rotating discs showing that the reaction rate was not influenced by the disc rotation speed, i.e. the rate of mass transfer at high zinc concentrations in solution. The relatively high activation energies determined by Fugleberg et al (1993) for cobalt precipitation using zinc cementation support this notion, as will be discussed in more detail in Section 2.5.2 on determining the activation energy. However, it is possible that the passivation of the zinc surface by the precipitation of hydroxides and basic sulfates will reduce the rate of zinc dissolution such that it may become the rate determining step, as indeed typically occurs if cobalt cementation is attempted without arsenic activation (Oghai

et al, 1998). This is discussed in more detail in terms of the hydroxide suppression mechanism in Section 2.3.4 on the effects of the zinc ion on cobalt cementation.

The availability of exposed and active reaction surface area is an important consideration in improving the cobalt removal rate through provision of reaction surface area not passified by basic zinc sulfate or zinc hydroxide. In addition, the rate at which cobalt is removed from solution is influenced by reactant concentration and temperature, all of which is discussed in detail in the sections following.

A discussion of the factors that influence the rate at which cobalt is removed from solution may best proceed by a discussion of the applicable rate laws and the temperature dependence of the rate constants.

2.3.1 Rate equation

The cobalt cementation reaction rate r is defined as the number of mols of cobalt reacted per unit time per unit volume of solution or in terms of standard symbols as follows:

$$r = kC_m \quad \text{.....} \quad (34)$$

Where k is the reaction rate constant with unit s^{-1} and C_m is the concentration of cobalt in solution in mol/m^3. The general mol balance for any reactor with constant volume can then be written as:

$$Mols_{in} - Mols_{out} - Mols_{conv} = Mols_{accum} \quad \text{.....} \quad (35)$$

Where $Mols_{in}$ is the rate of flow of cobalt into the reactor, $Mols_{out}$ is the rate flow of cobalt flowing out of the reactor, $Mols_{conv}$ is the rate at which cobalt in solution is converted to cement and $Mols_{accum}$ is the rate at which dissolved cobalt accumulates in the reactor, all with units of $mols.min^{-1}$. For a well-mixed batch reactor and with no flow in or out of the reactor and for decreasing cobalt concentration, Equation 35 becomes:

$$-rV = {}^{dN}/_{dt} \quad \ldots\ldots\ldots\ldots\ldots\ldots\ldots\ldots\ldots\ldots\ldots\ldots\ldots\ldots\ldots\ldots\ldots\ldots\ldots\ldots\ldots\ldots \quad (36)$$

Where –r is the cobalt cementation rate in a reactor with volume V (m^3) and where dN/dt is the rate of accumulation of cobalt in solution in the reactor in mols per minute. Combining the rate equation, Equation 34, and the mole balance for a fixed-volume batch reactor with well-mixed content, Equation 35, yields the following:

$$-r = -kC_m = \frac{dN/V}{dt} = {}^{dC_m}/_{dt} \quad \ldots\ldots\ldots\ldots\ldots\ldots\ldots\ldots\ldots\ldots\ldots\ldots\ldots\ldots\ldots\ldots\ldots\ldots\ldots\ldots\ldots\ldots \quad (37)$$

Equation 37 multiplied by the molar mass (g/mol) on both sides gives the rate at which cobalt precipitates, or the rate at which the cobalt concentration (C) in solution decreases over time as:

$$-\frac{dC}{dt} = kC \quad \ldots\ldots\ldots\ldots\ldots\ldots\ldots\ldots\ldots\ldots\ldots\ldots\ldots\ldots\ldots\ldots\ldots\ldots\ldots\ldots\ldots\ldots \quad (38)$$

With units of concentration kg/m^3 or equivalent. The term k represents the apparent rate constant that incorporates the effects of temperature and zinc dust or activated surface area (cementation products), depending on whether one or both of these surfaces support the rate determining half cell with unit “per minute” if it is elected to measure reaction time in minutes, as was done in this work and as was done in other similar investigations (Fugleberg et al, 1993; Tozawa et al, 1992; Yamashita et al, 1997). The cobalt removed as a function of time in an ideal batch reactor, assuming that the surface area remains constant, is then given by the integral:

$$-ln\frac{C}{C_o} = kt \quad \ldots\ldots\ldots\ldots\ldots\ldots\ldots\ldots\ldots\ldots\ldots\ldots\ldots\ldots\ldots\ldots\ldots\ldots\ldots\ldots\ldots\ldots \quad (39)$$

With C_o the initial cobalt concentration and C the cobalt concentration at any time thereafter. Equation 38 can be developed further by accounting for the effect of reaction surface area on the cobalt removal rate as a separate term in the rate function, as follows:

$$-\frac{dC}{dt} = k' A C \quad \ldots\ldots\ldots\ldots\ldots\ldots\ldots\ldots\ldots\ldots\ldots\ldots\ldots\ldots\ldots\ldots\ldots\ldots \quad (40)$$

Where A represents the surface area of the zinc dust or the activated surface area in m^2 for example, and where k' represents the true rate constant with unit $min^{-1}.m^{-2}$. Näsi (2004) developed the reaction rate equation further with consideration of the reactor volume by defining the reaction surface area in terms of a reaction surface area concentration, as follows:

$$-\frac{dC}{dt} = k'' \frac{A_{seed}}{V_{reactor}} C \quad \ldots\ldots\ldots\ldots\ldots\ldots\ldots\ldots\ldots\ldots\ldots\ldots\ldots\ldots\ldots\ldots\ldots\ldots \quad (41)$$

Where $A_{seed}/V_{reactor}$ represents the reaction surface area concentration or the reaction surface area per unit volume of solution in the reactor with units m^2/m^3. The true rate constant is now represented by k", but with units $m.min^{-1}$. Reactor volume, or more accurately the volume of solution in the reactor is relevant here only in terms of defining the reaction surface area concentration. The solution volume relative to the cobalt may change with time if significant evaporation of water occurs, but this effect is typically small and is assumed to be insignificant in the present case.

The active reaction surface area is provided by zinc dust and by cementation products, with the cementation product surface area likely to control the cobalt reaction rate, as will be discussed later. Surface area concentration defined per unit volume provides a sufficiently comparative base for cementation reactions in an aqueous medium contained in different reactor volumes, rather than surface per unit mass of dry solids, which is useful for comparing surface area on a dry basis only. An argument could be made for keeping the reaction surface area inside the rate constant, as with equation 38, if the reaction surface area remains relatively constant.

It is considered that the reaction surface area remains relatively constant in operating plants in a well-mixed reactor and a continuously operated system, because consumed zinc is replaced constantly with fresh zinc and the cobalt arsenide precipitation is supported by an excess of arsenic and such copper as may be required to maintain the activity of the surface. Moreover, zinc is added in large

stoichiometric excess and the zinc reaction surface area relative to cobalt in solution may not change much. Also, whatever zinc is consumed, assuming sufficient zinc remains to keep providing electrons, is replaced with active reaction surface area of cementation products. In batch processes, even though consumed zinc is not replaced continuously, the change in reaction surface area may be insignificant with respect to decreasing cobalt in solution and in terms of the effect on cobalt cementation rate. As with the continuous process, only a fraction of added zinc is consumed during the cementation process and if enough zinc surface area is available it is possible that the zinc dissolution reaction will not become rate determining during the experiment. If, as expected, the rate of the precipitation of the cobalt as arsenide on the existing arsenide surface is rate determining, then it would be necessary for this area to remain relatively constant, as would be the case if the precipitate only becomes thicker, i.e. little additional surface area is created.

The importance of the activated cathodic surface area was noted by both Fugleberg et al (1993) and Näsi (2004) who incorporated the effects of the surface area of recirculated cobalt precipitate to describe the kinetics of cobalt cementation in a batch process after observing that the presence of cobalt seed significantly increased the rate of cobalt removal. Cobalt precipitate in this case would contain a combination of unreacted zinc as well as precipitated copper and copper, cobalt and nickel arsenides. If the overall rate of cobalt precipitation is indeed limited by the rate of cobalt precipitation, and thus the activated surface area, there is a possibility that this surface area will remain relatively unchanged during the course of the precipitation process and that the simplified kinetic equation without an explicit and correlated area term might suffice.

Näsi (2004) suggested the use of deposition efficiency instead of the reaction rate constant to measure effectiveness of continuous purification processes (as opposed to batch processes) in continuously stirred tank reactors. His test setup consisted of four equally sized continuously stirred tank reactors (CSTRs) in series and a thickener for increasing the density of the slurry containing cobalt precipitate that is recirculated back to the first reactor. Deposition efficiency is expressed in terms of concentration differences between reactors, the amount of feed flow and the volume of the reactor for continuous flow conditions.

$$C_{eff} = \frac{(C_{in} - C_{out})F}{C_{out}V} \quad \text{.....} \quad (42)$$

With C_{eff} the deposition efficiency, i.e. the first order rate constant for the reactor, C_{in} the concentration of cobalt in the feed to the reactor, and C_{out} the concentration of cobalt flowing out as well as in the reactor itself. The residence time in the reactor is described by the ratio of F, the feed flow rate and V, the reactor volume. Equation 42 is the rate function for a well-mixed reactor with continuous flow in and out, with terms re-organized to calculate the rate constant. It is derived from the mass balance for a continuously stirred tank reactor combined with the rate law where the mass of cobalt into the reactor plus the mass of cobalt reacted or removed from solution via the various reactions (kAC) is equal to the mass of cobalt out of the reactor. This can be expressed as follows:

$$C_{in}F - k'''AC_{out}V = C_{out}F \quad \text{.....} \quad (43)$$

With C_{in}, C_{out}, F and V as above, with A the reaction surface area of zinc dust or activated surface area and with k''' the reaction rate constant with units of $min^{-1}.m^{-2}$. Equation 43 can be rearranged to the format of equation 42, with k''' equal to the deposition efficiency C_{eff} in Näsi's equation. Equation 43 can be rearranged further to include reaction time calculated as V/F, to describe the rate equation for a CSTR as follows:

$$\frac{C_{in} - C_{out}}{C_{out}} = k'''A\,\Delta t \quad \text{.....} \quad (44)$$

The deposition efficiency C_{eff} in equation 42 was shown to be affected by many process variables. The highest reported efficiency was achieved with a high copper concentration, a low arsenic concentration and a high zinc dust feed rate. Deposition efficiency was reported to have decreased during the course of a test campaign, and was attributed to changes in the deposit quality after continuous recirculation of the same cobalt precipitate. This indicates that the nature of the activated surface is not constant, but that it only changes relatively slowly. It was also found that the

efficiency could be maintained for longer times by raising the copper concentration in the feed. This confirms the importance of continued copper addition, even if intermittent and in small concentrations, if the activity of the cobalt precipitate is to be maintained. It is suggested that sufficient new copper is required to maintain the available unaltered reaction surface area with low cobalt deposition overpotential, because the surface of cobalt and copper precipitate that has been recirculated continuously for some time may be passivated through zinc hydroxide or basic zinc sulfate deposition or by reducing its surface roughness.

2.3.2 Cobalt precipitation rate constant

The temperature dependence of the apparent rate constant used in Equation 38 can typically be described by an Arrhenius type relationship:

$$k = Ae^{-E/RT} \quad \text{.....} \quad (45)$$

With A the pre-exponential factor, E the activation energy, R the universal gas constant and T the absolute temperature. The Arrhenius relationship is best regarded as an empirical relationship and typically holds true over a limited temperature range. Despite the theorizing in literature about the true meaning of the activation energy other than the observation that it exists, the activation energy is often used to provide an indication of the type of rate limitation that would govern a particular deposition reaction. A low value for the activation energy, typically less than 15 kJ/mol, indicates that some form of mass transfer limits the overall rate of the process. Mass transfer limitations are normally associated with low reactant concentrations and the development of mass transfer limiting product layers. A high value for the activation energy, typically 50 to 100 kJ/mol, suggests that the rate of reaction is limited by the actual chemical reaction itself (Fugleberg et al, 1993).

Reference is made in literature on cementation processes of an initial and an enhanced rate regime with different activation energies (Lawson & Nahn, 1981). The initial low cobalt deposition rate may be related to the creation of an activated surface for the cathodic cobalt precipitation reaction, followed by cobalt deposition without

changing this surface area significantly. High activation energies for both the initial (40 kJ/mol) and enhanced (60 kJ/mol) rate regimes indicated that the rate of the reaction itself controlled the rate during both stages of precipitation in this particular case.

2.3.3 Effects of temperature on precipitation processes

It is commonly reported that the reaction rate of cobalt removal from zinc sulfate electrolytes increases with an increase in solution temperature with copper and arsenic as activators, as would be expected (Boyanov et al, 2004; Fugleberg et al, 1993; Lawson and Nahn, 1981; Tozawa et al, 1992; Yamashita et al, 1989).

However, a decrease in rate is reported when exceeding a certain maximum temperature. This may be attributed to hydrogen evolution, which becomes the most prominent reaction at higher temperatures (Yamashita et al, 1997). Although this may ostensibly be due to a higher activation energy for the hydrogen evolution reaction, it is also possible that it may be a secondary effect due to passivation of the zinc dust surface by the higher surface pH values caused by the increased rate of hydrogen evolution.

The optimum temperature for cobalt cementation is typically between 80°C and 90°C under normal operating conditions. Operating at lower temperatures may be beneficial because it lowers energy consumption in the purification stage in addition to decreasing the amount of cooling necessary before electrowinning, but may require longer retention times. Yamashita et al (1997) in tests with galvanic cells reported that cobalt removal does not improve much above 60°C, although the galvanic current increased. This is not in agreement with observations of most authors and may be related to the generation of hydrogen at the higher temperatures and at the low pH (3.8) used. Also, a potential problem with the use of galvanic cells in experiments may be that the anodic and cathodic sites are spatially significantly separated, which is not the case in practice.

Fugleberg et al (1993) was able to reduce the cobalt concentration in zinc solutions to acceptable levels using zinc cementation at temperatures between 70 and 75 °C

(down from 80 °C) by increasing the catalytic surface area through recirculation of cobalt cement. Raghavan et al (1999) reported that increasing the zinc dust addition rate could compensate for the negative effect of a slight loss in temperature on the cobalt removal rate. There is however limited scope for this as the more negative potentials attained may stimulate hydrogen ion reduction such that basic zinc deposits passify the zinc surface.

Temperature also plays a role in determining what intermetallic species will form. Sinclair (2005) reported that intermetallics such as CoAs and $CoAs_2$ appear to be stable above 75 to 80 °C. Lawson & Nahn (1981) analysed cobalt deposits formed during zinc cementation and found that CoAs forms preferentially below 80 °C while $CoAs_2$ do so above 80 °C.

2.3.4 Effects of zinc ion on precipitation processes

Zinc in solution in the concentrations commonly associated with zinc refining inhibits cobalt cementation. A number of passivation mechanisms have been proposed of which the hydroxide suppression mechanism is most prominent. According to this mechanism the deposition sites for iron-group metals are limited and may further be occupied by foreign substances, like zinc hydroxide ($Zn(OH)_2$, $Zn(OH)^+$) or basic zinc sulfate ($ZnSO_4.Zn(OH)_2$) to limit the rate of the cathodic half cell (Oghai et al, 1998).

An investigation into the deposition overpotential of cobalt on zinc indicated that the potential at which cobalt begins to deposit, in sulfate solutions containing high zinc ion concentrations without activators, is polarized to almost the equilibrium potential of zinc (Ohgai et al, 1998). The slow cementation rate of cobalt in zinc sulfate solutions is attributed to this peculiar trait. In the presence of arsenic and copper ions however, the cobalt polarization curves are shifted in a more noble direction.

Cobalt begins to deposit at the reversible potential for cobalt arsenide in sulfate solutions free from zinc ions, but containing arsenic ions. In a sulfate solution not containing arsenic ions, the deposition of cobalt is polarized by roughly 0.15 V, even in the absence of zinc ions. A minimum overpotential is therefore required to initiate cobalt deposition. This minimum overpotential is reduced at elevated temperatures

emphasizing the need to operate cobalt removal processes at elevated temperatures. In the presence of zinc ions the potential at which cobalt deposition begins, is further polarized to reach the equilibrium potential of zinc. The observed increase in deposition potential is attributed to zinc hydroxide adsorbed on deposition sites on the cathode according to the hydroxide suppression mechanism.

The deposition of cobalt is kinetically suppressed as is indicated by the measured overpotentials (Ohgai et al, 1998). It is suggested that arsenic and copper work as catalysts to reduce the cobalt cathodic overpotential by increasing the exchange current density of the cobalt half cell such that the mixed potential with zinc is close to the reversible potential for cobalt precipitation.

Nelson et al (2000) found a strong correlation between the ability of a metal to act as activator for cobalt deposition and its hydrolysis constant (K_{OH}) for the predominant hydrolysis product. Based on this finding it was suggested that zinc adsorbs as $Zn(OH)^{+}$ on the surface of solid zinc, which is the stable hydroxide species at pH 4, thereby effectively blocking the surface for adsorption of other metals in support of the hydroxide suppression mechanism. It is suggested therefore that a depositing metal ion first undergoes hydrolysis before being adsorbed onto the surface of the zinc dust. Once adsorbed the metal ion is reduced to its elemental state. Effective activators have a large hydrolysis constant compared to zinc, which forms relatively little hydrolysis product. According to this mechanism an effective activator would adsorb in preference to zinc, thereby providing a surface on which zinc hydroxide does not adsorb, allowing cobalt to reach the zinc dust surface.

Xiong & Richie (1988) found that the polarization curve for cobalt deposition is shifted to more negative potentials in the presence of a high concentration of zinc ions. They proposed that the effect of the zinc ions is to reduce cobalt deposition by a double layer effect. According to the double layer theory the zinc cation in an electrolyte such as acidic zinc sulfate can affect the potential at the outer Helmholtz plane as a result of its adsorption. Cation adsorption causes this potential to become positive, increasing the repulsion of a cation like cobalt with resultant lower deposition rates.

The aim with the present investigation was not to further investigate the mechanism of cobalt cementation, but rather to optimize the operation of an existing plant. It is therefore suggested that the function of activators be regarded as that suggested by Nelson et al (2000), i.e. that is to provide a surface on which zinc does not significantly adsorb or upon which the relative rate of cobalt adsorption is higher.

2.3.5 Effects of cobalt concentration on precipitation processes

Zinc dust consumption increases with increasing feed cobalt concentration, as is expected (Fugleberg et al, 1980). A study of the effect of increasing initial cobalt concentration on the initial cobalt cementation rate with antimony activation indicated that the initial cobalt removal rate was independent of the initial cobalt concentration (Dreher et al, 2001) confirming that the same kinetic model applied for all their tests. Comparative results for arsenic were not found in the literature.

2.3.6 Effects of zinc dust properties and addition rate on precipitation processes

Cementation processes involve the galvanic coupling of anodic and cathodic reactions occurring on sites on the sacrificial metal (Yamashita et al, 1989; 1997). The nature of the deposited metal and the sustenance of conditions favourable to the precipitation of the impurities are likely to be influenced by the nature and dosage rate of the metal used. It is proposed that an optimum zinc dust dosing configuration exists in terms of dosage distribution, concentration and size distribution for the precipitation of cobalt from the zinc sulfate solutions. A large zinc dust surface area concentration (m^2/L) either through high zinc dust loading or fine zinc dust, i.e. with a higher surface area per mass, leads to an increase in the cobalt cementation rate (Van der Pas and Dreisinger, 1996). Fine zinc dust gives the greatest surface area per mass of zinc, but is more difficult to produce and a higher degree of prior oxidation loss per mass is likely (Sinclair, 2005).

In practice it is found that copper and cadmium removal is more efficient with a coarser zinc dust than that typically used for cobalt. Bøckman and Østvold (2000) reported that cobalt was prone to redissolution when using fine zinc dust (< 36µm),

while larger zinc particles showed no cobalt redissolution. This is related to redissolution of basic cobalt hydroxide ($Co(OH)_2$) which formed under localized conditions of higher pH during hydrogen evolution. The driving force for hydrogen evolution, and thus the higher surface pH, disappears when the fine zinc dust cores are consumed, leading to redissolution of formed $Co(OH)_2$ to again increase the cobalt in solution.

Coarse zinc dust is usually in the range 100 µm to 200 µm, while fine zinc dust can range from 15 µm to 40 µm (Sinclair, 2005). A quoted average zinc dust particle size used in industry for cobalt removal is between 50 µm and 75 µm with a surface area of 1.74 m^2/gram (Nelson et al, 2000; Dreher et al, 2001). Elsewhere, wet atomized zinc dust with particle size between 74 µm and 105 µm was used (Van der Pas and Dreisinger, 1996).

The opportunity for redissolution of precipitated cobalt decreases with increasing zinc dust concentration (Bøckman and Østvold, 2000). Reducing conditions improve as is indicated by a decrease in the reducing potential (more negative mixed potential) associated with an increased zinc dust concentration. The rate of the cobalt cementation reaction increases due to the related increase in reaction surface area, as is indicated by the increase in magnitude of the apparent rate constant.

A limit exists to the benefit derived from increasing the zinc dust addition rate (Singh, 1994). A maximum zinc dust concentration exists, beyond which the cobalt removal rate decreases again, even though the reducing potential continues to improve by becoming more negative as the zinc dust concentration increases. Cobalt is known as a good catalyst for the hydrogen evolution reaction. The observed decrease in the cobalt precipitation rate above a certain zinc dust concentration was subsequently attributed to hydrogen evolution (Fugleberg et al, 1993), which progressively consumes a greater fraction of the current at the expense of the cobalt precipitation reaction.

Dreher et al (2001) reported that the initial rate constant increased with increasing zinc dust surface area up until a peak value, where after a plateau was observed. This peak value was approximately 6 m^2/L or 3.5 g/L zinc dust in tests with antimony

trioxide. It was proposed that the cobalt removal rate initially depended upon establishment of active sites on the zinc dust surface area. An optimum number of active sites existed for the available zinc dust surface area and activator concentration beyond which no further increases in the cobalt removal rate were observed. This was attributed to hydrogen evolution.

Significant co-precipitation of cadmium occurs in the cobalt section when a high stoichiometric excess of zinc dust is added (Heukelman, 2006; Fugleberg et al, 1980). Fugleberg et al (1984) reported that co-precipitation of cadmium decreased after optimisation and reduction of zinc dust addition in the cobalt removal circuit, due to increased selectivity of the cobalt circuit. This will invariably increase the loading on and sensitivity of the cadmium circuit.

For economic reasons the zinc dust concentration should be minimized. However, a certain excess of zinc dust is required to maintain a sufficiently reducing environment to prevent the redissolution of the precipitated cobalt. This is related to maintaining a sufficient ratio of cobalt precipitation sites (reduction surface area) compared to zinc dissolution sites (oxidation surface area). This excess zinc dust is required to counter kinetic limitations and the degree of excess required to sustain cobalt deposition is determined by parameters such as particle size distribution or available reaction surface area. Consequently redissolution of deposited cobalt will occur when the zinc dust concentration decreases below a certain critical level.

A lower zinc dust concentration will also lead to a decrease in the number of areas with localized high pH, normally associated with hydrogen ion consumption or hydrogen evolution, due to maintenance of a more positive mixed potential where hydrogen evolution occurs at a lower rate (Fugleberg et al, 1980). As a result the precipitation of easily redissolvable basic metal salts will decrease, ensuring better overall performance of the purification circuit.

2.3.7 Effects of copper on precipitation processes

Precipitation of cobalt by cementation on zinc is catalyzed by the presence of precipitated elemental copper (Näsi, 2003; Yamashita et al, 1997; Tozawa et al,

1992; Fugleberg et al, 1980), as well as by the precipitated copper arsenide (Fugleberg et al, 1976). Reports that dissolution of cobalt occurs without the added presence of arsenic suggest that although elemental copper may be instrumental in catalyzing cobalt precipitation, it does not prevent redissolution of cobalt, whereas copper arsenide does (Yamashita et al, 1997).

It was observed that copper precipitates first, followed by precipitation of cobalt (Ohgai et al, 1998), giving support to the notion that copper aids in the cobalt precipitation process by providing additional reaction surface area with low cobalt deposition overpotential on the surface of the zinc dust (Yamashita et al, 1997). It is suggested that reactive reaction surface, which is not covered with deposits of basic zinc sulfate and zinc hydroxide is provided through continuous replenishment with new copper precipitate. It is assumed that any new surface will not have an opportunity to passivate by deposition of basic zinc sulfate due to more favourable reaction kinetics, because arsenic and cobalt precipitates faster than the rate at which basic zinc sulfate forms or the rate at which zinc hydroxide is adsorbed onto the newly formed copper and Cu_3As surfaces.

According to Yamashita et al (1997) copper enhances the hydrogen evolution reaction such that the mixed potential becomes more positive and such that the precipitation of cobalt arsenide rather than cobalt occurs. Consequently, the catalyzing effect of copper leads to a reduction in the required zinc dust concentration compared to conditions where none or insufficient copper is available.

From descriptions of early investigations and of older zinc refining processes it is clear that copper concentrations of up to 400 mg/L was deemed necessary for sufficient catalysis of cobalt cementation. Fugleberg et al (1993) showed that the requirement for new copper may be reduced with circulation of cobalt cement and the required copper concentration could be reduced to 50 mg/L. Additional copper led only to a marginal improvement in the cobalt removal rate.

The cobalt deposition rate increases with increasing copper concentration as indicated by Figure 6 (Tozawa et al, 1992).

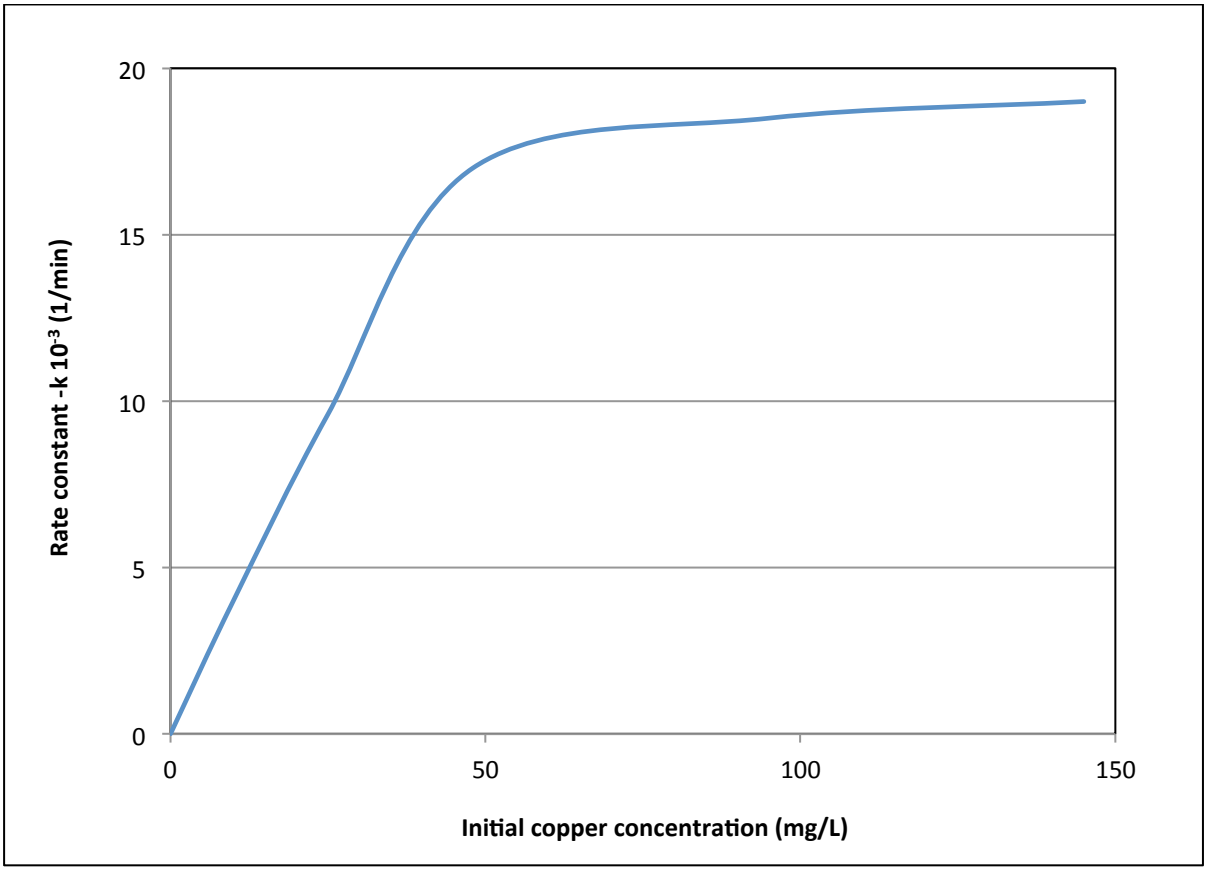

Figure 6: Cobalt cementation rate constant as a function of initial copper concentration with pH 3.3, temperature 90 °C, initial concentrations (g/L) of Zn: 150, Co: 0.01, As: 0.01 (after Tozawa et al, 1992).

The rate at which the cobalt cementation rate constant increases, is reduced however, above a certain copper concentration. The transition from a high rate of increase to a low rate of increase occurring at 50 mg/L is quite abrupt and may be related to having reached the maximum number of active sites proposed by Dreher et al (2001). It is suggested that the observed reduction in the rate of increasing cobalt rate constant is determined by a fixed and finite arsenic concentration determining the copper concentration, above which the deposition of copper is favoured above that of Cu_3As. It is suggested that not enough arsenic was available to sustain the reaction with the increasing copper concentration. This illustrates the importance of arsenic as activator with copper to sustain cobalt deposition and to prevent redissolution of precipitated cobalt.

The cobalt precipitate may be heavily contaminated with copper, as a result of high copper feed concentrations. An economic incentive exists to minimize the requirement for copper in the feed to the cobalt removal circuit, and to remove the bulk of the copper as a clean copper product in the copper removal circuit for further refining. These tests were conducted with a fixed arsenic concentration, suggesting that the increase in the number of active sites (Cu_3As deposition sites) is finite and a function of copper concentration, arsenic concentration and available zinc dust surface area. Deposition of elemental copper will continue once arsenic has been depleted. The cobalt deposition rate increases quickly with sufficient copper and arsenic in solution until a maximum number of reaction sites have been established for the available zinc surface area and available arsenic in solution.

A rather abrupt change in the reaction kinetics is noticeable after approximately 100 minutes of the test had passed, as indicated in Figure 7, with the rate constant decreasing from 0.018 per minute to 0.0013 per minute. It is suggested that the decrease in the rate constant as indicated by the decrease in slope in the second rate regime was not caused by passivation of the zinc dust surface, due to the low pH (3.3) at which the test was conducted and the observed continuation in the decrease of the bulk cobalt concentration. The changeover point from one rate limiting regime to the other appears to be related to the cobalt concentration as well as to the catalytic reaction surface area created by cemented copper.

It follows from the above and previous discussion that although finer zinc powder will favour precipitation by providing a larger surface area per mass of zinc, it is critical that the right balance between the anodic and cathodic sites favourable for cobalt precipitation, but not hydrogen ion reduction, is achieved. A larger surface area favourable for cobalt precipitation may reduce the specific rate of cobalt precipitation i.e. the rate per area, such that cobalt precipitation will not become mass transfer controlled.

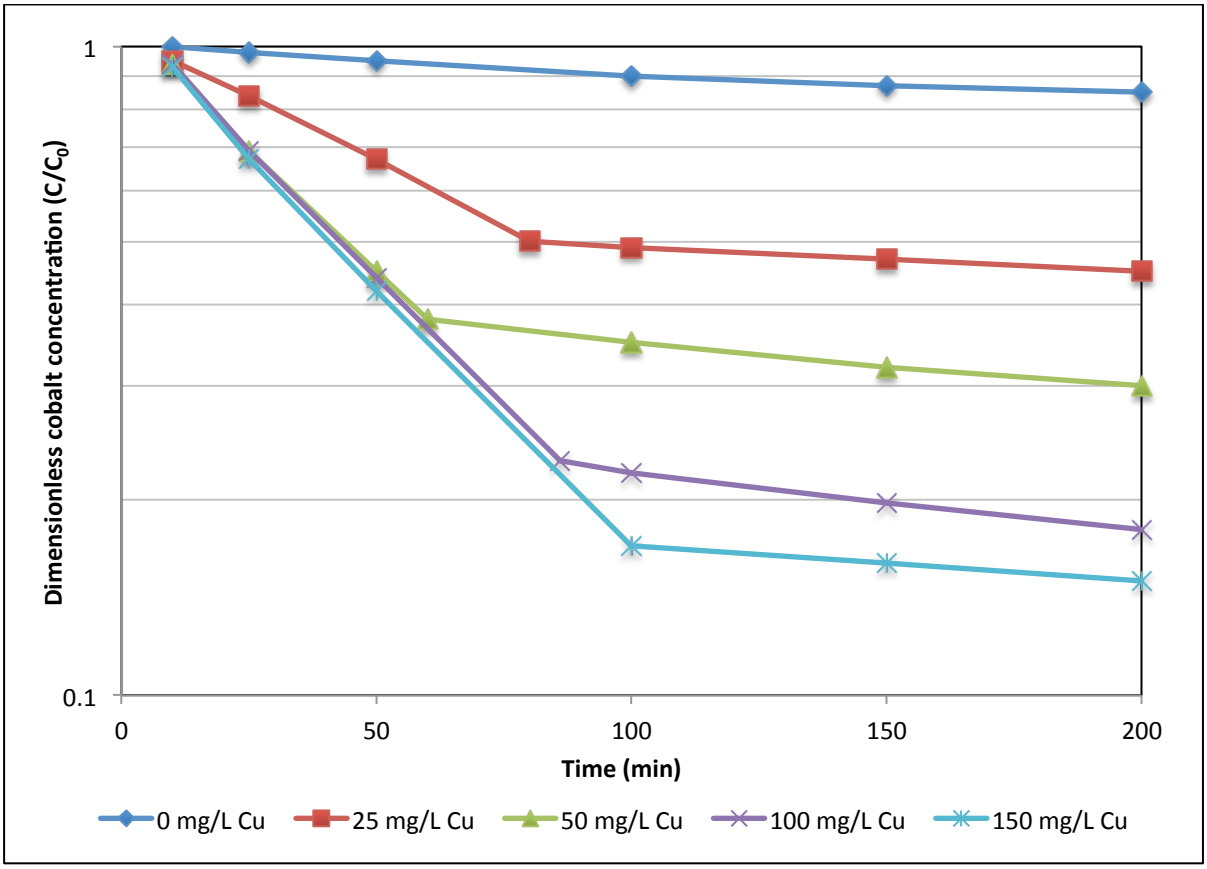

Figure 7: Dimensionless cobalt concentration as a function of time and initial copper concentration with pH 3.3, temperature 90 °C, initial concentrations (g/L) of Zn: 150, Co: 0.01, As: 0.02 (after Tozawa et al, 1992).

2.3.8 Effects of arsenic on precipitation processes

Arsenic, generally taken to be in the form As_2O_3 (arsenic trioxide) when received as pellets, is used as activator for cobalt cementation together with copper. It had been suggested by some (Lawson and Nahn, 1982) that arsenic hydrolyses to the form $HAsO_2$ during the basic leaching process used in preparation of the arsenic rich solution normally added to the cobalt precipitation reactors. This is also the stable form as predicted by the Pourbaix diagram for the As-H_2O system (Figure 2) for the pH and potential conditions normally associated with the purification process. The precipitation chemistry that follows in both cases is the same, with the oxidation state of the arsenic remaining 3+. However, solubilized arsenic increases the efficiency of

the reactions, due to the instant availability of the trivalent arsenic ion in solution (Yamashita et al, 1997).

The cobalt removal rate increases with increasing arsenic concentration, but only when used simultaneously with copper (Tozawa et al, 1992) and only to a certain optimum arsenic concentration (Lawson and Nahn, 1981). Yamashita et al (1997) observed that an excess concentration of arsenic is detrimental to cobalt removal and further reported that arsenic without the presence of copper does not contribute actively towards cobalt deposition. Arsenic added in the concentration determined by the stoichiometric requirement of the relevant chemical reactions is sufficient for effective removal of cobalt and an excess of arsenic is not required. Appendix B on the calculation of the zinc dust dosage provides a detailed account of the stoichiometric requirements and the relevant electrochemical reactions.

Fugleberg and Rastas (1976) determined that arsenic first reacts with copper to form a catalyzing surface (Cu_3As) upon which both cobalt and nickel are deposited as arsenides. This is discussed in more detail in Section 2.3.7 on the effects of copper on precipitation. It appears that complexing of cobalt with arsenic leads to a more stable precipitate. Arsenic affords the opportunity to precipitate cobalt in a stable form at lower pH, thereby decreasing the risk of precipitating cobalt together with a basic zinc sulfate.

It is reported that use of arsenic only, without copper, also increases formation of basic zinc sulfate (Tozawa et al, 1992). This is likely to be caused by localized increases in pH as hydrogen is consumed in reaction between arsenic and zinc dust by the following half cell reaction proposed by Yamashita et al (1997):

$$HAsO_2(aq) + 3H^+ + 3e = As^0 + 2H_2O \quad \ldots\ldots (46)$$

The reversible half cell potential of reaction 46 is +247 mV(SHE) and the thermodynamic driving force for deposition of elemental arsenic in the reaction with zinc is therefore almost as high as that of copper (E^0 = +337 mV(SHE)).

Arsenic reacts with nascent hydrogen to form arsine gas (H_3As), which is why antimony is preferred as activator, even though arsenic is a more efficient activator when used with copper (Tozawa et al, 1992). This gas is lethal and the process should be designed and operated such that arsine is not formed and if formed is properly contained or diluted.

2.3.9 Effects of cadmium on precipitation processes

Cadmium is regarded as an important activator, which enhances the cobalt removal efficiency. Complete removal of cadmium may be detrimental to the cobalt removal efficiency in zinc refineries where cadmium is precipitated before cobalt (Yang et al, 2006). In processes where cadmium is removed after cobalt the cadmium precipitation circuit is sometimes referred to as the cadmium scavenger circuit, because a large fraction of cadmium co-precipitates with cobalt in the preceding cobalt precipitation circuit due to the large stoichiometric excess of zinc dust being added (Fugleberg et al, 1980). It was observed in the Zincor process that precipitated cadmium redissolves readily in the subsequent pressure filtration step, where the CoAs precipitate is removed from the partially purified zinc sulfate solution, leaving the cadmium concentration in the feed to the cadmium scavenger circuit almost as high as in the feed to the cobalt circuit. An increase of up to 400% had been recorded at Zincor, i.e. from 50 mg/L up to a 200 mg/L in one case.

The cobalt precipitation rate constant was found to be dependent on specific ranges of cadmium present in the solution. Yang et al (2006) found that the rate and extent of cobalt removal is inhibited when cobalt cementation is done in the presence of more than 400 mg/L cadmium in solution as indicated in Figure 8. Nelson et al (2000) reported that cadmium impacted negatively on cobalt removal efficiency above 100 mg/L. This observed limit to the positive effects of cadmium was attributed to competitive adsorption, where a very large concentration of one reactant causes the other reactants (antimony, copper) to desorb with detrimental effects on cobalt removal efficiency (Dreher et al, 2000).

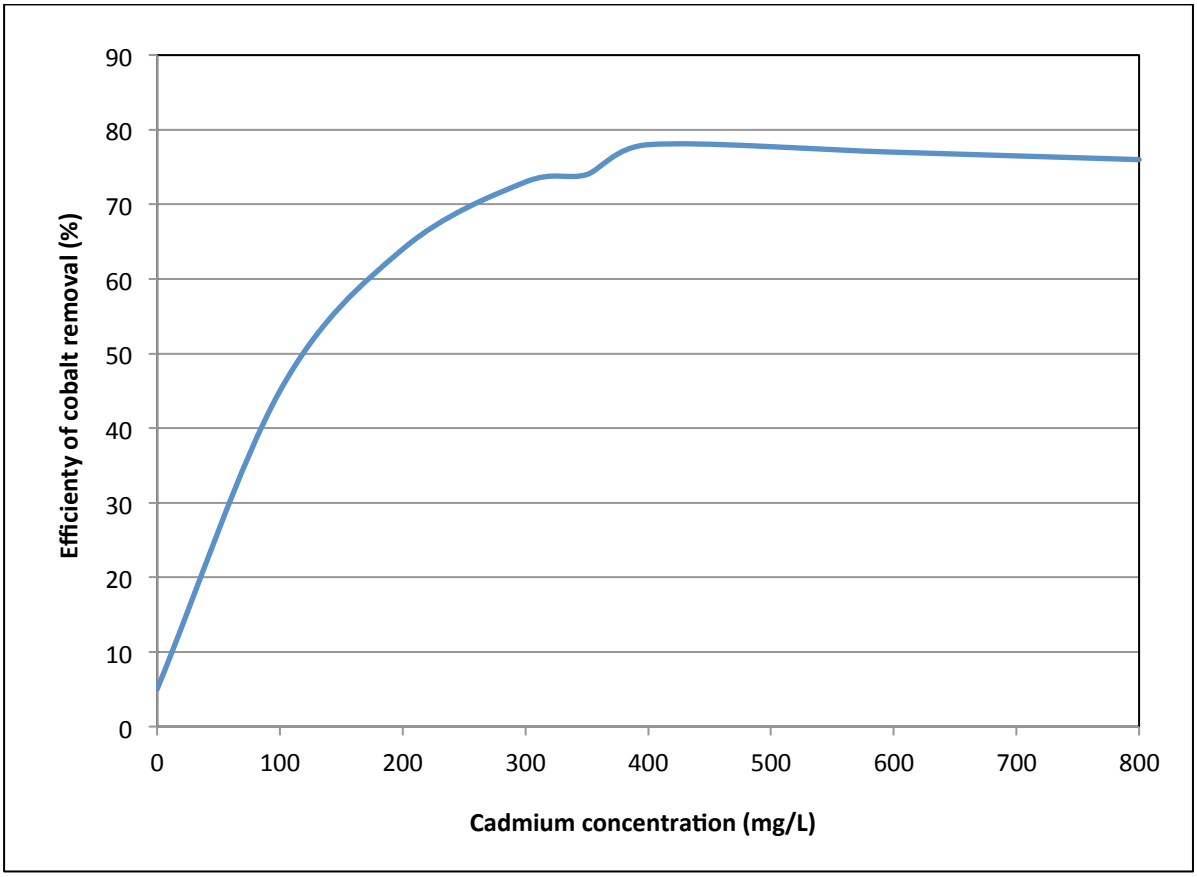

Figure 8: Efficiency of cobalt removal as a function of cadmium concentration with pH 4, temperature 90 °C, initial concentrations (g/L) of Zn: 140, cobalt not specified (after Yang et al, 2006).

During tests with and without copper, but without other activators like antimony or arsenic, it was found that the presence of cadmium inhibits the formation of basic zinc sulfate (Yang et al, 2006). It is assumed that the role of cadmium would be similar in the presence of other activators following on a suggestion by Nelson et al (2000) that cadmium may favour cobalt deposition by forming a dendritic deposit, which increases the reaction surface area in the same manner as copper. The best results were obtained when cadmium was present in combination with copper.

2.3.10 Effects of recirculated cobalt precipitate on precipitation processes

The solids resulting from cobalt precipitation typically contains residual elemental zinc, elemental copper and the arsenides of the precipitated activators and of cobalt and is typically described as 'cobalt precipitate' or 'cobalt cement' although it is of course not pure. This precipitate may galvanically interact with added zinc powder to significantly accelerate the precipitation of cobalt if it is for instance recirculated to a precipitation stage (Fugleberg et al, 1976; Singh, 1996). The zinc dust consumption could in this way be reduced significantly, i.e. from 5% to 2% of cathode zinc (Fugleberg et al, 1993). A further advantage of recirculating cobalt precipitate is that unwanted increases in pH and thus the propensity for basic zinc sulfate precipitation is also reduced (Fugleberg et al, 1980). In addition the requirement for new copper was also decreased considerably. Copper should however not be removed from solution completely as the renewal of the catalytic surface is required continuously (Näsi, 2004).

The advantage of this process is that a large proportion of copper in the feed to the purification circuit can be cemented out as relatively pure copper cement, which is suitable for re-leaching and electrowinning or as feed to a copper smelter. The cobalt cement produced in this way also contains less zinc. In addition, an effective chloride bleed from the system is provided as chloride precipitates with copper as CuCl in the copper cement section, which further reduces the zinc required. Another recorded advantage of recirculation of cobalt cement is a decrease in the required operating temperature from 90°C to between 70°C and 75° due to the increase in reaction surface area and the lowering of kinetic constraints (Fugleberg et al, 1980). The most effective concentration of recirculated cement was reported to be in the range 30 g/L to 50 g/L solution (Fugleberg et al, 1993).

The mechanism through which cobalt removal kinetics is improved is through an increase in the available cobalt deposition sites by the extra reaction surface area created by Cu_3As, arsenic, copper and cadmium precipitates on the zinc dust surface.

2.3.11 Effects of pH on precipitation processes

Solution pH is a critical parameter in determining the nature and stability of cementation reaction products from a thermodynamic perspective. In addition the pH influences side reactions, which has direct bearing on reaction kinetics and cobalt removal efficiency. Cobalt removal efficiency improves with increasing pH (Nelson et al, 2000; Bøckman and Østvold, 2000; Van der Pas and Dreisinger, 1996). The pH rises during cobalt cementation mainly due to consumption of hydronium ions by the hydrogen evolution reaction. The increase in cobalt removal efficiency was attributed to the resultant decrease in the number of protons competing for reaction sites on the zinc dust surface (Nelson et al, 2000). However, a too high pH will lead to the formation of zinc hydroxide and basic zinc sulfate, which has a detrimental impact on the filtration process following cementation in addition to passivating the zinc dust surface, as discussed previously.

The presence of basic zinc sulfate is recognizable being a white precipitate, which forms a telltale milky, white suspension in the impure zinc sulfate solution. De Blander and Winand, referred to by Xiong and Richie (1988), identified the substances forming in the zinc dust surface at pH 5.4 and in the absence of activators as a mixture of basic salts, namely $ZnSO_4.3Zn(OH)_2.4H_2O$ and $ZnSO_4.6Zn(OH)_2$. Yang et al (2006) confirmed the presence of a covering layer of basic zinc sulfate on the precipitate at higher pH values using image analyses with energy dispersive spectroscopy.

Nelson et al (2000) reported that the pH will stabilize and become self-regulating, if left uncontrolled, as is displayed in Figure 9. They also reported that the zinc dust surface does not become passivated with basic zinc sulfate until after cementation was completed. The observed transition from variable pH to stable pH corresponds with an apparent transition from a period where cobalt is obviously being precipitated during the first 30 to 40 minutes to a period thereafter where no cobalt appears to be precipitated at all. It is suggested that apparent stabilization of pH was more likely the result of zinc dust surface passivation, as more than 0.6 mg/L of cobalt still remains in solution, even though the zinc dust concentration was high to start with.

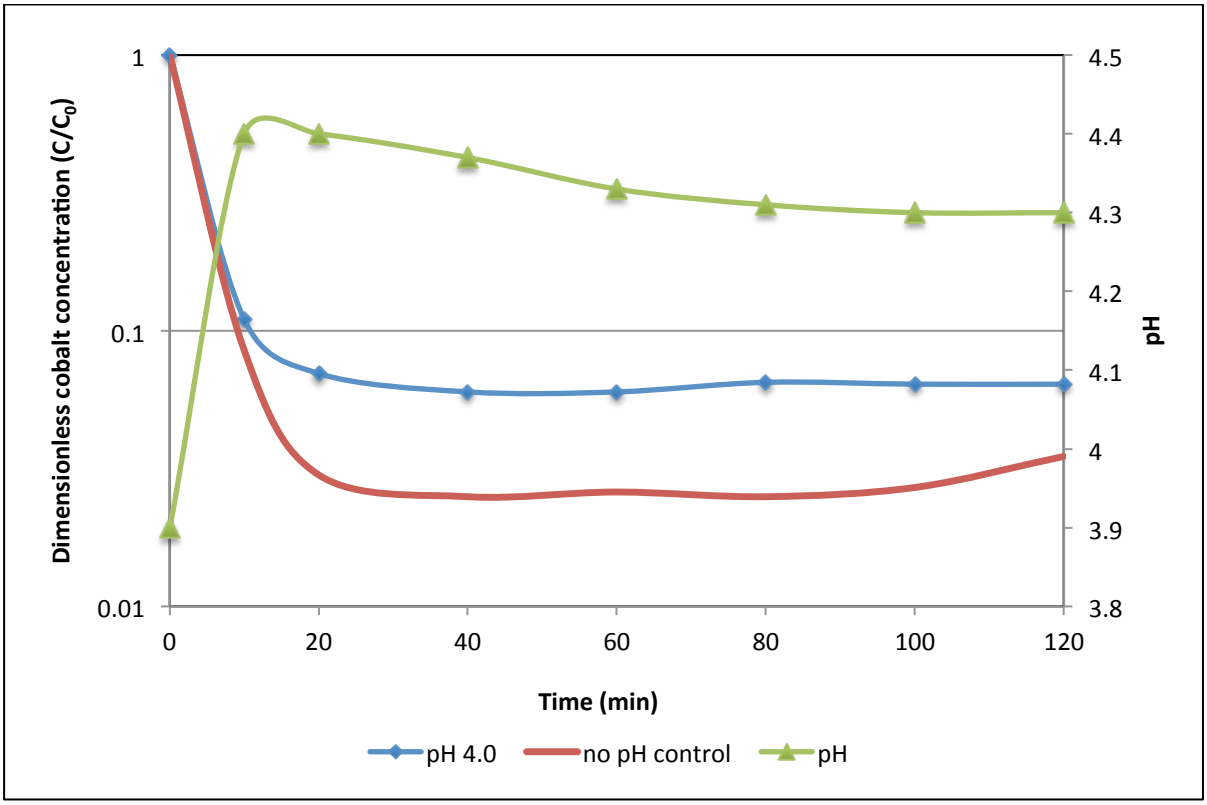

Figure 9: Dimensionless cobalt concentration and pH as a function of time for cobalt cementation on zinc with temperature 95°C, initial concentrations (g/L) of Zn dust: 5, $ZnSO_4$: 150, Co: 0.01, Cu: 0.03, Sb: 0.002 (after Nelson et al, 2000).

Conversely, a too low pH impacts negatively on cobalt cementation. Adsorption of hydronium ions at lower pH (<4) inhibits cobalt deposition by reducing the available reaction surface area for cobalt (Xiong & Richie, 1988). Decreasing the pH to too low levels is detrimental because more zinc dust is consumed directly in reaction with hydrogen. In addition the risk of redissolution of precipitated cobalt increases due to the consequent reduced availability of zinc dust. The pH is normally adjusted towards the end of cobalt removal by addition of sulfuric acid in order to remove the basic zinc sulfate.

Various attempts have been made to optimise the pH at which cobalt removal should be done. Tozawa et al (1992) suggested in tests with antimony that the maximum cobalt removal rate is achieved at a pH of between 3.30 and 3.75. Raghavan et al (1999) suggested that the optimum pH range is between 4 and 5 with values greater than 5 leading to formation of basic zinc sulfate and also that a lower final cobalt

concentration could be achieved with a feed solution pH of 4.5 compared to a feed solution pH of 5. Yamashita et al (1997) reported a decrease in the rate of cobalt removal at pH 3.3 with dissolution of already precipitated cobalt at lower pH.

Cobalt is also removed by forming easily dissolvable cobalt salts under localized basic conditions. Localized conditions of high pH are created close to the surface of metallic zinc due to hydrogen ion depletion, which is caused by hydrogen evolution (Bøckman & Østvold, 2000). These basic deposits ($Co(OH)_2$) are not very stable and a slight decrease in pH will lead to dissolution of the precipitated cobalt salt, usually also when metallic zinc had been depleted.

2.3.12 Effects of oxygen on precipitation processes

Exposure to oxygen (in solution) increases the risk of oxidation and redissolution of cemented cobalt, copper and cadmium (Fugleberg et al, 1984; Lawson and Nahn, 1981). Oxygen reduction at the zinc surface or more likely at the metal-arsenic surfaces would increase the consumption of zinc and possibly enhance redissolution of cobalt by completely consuming the zinc. Conducting cobalt deposition in an inert nitrogen atmosphere had been suggested to improve cobalt removal kinetics.

Xiong and Richie (1988) conducted cobalt deposition tests in the presence of air as well as in a de-aerated environment. They found that interfacial capacitance of the zinc dust surface increased rapidly in the presence of air, suggesting that a build-up of oxygen on the surface of the zinc may lead to passivation of the zinc dust surface and a less conducting interface.

The surface of zinc metal passivates when exposed to an atmosphere of air and moisture. Zinc oxide forms in the absence of moisture and zinc hydroxide forms in the presence of air and moisture. It is assumed that this oxidized layer dissolves readily when exposed to the post leach zinc sulfate solution. Schweitzer (1999), as quoted by Ahmad (2006), suggested that long term atmospheric exposure of zinc leads to formation of hydrozincate ($Zn_5(OH)_6(CO_3)_2$) due to the reaction of zinc hydroxide with carbon dioxide in the atmosphere, which dissolves readily in strong

acids only. This could be a contributing factor in the observed slow initial cobalt precipitation rate.

2.4 Deposition morphology and deposition mechanism

Various mechanisms have been proposed for cobalt precipitation with arsenic trioxide as activator in the presence of copper. Cobalt removal occurs through deposition of intermetallic compounds on the zinc dust surface, which can reduce the cobalt deposition overpotential or provide active sites with lower overpotentials for cobalt deposition (Sinclair, 2005). Active sites are established by the adsorptive action of the activators and for a given concentration of activator there are a maximum number of active sites, which can be formed (Dreher et al, 2001). As soon as this number is reached, further increases in zinc dust concentration (surface area) result in no further increase in the rate of cobalt removal. It was suggested that the cobalt removal rate initially depended on the zinc dust concentration (surface area more specifically) due to the formation of these active sites. A higher zinc dust surface area should therefore lead to an increase in the cobalt removal rate. The reactions are coupled and the slowest reaction would be overall rate determining.

Tozawa et al (1992) concluded from a study of the Pourbaix diagram for the Co-As-SO_4 system that the intermetallic compounds were cobalt arsenide (CoAs). The Pourbaix diagram was constructed from standard free energy data obtained from the NBS tables of chemical thermodynamic properties compiled by Wagman et al (1982) for compounds and ionic species of arsenic and from data compiled by Kubaschewski et al (1979) and Barin et al (1977) for metal arsenides. Subsequent observations with a scanning electron microscope and measurement of characteristic X-ray images confirmed the presence of CoAs. They also found that cobalt, arsenic and copper were deposited on the same sites.

Metallic copper and Cu_3As could be identified with analyses of the cobalt cementation residue by X-ray diffraction, but not cobalt compounds (Fugleberg et al, 1980). Through further investigation of the residue with energy dispersive spectroscopy it was established that cobalt was not significantly mixed with copper compounds, but formed as separate compounds with arsenic, namely CoAs, that

was substantially copper free. As cobalt could only be precipitated at acceptable rates in the presence of both arsenic and copper, it was concluded was that Cu_3As formed first, thereby creating a substrate for cementation of CoAs. Ohgai et al (1998) concluded that copper precipitates first, followed by precipitation of cobalt, suggesting that both elemental copper and copper arsenide enhances cobalt cementation through the contribution of their respective surface areas.

Precipitation of cobalt with only arsenic as activator and with no copper at all in the solution is possible, but occurs at an unacceptable rate (Fugleberg et al, 1993). Copper in solution could be substituted partially by recycling of cobalt cement without detriment to the cobalt removal efficiency. However, the rate of cobalt removal decreased over time and reactivation of aged cobalt cement with fresh copper was necessary to replenish the supply of new Cu_3As (Näsi, 2004). Näsi (2004) also reported that cobalt deposition proceeds more slowly than copper and arsenic in support of the suggestion that deposited copper provides a nucleation site for cobalt deposition.

2.5 Review of testwork practices

Most tests, upon which published results are based, were conducted with batch reactors with either zinc dust (Fugleberg et al, 1993; Näsi, 2004) or a rotating zinc disc (Tozawa et al, 1992). Näsi (2004) used a purpose-built pilot plant with small reactors in series with a pilot thickener operating in parallel with which to concentrate and circulate cobalt precipitate back into the first reactor. Stock impure solution samples were either drawn from the plant or prepared by dissolving impurities in a purified zinc sulfate solution.

Not much information is shared in the literature with regard to the way in which zinc dust is added in the various tests. Fugleberg et al (1993) added zinc dust at a constant rate until a preset mixed potential has developed which was then used to control further additions of zinc. Some time passed before a sufficiently negative (reducing) mixed potential developed during batch cementation tests, and was attributed to the period required to establish active reducing sites for cobalt deposition, i.e. initial precipitation of Cu_3As and elemental copper followed by cobalt

precipitation as CoAs (Fugleberg et al, 1993). The target mixed potential at the Zincor Zinc Refinery in Springs, South Africa, is -680 mV SHE. A value of between -550 and -650 mV SHE is usually attained, depending on operating conditions.

Of interest though is the rate at which the cobalt concentration decreases with time. Samples of fixed volume were typically drawn from the test solution at regular intervals for determining of diminishing cobalt concentration (Ohgai et al, 1998; Dreher et al, 2001). Cobalt concentration is typically determined with colorimetric analyses using nitroso-R salt (Fugleberg et al, 1993).

Some investigators controlled the pH during experiments (Tozawa et al, 1992; Yamashita et al, 1997; Dreher et al, 2001; Yang et al, 2006). This could be done when the experimental setup was sophisticated enough to enable such control. An operating pH of between 4 and 4.5 appears to be used frequently and adjustments down to pH 3.5 have been made. Others conducted tests with a solution pH resembling a specific industry standard and elected to rather monitor the pH as each test progresses, but not to intervene with any pH adjustment (Bøckman and Østvold, 2000; Lawson and Nahn, 1981; Ohgai et al, 1998; Yamashita et al, 1989). Raghavan et al (1999) made a final adjustment to a lower pH at the end of each experiment to presumably dissolve precipitated zinc salts. The cobalt removal section in the Zincor Zinc Refinery in Springs, South Africa, which served as comparative basis for this study, receives an impure solution from the preceding neutral leach section with a pH of 5.1 to 5.3. Cementation of cobalt runs its course without pH control, but the solution pH is adjusted down to pH 4.66 with spent electrolyte in the final cementation reactor to dissolve any basic zinc sulfate that may have formed, which would otherwise interfere with the filtration step that follows. The value of 4.66 is an arbitrary value, which was selected based on past experience that appears to satisfy the need for efficient filtration without redissolution of precipitated cobalt.

2.5.1 Determining the apparent rate constant

Some effort has gone into extracting kinetic data for the Kokkola process from the literature, due to similarities with the Zincor process. It is therefore assumed that the published data could provide a baseline in terms of the performance that could be

aspired to. In addition, comparative kinetic data for the hot arsenic process are not readily available in literature.

Fugleberg et al (1993) plotted the logarithms of decreasing cobalt concentrations against time during batch cementation tests and the linear parts were used to determine kinetic rate constants. A description of the procedure followed to extract kinetic data from the plots is provided in Appendix A.

The rate constants derived by Fugleberg et al (1993) for cobalt removal at various temperatures are displayed in Table 4. Only a few other comparative apparent rate constants could be found for the hot arsenic process in the literature and these too are displayed.

Table 4: Comparative apparent rate constants for the hot arsenic process.

Temperature	**Fugleberg et al (1993)**	**Tozawa et al (1992)**	**Yamashita et al (1997)**
(°C)	k (per minute)	k (per minute)	k (per minute)
45			0.010
50	0.016		
60	0.035		0.019
70	0.072		0.021
80	0.140		
90		0.018	

Test conditions for rate constant are displayed in Table 5 Fugleberg et al (1993) determined the apparent rate constant under optimised conditions with circulation of cobalt seed to increase the catalytic surface area.

Table 5: Comparative test conditions for determining cobalt cementation rate constants in a zinc sulfate solution.

Parameter	Unit	Fugleberg et al (1993)	Tozawa et al (1992)	Yamashita et al (1997)
Test type		Batch reactor	Rotating zinc disc	Galvanic cell (Cu/Zn)
Cobalt seed surface area	m^2/L	750	None	None
Zinc dust	g/L	0.58	None	Solid plate
Zinc in solution	g/L	$140_{(assumed)}$	150	150
Copper in solution	mg/L	50	0 - 150	3300
Cobalt in solution	mg/L	32	10	20
Arsenic in solution	mg/L	Unknown	20	75
pH		Unknown	3.3	3.8

Tozawa et al (1992) used a rotating zinc disc instead of zinc dust and no cobalt seed to determine cobalt cementation kinetics. The relatively low apparent rate constant derived by Tozawa et al (1992) compared to that derived by Fugleberg et al (1993) can be explained by the difference in reaction surface areas involved.

Yamashita et al (1997) used a galvanic cell to determine cobalt deposition kinetics. This cell was separated into two compartments by an anionic membrane with both compartments filled with a zinc sulfate solution. A zinc metal plate in one compartment was then connected externally to a copper metal plate with similar dimensions in the other compartment. The electrolyte in the side with the copper plate contained cobalt and arsenic ions and a high concentration of copper powder in addition. Cobalt deposited onto the copper electrode and onto the copper powder (<150 µm) as a result of the galvanic current created by the Cu/Zn couple. Yamashita et al's apparent rate constants presented in Table 4 was derived from the results of their investigation into the effect of temperature on cobalt removal rate presented in Figure 10.

The apparent rate constants derived by Yamashita et al (1997) were significantly lower than that derived by Fugleberg et al (1993), but still higher than that derived by Tozawa et al (1992). This can be explained in terms of the reaction surface area. Fugleberg et al (1993) maintained the highest cobalt removal rate through provision of a high reaction surface area by circulation of cobalt seed. Tozawa et al (1992) provided the lowest reaction surface area with only a zinc disc for deposition. Yamashita et al (1997) increased the reaction surface area by addition of copper powder. This confirms that elemental copper as well as Cu_3As provides an effective deposition surface for CoAs. Fugleberg et al (1993) further reported that the relationship between the relative rate constant, assumed to be derived from the apparent rate constant, increases with increasing catalytic surface area.

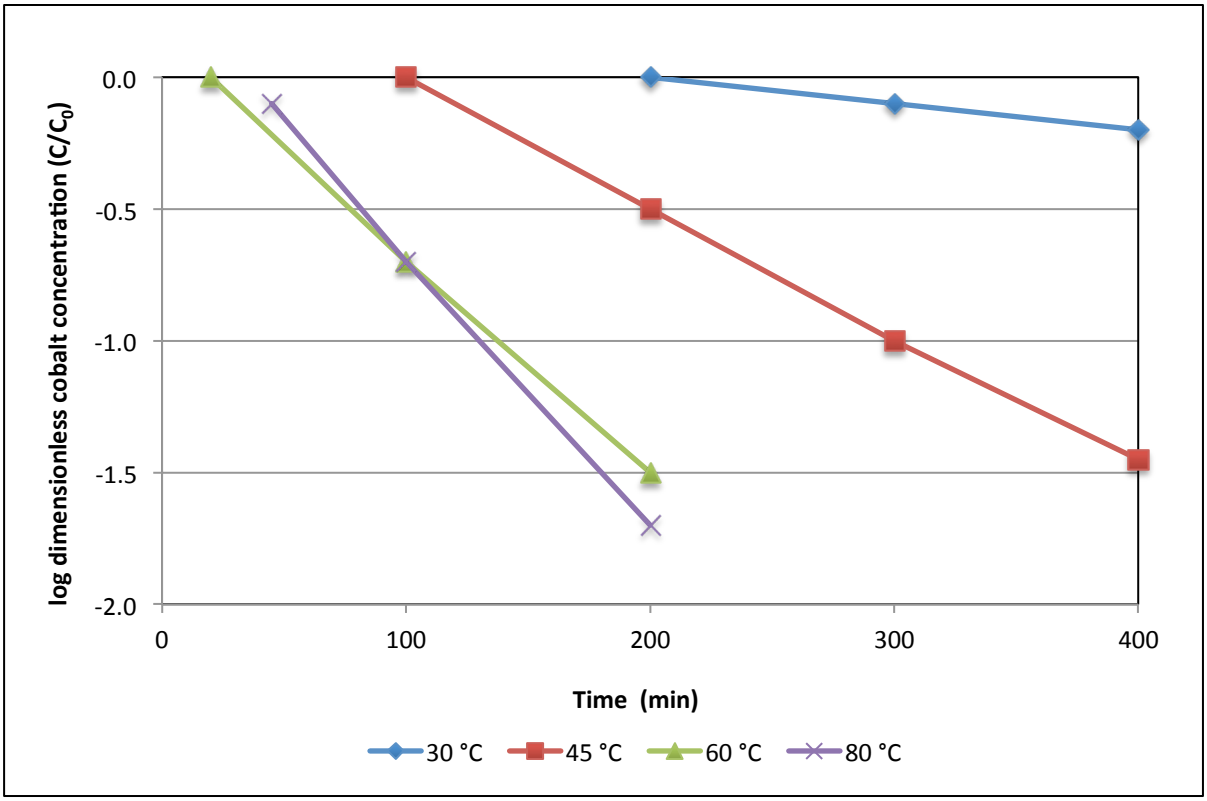

Figure 10: Logarithm of the dimensionless cobalt concentration in an industrial zinc sulfate solution during cobalt cementation on copper in a galvanic cell and in reaction with zinc as a function of time and temperature with pH 3.8, initial concentrations (g/L) of Zn: 150, Co: 0.020, Cu: 3.3, As: 0.100 (after Yamashita et al, 1997).

Maintaining a high enough temperature together with providing sufficient reaction area appears to be the two main drivers by which cobalt removal may be optimised, whilst assuring that sufficient arsenic and copper are available in solution and that the pH is not too high so as to cause precipitation of basic zinc sulfate or too low so as to enhance hydrogen evolution. These will then also be the drivers for producing the most negative or reducing mixed potential.

2.5.2 Determining the activation energy

The apparent activation energy may be calculated from a plot of ln k vs 1/T as was done by Fugleberg et al (1993) and as illustrated in Figure 11, if it is assumed that the temperature dependence of the rate constant can be described by an Arrhenius type relationship.

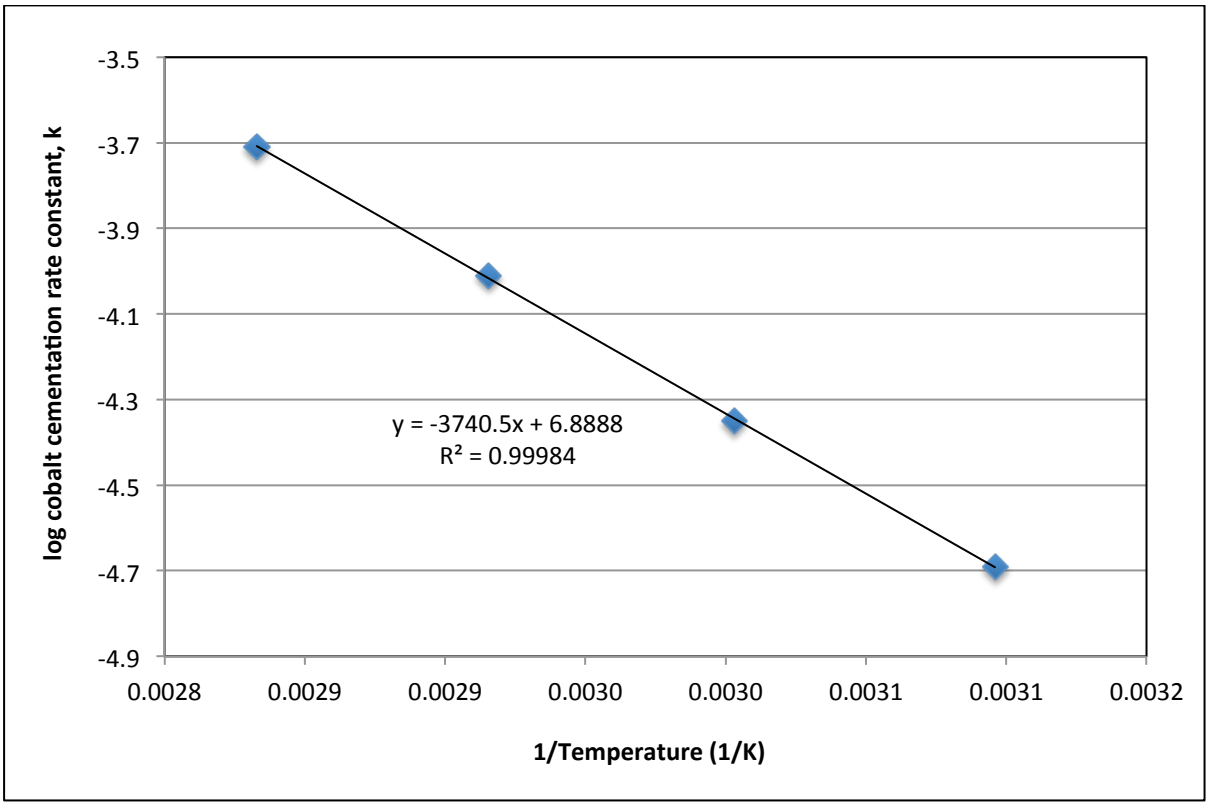

Figure 11: Logarithm of cobalt cementation rate constant as a function of inverse temperature with pH not specified, initial concentrations (g/L) of Zn: 140, Co: 0.032, Cu: 0.05, As: not specified (after Fugleberg et al, 1993).

Comparative activation energies for the rate constant for cobalt cementation are given in Table 6. The rather high values for the activation energy suggest that the cementation process is under activation control rather than mass transfer control.

Table 6: Activation energies for cobalt from acidic zinc sulfate solutions.

Element	Fugleberg et al (1993)	Yamashita et al (1997)	Lawson & Nahn (1981)
	kJ/mol	kJ/mol	kJ/mol
Cobalt	70	72	60[1]

Note 1: Lawson & Nahn (1981) did not use copper as an additional catalyst with arsenic

2.5.3 Summary of analytical techniques

Various analytical techniques are mentioned in literature for identifying and determination of concentrations of the relevant elements. Table 7 provides a summary of analytical techniques used to determine concentrations of elements in solution and in deposits.

Table 7: Comparative analytical techniques used by investigators to determine metal assays.

Element	Method or instrument	Reference
Metal in solution (general)	Thermo Jarrell Ash ICP-MS (Model POEMS II) with detection limit of 0.1 µg/LL	Dreher et al (2001)
	Inductively coupled plasma-atomic emission spectrometer (ICP-AES).	Näsi (2004)
	Atomic Absorption Spectrometry	Van der Pas and Dreisinger (1996)
	Metrohm polarograph High sensitivity DP-MODE-differential pulse voltammetry and separating capacity of 1:50 000	Boyanov et al (2004)

Element	Method or instrument	Reference
Metal deposit (general)	XRF (Al, Fe, Co, Ni, Cu, Zn, Ge, As, Cd, Sb, Si, Ca)	Näsi (2004)
	Scanning Electron Microscopy	Tozawa et al (1992)
Cobalt deposit	Scanning Electron Microscopy and Energy Dispersive Spectrometry	Van der Pas and Dreisinger (1996)
Cobalt in solution	Atomic Absorption Spectrometry	Tozawa et al (1992) Yamashita et al (1997)
	Colorimetric method (nitroso R-salt method)[1]	Raghavan et al (1999) Van der Pas and Dreisinger (1996)
Copper in solution	Atomic Absorption Spectrometry	Tozawa et al (1992) Raghavan et al (1999) Yamashita et al (1997)
Arsenic in solution	Colorimetric procedure	Tozawa et al (1992)
	Hybrid ICP-AES technique	Näsi (2004)
	AsH_3-AgDDC-brucin-chloroform spectrophotometer	Yamashita et al (1997)
Arsine gas	Test paper	Yamashita et al (1997)
Antimony in solution	Atomic Absorption Spectrometry	Tozawa et al (1992)
	Hybrid ICP-AES technique	Näsi (2004)

Element	Method or instrument	Reference
	Inverse voltammetric technique	Raghavan et al (1999)
Cadmium in solution	Atomic Absorption Spectrometry	Raghavan et al (1999)
Nickel in solution	Spectrophotometric method using dimethylglyoxime	Raghavan et al (1999)
Iron deposit	Photometrically at 510 nm wavelength	Näsi (2004)

Note 1: Also the method used at Zincor for determining cobalt concentration

2.5.4 Comparative operating parameters

Published work on the arsenic process in general does not disclose much detail in terms of operating parameters. Table 8 below provides a summary of comparative operating parameter values extracted from the literature for the hot arsenic process for which kinetic data were also available. Operating conditions were compared with that of the cobalt removal process used at the Zincor refinery in South Africa, which was used as the comparative base for all experimental work done in this study.

Table 8: Comparative operating parameters for cobalt precipitation in an acidic zinc sulfate solution (arsenic as activator).

Parameter	Unit	Tozawa et al (1992)	Fugleberg et al (1993)	Zincor (current)
Zinc in solution	g/L	150	140	138 - 146
Cobalt in solution	mg/L	10	31	25 - 30
Cadmium in solution	mg/L	None	400	250 - 350
Copper in solution	mg/L	150	50	650 - 850

Parameter	Unit	Tozawa et al (1992)	Fugleberg et al (1993)	Zincor (current)
Arsenic in solution	mg/L	20	Not available	75
Cobalt removal	%	86	99.5	99.4
Temperature	°C	90	70 - 75	80 - 85
Retention time	min	250	60	320
As:Co	ratio	2 : 1	Not available	2.5 : 1
Zinc dust concentration	g/L	Rotating disc	0.58	4.5
Zinc dust stoichiometry	Times excess	NA	1.5	6.5 - 7.5
Zinc dust PSD	µm	NA	Not available	d_{90} = 330 µm d_{50} =150 µm
Zinc dust surface area	m^2/L	0.0013 (calc)	Not available	0.06
Catalytic surface area (cobalt seed)	m^2/L	None	750	92
Operating pH	pH	3.30 – 3.75	Not disclosed	5.1 – 5.3
pH adjustment	pH	None	Not disclosed	4.55 – 4.65
Mixed potential	mV SHE	Not measured	-600 (controlled)	-600 – (-660)

3. EXPERIMENTAL AND ANALYSES

Experiments to optimise zinc sulfate solution purification at the Zincor refinery were conducted in batch reactors in the on-site laboratory. Zinc dust consumption and corresponding cobalt removal rates were determined for varying operating conditions. In addition the cobalt cementation kinetics was defined in terms of the rate constant and activation energy.

3.1 Experimental procedure

Impure solution taken from the plant was used for all test work. Two impure solution stock samples were taken, an initial sample that was used for most of the test work and a later one, which was used for final optimisation test work. The stock sample compositions were typical for Zincor. The composition of the stock samples are displayed in Table 9 together with concentrations used for equilibrium calculations for Figure 3 and Figure 4.

Table 9: Impure solution properties for the two different stock samples used for testwork.

Composition	Unit	Sample 1	Sample 2	Values used for equilibrium calculations
Cobalt	mg/L	39	18	50
Copper	mg/L	880	422	1000
Cadmium	mg/L	266	380	300
Zinc	g/L	139	135	150
Sulfate[1]	g/L	288	288	300
Acid	mg/L	0.0132	0.0079	
	pH	4.9	5.1	4

Note 1:The exact sulfate concentration was not measured in the stock samples and instead an average concentration of 3M was assumed, based on an average operational value.

The difference in cobalt concentration between the two stock samples is deemed not to have impacted on testwork results as it was found that the initial cobalt removal rate is independent of initial cobalt concentration as indicated in Figure 12 and predicted in Section 2.3.5 on the effects of initial cobalt concentration on cobalt cementation rate.

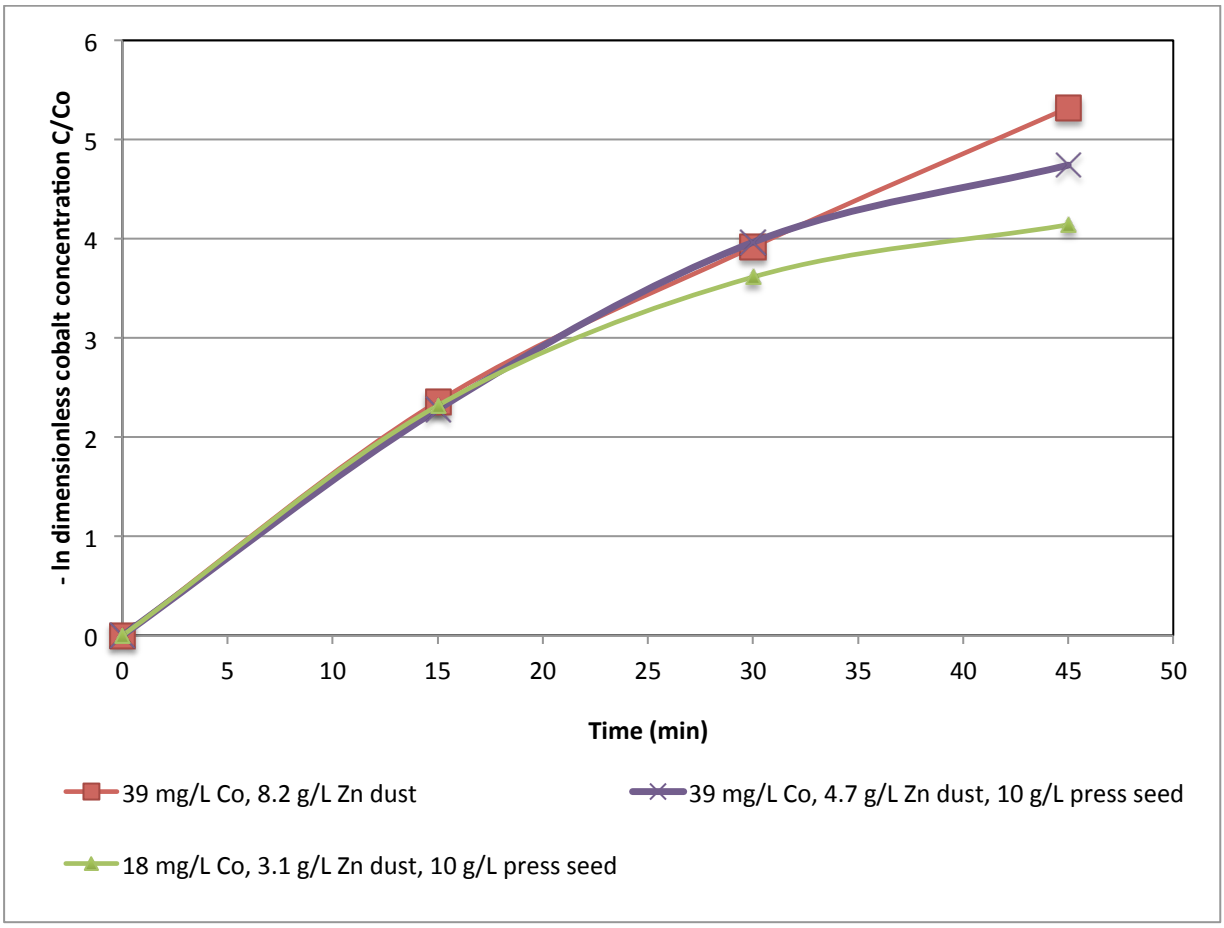

Figure 12: Negative natural log of dimensionless cobalt concentration as a function of time. Initial concentrations of zinc, copper, arsenic and cadmium and pH as per Table 9 for the two stock samples used.

Batch tests were conducted in 5L cylinders in the metallurgical laboratory for all the laboratory-based trials. All tests were conducted in a fume cupboard equipped with an extraction fan to prevent exposure to harmful emissions like arsine and hydrogen. Two tests were always conducted simultaneously and the measurements made during each test were used to verify the integrity of the other.

Impure solution samples were pre-heated to the required temperature on Heidolph 30001 K type hot plates with the temperature controlled automatically through the unit's thermostat throughout each test. Temperature was measured at regular intervals with a portable Knick Portamess pH probe. Solution temperature varied within 1°C above and below the target temperature with variations within 2°C above and below target temperature occurring infrequently.

Mixed potential and pH were measured initially, but attempts to measure these parameters were aborted due to repeated probe failures. It is suspected that the probes failed in regards to measuring pH and the mixed potential due to the high solution temperature, even though they were rated to withstand temperatures of up to 80 °C. No pH control was done during tests.

The measured evaporation rate was 4.3 ml/min at 80°C. An increase in the concentration of all the dissolved species, that presumably did not evaporate, occurred during the experiments, as a result. This change in concentration is assumed to be proportional to the change in solution volume due to evaporation. This should have favoured the cobalt removal rate, as the removal rate is proportional to the concentration at any time. A maximum bias of 11.8% was measured after 105 minutes. Tests at lower temperatures were obviously affected less by evaporation, while tests at 80°C were all affected similarly. The effect of evaporation was quantified for reaction time in indicating the increase in cobalt concentration with time. The effect of evaporation on test results was regarded as insignificant as at least 90% of cobalt is removed after 15 minutes and after an estimated 1.5% change in solution volume and virtually all cobalt (>98%) is removed after 30 minutes after an estimated 3% change in solution volume for tests at 80 °C. No correction factor was therefore applied to any test results. The impure solution in the actual operating plant is subjected to similar evaporation at 80°C, where each reactor is covered to protect operating personnel, and all gasses including evaporated water are discharged into the atmosphere via exhaust stacks with extraction fans.

Table 10: Concentration bias due to evaporation at 80°C

Time	Bias
Time lapsed in minutes	**% Increase in cobalt concentration**
0	0
15	1.5
30	3.0
45	4.6
60	6.3
75	8.0
90	9.9
105	11.8

Reactor content was agitated with VELP Scientifica overhead type stirrers at a rotational speed setting of 6 to keep the solids in suspension without causing cavitation around the impellor. The stirrer's rotational speed was not measured. High activation energies achieved during testwork discussed in Section 4.2 on cobalt precipitation kinetics indicated that agitation rates were sufficiently high so as not to cause mass transfer limitations.

Samples with a volume of 160 ml each were extracted from the reactor every 15 minutes with a calibrated glass beaker until each test was complete. The agitator was kept running throughout each test and it was assumed that the solids to liquid ratio was the same in both the sampling beaker as well as in the reactor. The effects of changes to the reaction surface area concentration in the reactor on cobalt removal rate due to sampling bias, if any, is expected to be insignificant as a maximum of 7 samples were taken for each test with only 3% of the reactor volume removed with the first sample increasing to approximately 4% of the reactor volume removed with the seventh sample due to the decrease of the bulk solution volume in relation to the constant sample volume. All solid particles i.e. unreacted zinc dust with cementation products were removed from the sample solution immediately after taking each sample by filtering through filter paper over glass beakers to ensure that reactions did not proceed further.

Particles on filter paper destined for energy dispersive analyses containing remaining zinc dust with cementation products were allowed to air dry. Each filter paper was folded to preserve the contents once dried and transferred to sample containers for safekeeping.

A stock sample containing 24 g/L of arsenic was taken at the arsenic trioxide plant where As_2O_3 pebbles are leached under alkaline conditions with sodium hydroxide. The required volume of arsenic solution was added when each test was about to start, i.e. once the desired solution temperature was reached and just before adding the zinc dust.

The required amount of dry zinc dust particles was added in a single dose at the beginning of each test. Tests lasted between 90 and 105 minutes. Raw data for all tests are provided in Appendix D.

The required amount of cobalt seed was added to the reactor before the start of those tests requiring cobalt seed, before adding arsenic and zinc dust.

The cobalt concentration of the filtrates was measured with a colorific method using Nitroso-R salt.

Specific surface area of both zinc dust and cobalt seed was measured by gas adsorption on the surface of the solid particles with the BET method.

3.2 Preparation of zinc dust

Zinc dust for all test work was taken from a zinc dust feeder in the cobalt section at Zincor's purification plant. Zincor manufactures zinc dust for own consumption. The zinc dust used was unaltered, as received from the manufacturing facility and as used in the plant to determine the apparent rate constant for the current, un-optimised operation (base case). A typical particle size distribution is presented in Table 11.

Table 11: Particle size distribution for standard Zincor zinc dust.

Screen size (µm)	% Passing	Standard deviation
500	98	0.2
300	88	0.2
212	72	0.2
106	32	0.2

The 7 kg stock sample was subdivided into 500 g sub-samples. Care was taken to prepare representative sub-samples from the stock sample. Minimal bias for the eight sub-samples was confirmed by an acceptable standard deviation on each of the size fractions. A Retsch 1000 sample splitter with three-way rotary divider with a variable speed vibratory feeder was used for initial splitting of the zinc dust sample.

A number of 500 g sub-samples were hand-screened manually with a set of screens. Zinc dust samples with 100 percent passing 300, 212 and 106 µm were prepared for optimisation of zinc dust particle size distribution from the parent sample with a 500 µm top size. Each of the 500 g samples was divided into ten 50 g samples using a ten-way rotary splitter from Dickey & Stockler. Each of the 50 g samples was split into eight equal and unbiased samples using an eight-way Quantachrome rotary splitter. Samples of 25 gram each were prepared by adding together four of the small sub-samples.

The effects of oxidation on the zinc dust surface on the test results, if any, are expected to be minimal, as any oxide would be removed relatively quickly in the slightly acidic spent electrolyte.

3.3 Preparation of cobalt seed

Cobalt precipitate for test work was harvested from the cobalt filter press section (press solids) from the bulk bags containing the cobalt filter press section solids for initial tests to quantify the impact of recirculated cement on cobalt removal. Zinc

sulfate solution had been adequately removed and the filter press solids contained roughly 40% moisture. The harvested cobalt precipitate was not allowed to dry and was stored in a container with closed, sealed lid for the testwork. The mass of seed required for specific tests was calculated on a dry basis taking the moisture content into consideration.

Cobalt cement harvested from the No. 2 cobalt tank reactor was used for the remainder of the tests, due to improved cobalt removal. Slurry taken from the No. 2 tank overflow was allowed to stand for a number of hours to allow the solids to settle and the clear supernatant was decanted thereafter. The mass of seed in the slurry taken from reactor 2 was calculated based on a relationship derived earlier of g/L vs ml/L (read from a 500 ml measuring cylinder) displayed in Figure 13. Cobalt seed from the No 2 reactor was stored with the lid closed after decanting the supernatant. Cobalt seed for tests was taken from this seed stock using a concentration of 200 gram seed per liter of stock to calculate the volume required for each test.

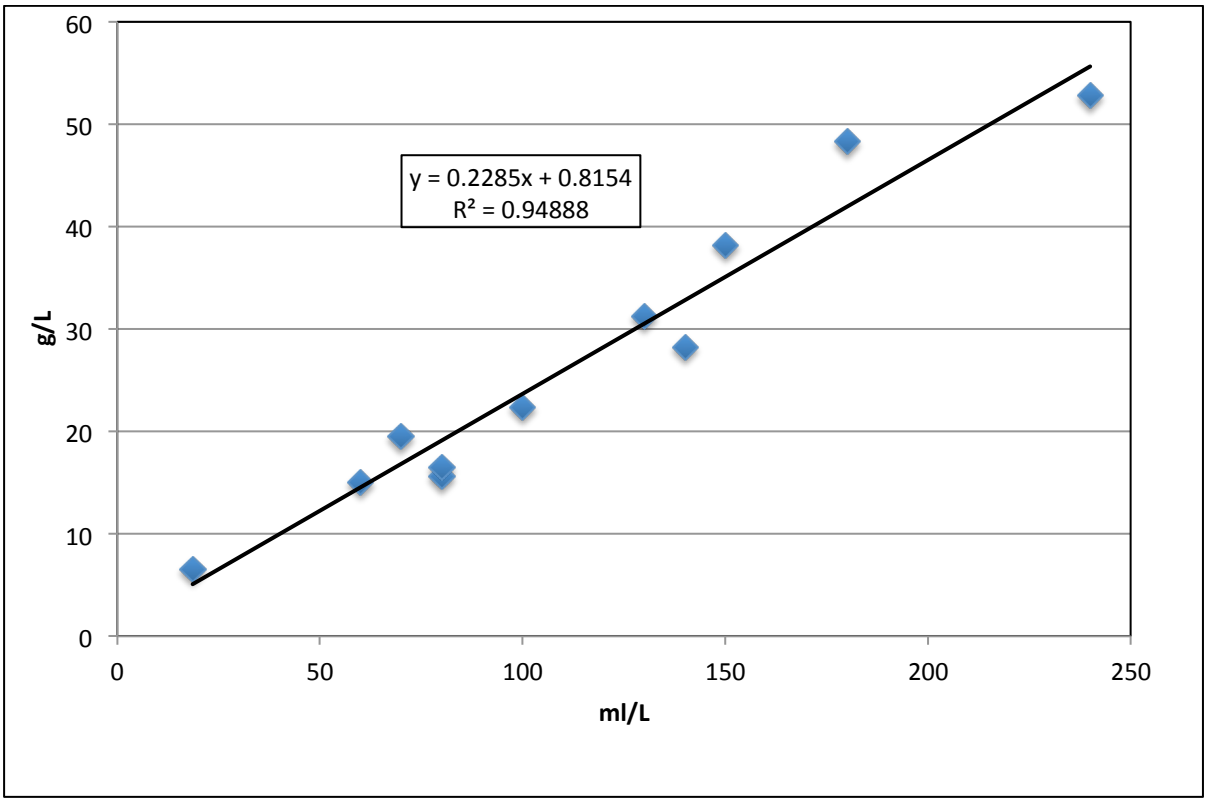

Figure 13: Conversion graph to convert cobalt precipitate (seed) concentration from ml/L to g/L.

The zinc remaining in the cobalt seed after each test was not measured. Further oxidation of the zinc remaining in the cobalt seed was not intentionally prevented, but was assumed to be minimal due to low hydrogen and oxygen content in the little bit of moisture left relative to the zinc and due to the relatively low ambient temperature at which the cobalt seed was stored. Surface exposure to atmosphere was low as interstitial voids were filled with purified solution i.e. void of copper, arsenic or cobalt. Any oxidation that did occur on the surface of the cobalt seed would have been removed quickly due to the acid in the slightly acidic stock solutions (spent electrolyte).

3.4 Laboratory test program

A base case test was prepared in the laboratory against which to compare changes in performance due to changes made to operating conditions. The results of all further optimisation work were compared against this base case. The criteria against which performance was measured were the removal rate of cobalt and the zinc dust concentration required to achieve an acceptable final cobalt concentration within an acceptable time frame. Tests to determine the base case were conducted at temperatures of 50, 60, 70 and 80 °C with standard zinc dust used in the cobalt section at Zincor's purification plant. Zinc dust was added at a stoichiometric excess of 7.5 times with respect to cobalt, copper and arsenic following the standard Zincor method. This is equivalent to a zinc dust concentration of 8.2 g/L. Arsenic was added at the stoichiometric requirement.

The rate constants, apparent rate constants and activation energy were determined for this base case from the cobalt removal data generated with varying temperature without adding cobalt precipitate.

The zinc dust particle size distribution was optimised first at a temperature of 80 °C without adding cobalt seed. Zinc dust was again added at 7.5 times the stoichiometric excess with respect to cobalt, copper and arsenic for a zinc dust addition of 8.2 g/L. The rate at which the cobalt ion concentration decreased was measured for zinc dust with maximum particle sizes equal to 106, 212, 300 and 500 micron.

This was followed by optimisation of the cobalt seed concentration at a temperature of 80°C using zinc dust with standard Zincor size distribution (unoptimised). The rate at which the cobalt ion concentration decreased was measured for cobalt precipitate additions of 10, 20, 30, 40 and 60 g/L. Zinc dust was added at a stoichiometric excess of four times for both cobalt and copper during this test or at an addition of 4.7 g/L. Cobalt seed was harvested from the cobalt filter presses for the first series of cobalt seed optimisation tests. A further series of tests were done with cobalt precipitate harvested from the No. 2 cobalt tank to test whether the source of cobalt seed made a difference to the cobalt removal efficiency.

The cobalt seed concentration and the zinc dust particle size distribution that showed the most favourable results were then used to determine a new optimised zinc dust concentration to achieve the desired cobalt removal rate. All tests were conducted at 80°C and the cobalt removal rate was determined for zinc dust concentrations of 1, 2 and 3.1 g/L.

Tests were concluded with an assessment of deposition morphology and composition for copper, cobalt and arsenic through investigation using scanning electron microscopy (SEM) and energy dispersive spectroscopy (EDS). A summary of the test program is provided in Table 12.

Table 12: Cobalt precipitation optimisation testwork program.

Test	Conditions	Purpose	Action
Base case – Cobalt cementation kinetics and effect of temperature defined	• Temperature = 50, 60, 70, 80 °C • No cobalt seed • Zinc dust = plant PSD • Zn dust = 8.2 g/L	• Determine apparent rate constant • Determine activation energy	• Measure cobalt concentration rate of change
Zn dust PSD optimised	• Temperature = 80 °C • No cobalt seed • Zn dust = 8.2 g/L	• Determine optimum zinc dust feed PSD • Test -106, -212, -300, -500 µm	• Measure cobalt concentration rate of change

Test	Conditions	Purpose	Action
Cobalt seed concentration optimised	• Temperature = 80 °C • Optimised Zn PSD • Zn dust = 4.7 g/L	• Determine optimum feed cobalt seed concentration • Test 10, 20, 30, 40, 60 g/L	• Measure cobalt concentration rate of change
Zinc dust concentration optimised	• Temperature = 80 °C • Optimised zinc dust PSD • Optimised cobalt seed concentration	• Determine minimum zinc dust consumption • Test 3.1, 2, 1 g/L	• Measure cobalt concentration rate of change
Copper deposition kinetics investigated	• Temperature = 80 °C • Purified solution with 800 mg/L copper • Zinc dust = 1x stoichiometric	• Determine copper ion removal rate in the presence of arsenic	• Measure copper concentration rate of change

3.5 Plant trial

A plant case was prepared during un-optimised plant operation for determining of the cobalt removal efficiency and associated kinetic constants from samples taken from Zincor's cobalt removal section. Slurry samples were taken of the feed to the cobalt circuit and the discharge of each of the four 212 m^3 continuously stirred tank reactors and were therefore representative of actual operating conditions. These samples were filtered with a small pressure filter and the filtrate was submitted to the laboratory for analyses. The properties on the day are displayed in Table 13:

Table 13: Impure solution properties for plant trial.

Element	Unit	Concentration
Cobalt	mg/L	28
Copper	mg/L	560
Cadmium	mg/L	300
Zinc	g/L	126

The operating conditions at the time that the sample was taken are displayed in Table 14 below.

Table 14: Un-optimised operating parameters – plant case.

Operating parameter	Unit	Value
Temperature	°C	72
Zinc dust concentration	g/L	3.4
Zinc dust PSD (500µm top size)	µm (d_{50})	154
	µm (d_{90})	327
Zinc dust surface area	m^2/g	0.0134
	m^2/L	0.046
Cobalt seed concentration	g/L	11
Cobalt seed surface area	m^2/g	8.34
	m^2/L	91.7
Volumetric flow rate	m^3/h	145
Retention time	min	351

3.6 Morphology and mechanism

Samples were taken from the 5 L laboratory reactor at specific intervals to investigate deposition morphology changes with time. Samples were drawn 5 minutes after addition of zinc dust, followed by samples at 10, 15, 20, 30 and 45 minutes. The tests were done without adding additional cobalt seed in order to study the physical characteristics of the precipitate of copper, arsenic and cobalt on fresh zinc dust.

The slurry samples were allowed to stand for a few minutes to allow the solids to settle. The solution was decanted after a few minutes and the remaining solids were placed onto filter paper and allowed to air dry. Special measures to prevent atmospheric surface oxidation were not taken while preparing samples for SEM and EDS analyses as it affects mainly zinc. Atmospheric oxidation of cementation

products was not considered, as cobalt arsenide and copper arsenide are very stable, while elemental copper and arsenic oxidises slowly in dry, cool conditions.

The dry samples were investigated with SEM at various magnifications. The composition of the particles was estimated with EDS. In addition an investigation into the deposition characteristics of the copper species was done by preparing samples with precipitation products for studying with SEM and EDS.

An industrial purified solution was spiked with copper sulfate ($CuSO_4$:$5H_2O$) to a concentration of 880 mg/L copper. Cementation of the copper species was done in the 5L reactor at 80 °C with the exact stoichiometric requirement of zinc and arsenic added (1x).

Samples were drawn 5 minutes after addition of zinc dust and again after 10, 15, 20, 30 and 45 minutes. Solid samples were prepared as above by decanting of the solution and by depositing of the solid fraction on the filter paper.

The solution fraction of each of the samples was submitted to the laboratory for analyses of the copper concentration in order to determine the copper removal rate.

4. RESULTS AND DISCUSSION

4.1 Effects of temperature on cobalt precipitation

The rate of cobalt cementation is significantly enhanced by increasing the temperature as indicated by the results shown in Figure 14 with the dimensionless ratio of actual cobalt concentration over initial cobalt concentration plotted against time for different solution temperatures. The rate at which cobalt is removed increases with increasing temperature from 50 to 80 °C as is predicted by the Arrhenius relationship between the reaction rate constant and temperature, discussed previously.

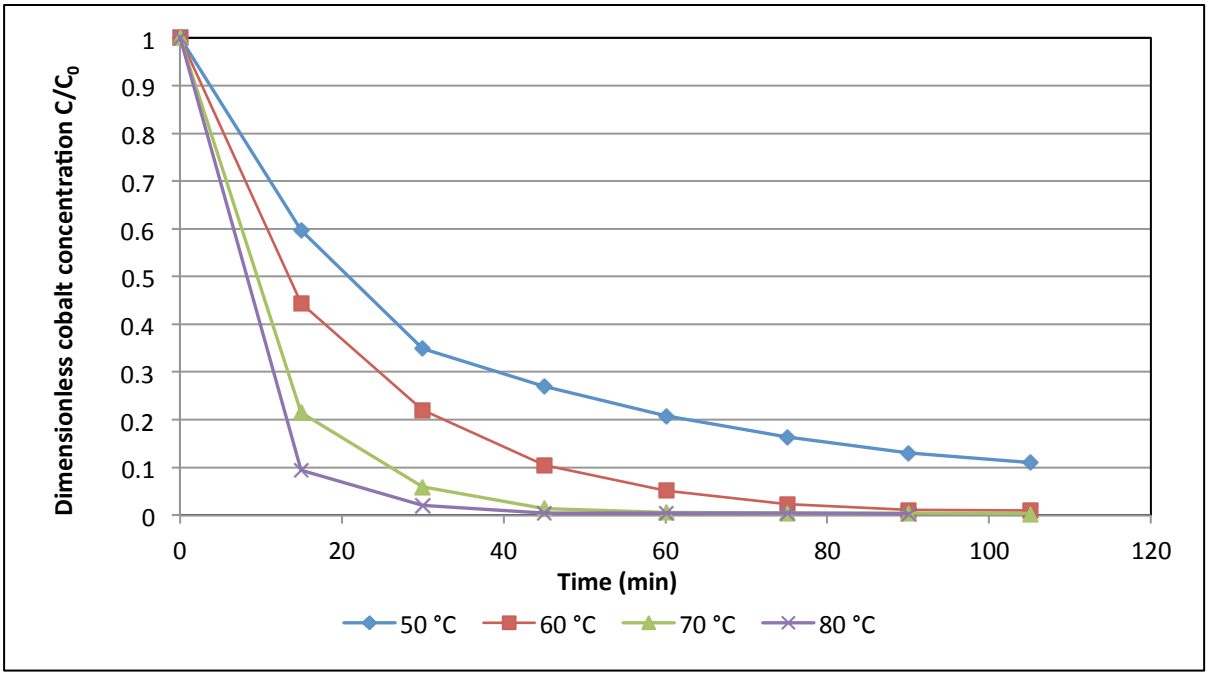

Figure 14: Dimensionless cobalt concentration in an industrial zinc sulfate solution during cobalt cementation on zinc in a stirred batch reactor as a function of time and temperature with pH 4.9 (uncontrolled), initial concentrations (g/L) of Zn dust: 8.2, Zn: 139: Co: 0.039, Cu: 0.880, As: 0.400, Cd: 0.266.

Moreover, arsenic precipitation is favoured by elevated temperature (Lawson and Nahn, 1981). An increased arsenic precipitation rate may therefore enhance the cobalt precipitation rate as cobalt precipitation follows after arsenic precipitation.

The section of the dimensionless cobalt concentration below 0.01 (y-axis) in Figure 14was magnified in Figure 15 to investigate an apparent change in the reaction rate. A change in reaction kinetics is observed at a certain low cobalt concentration, as is suggested by the rather abrupt decrease in cobalt deposition rate in Figure 15, after approximately 40 minutes for the reaction at 80 °C, and after 60 minutes for the test at 70 °C. This is explored further in Section 4.2 on cobalt precipitation kinetics.

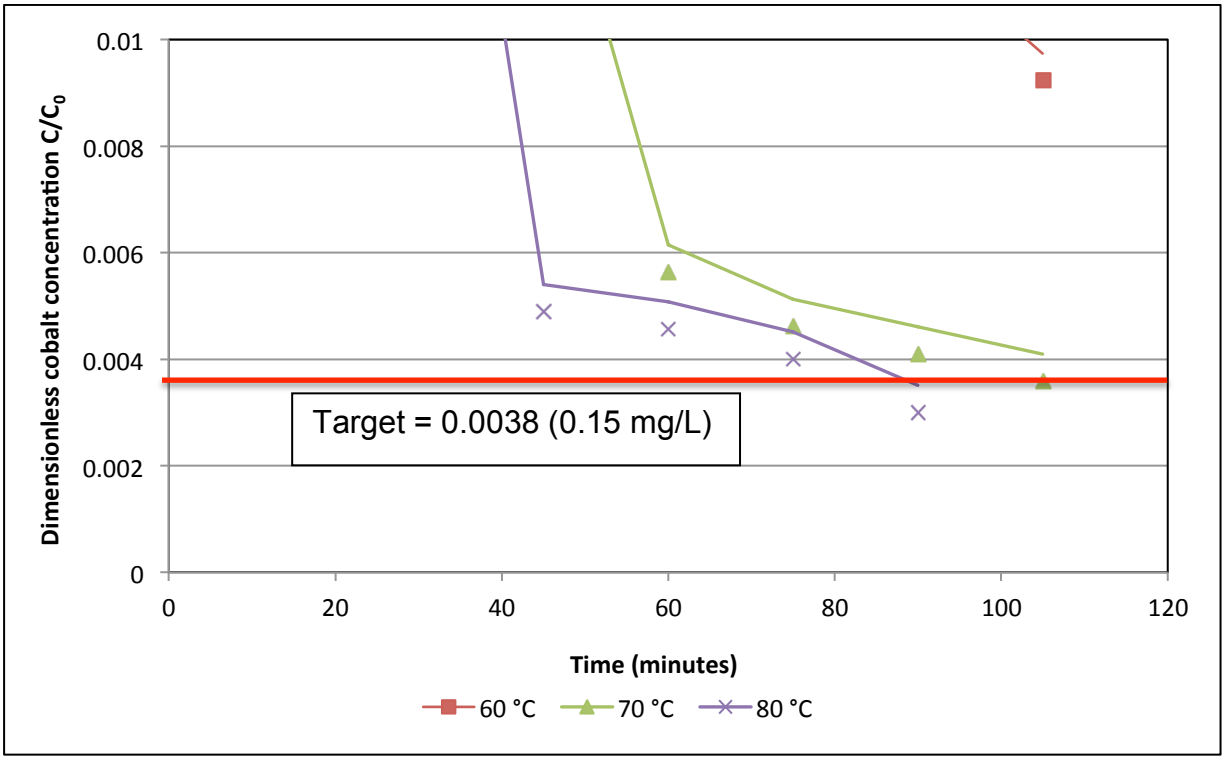

Figure 15: Dimensionless cobalt concentration (C/C_0) in an industrial zinc sulfate solution during cobalt cementation on zinc in a stirred batch reactor as a function of time and temperature – magnified at low concentration with pH 4.9 (uncontrolled), initial concentrations (g/L) of Zn dust: 8.2, Zn: 139, Co: 0.039, Cu: 0.880, As: 0.400, Cd: 0.266.

It is clear from Figure 15 that the target concentration of 0.15 mg/L, or 0.0038 as a dimensionless concentration ratio, is not achieved within the comparative time frame for the tests at 50 °C and 60 °C due to the low reaction rates.

4.2 Cobalt precipitation kinetics – base case

Tests were conducted with a standard set of operating conditions described previously to generate a base case against which performance of further optimisation tests may be compared. The logarithm of the cobalt concentration was plotted against time in order to determine the apparent rate constant for the reactions at various temperatures as is displayed in Figure 16.

Each test displayed an initial faster rate regime followed by a secondary slower rate regime. Figure 16 indicates that different rate limiting mechanisms control the reaction kinetics in the first and second rate regimes. It follows that achieving the target concentration is dependent on the properties of both the first rate regime and the second rate regime.

The solution temperature and cobalt concentration appear to be controlling parameters in determining when the transition occurs from one rate regime to the other. The transition from the first to the second rate limiting regimes typically occurs at a low cobalt concentration, which is reached sooner at higher temperatures. The early transition to the second rate regime at 50°C is unexpected and could not be explained. However, it is possible that the first two data points for the test at 50°C rather represent a transition into the first rate regime and that the test at 50 °C does not actually progress to the second rate regime within the observed time frame.

Straight lines were fitted to the data and the relationship between time and the logarithm of the concentration for each line as well as the quality of fit are displayed next to it. The results are summarised in Table 15.

The apparent rate constants for the first rate regime displayed a high temperature dependence and were comparable with values determined by Fugleberg et al (1993) for Kokkola and higher than those determined by Yamashita et al (1997) and Tozawa et al (1992) as were displayed previously in Table 4.

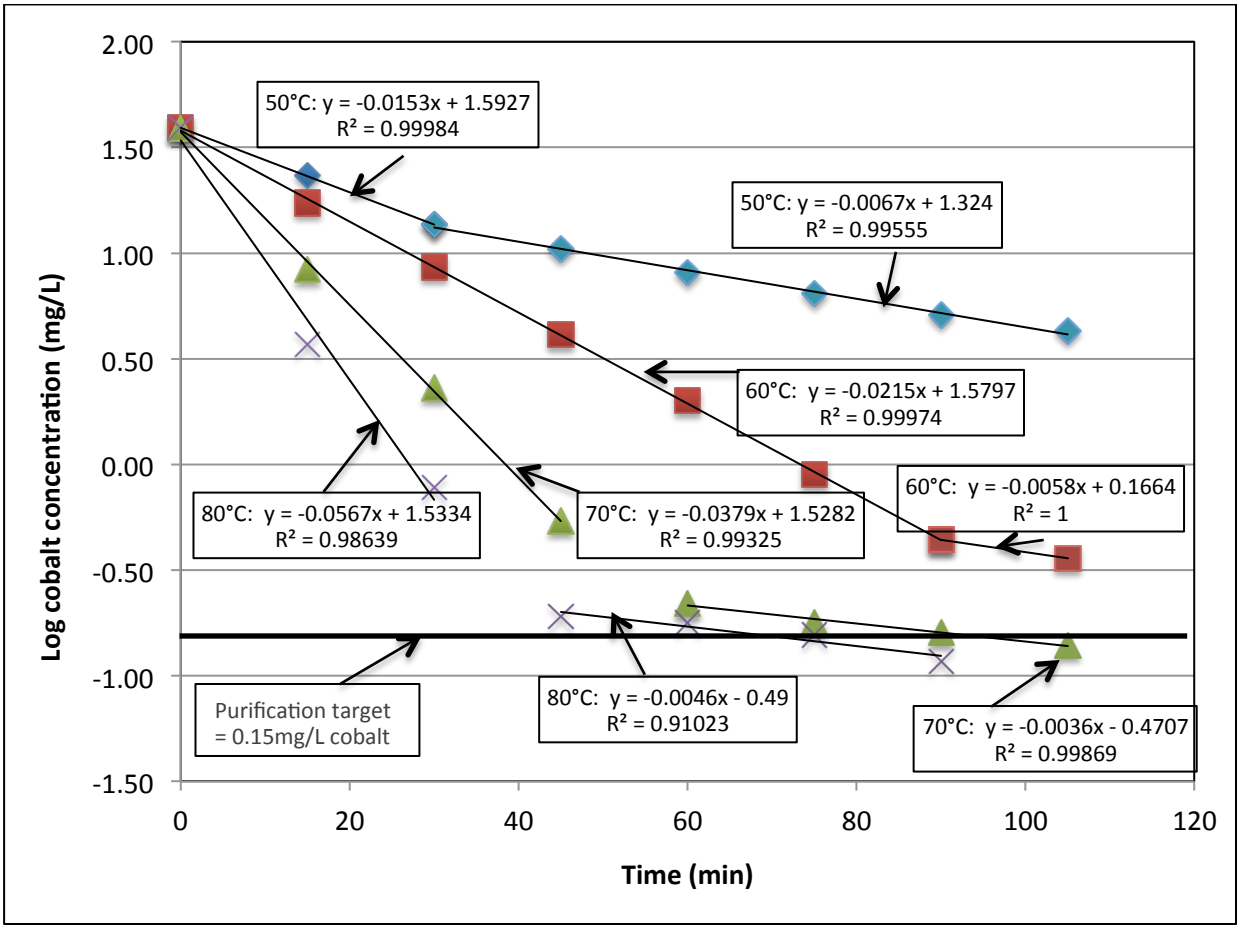

Figure 16: Logarithm of the cobalt concentration in an industrial zinc sulfate solution during cobalt cementation on zinc in a stirred batch reactor as a function of time and temperature with pH 4.9 (uncontrolled), initial concentrations (g/L) of Zn dust: 8.2, Zn: 139, Co: 0.039, Cu: 0.880, As: 0.400, Cd: 0.266.

Table 15: Initial apparent rate constants for the un-optimised base case.

Temperature	First rate regime		Second rate regime	
°C	Slope	k (per minute)	Slope	k (per minute)
50	-0.015	0.035	-0.0067	0.015
60	-0.021	0.049	-0.0058	0.013
70	-0.041	0.094	-0.0043	0.010
80	-0.057	0.131	-0.0046	0.011

The calculated values are considered to be high considering that no cobalt seed was used during the test. Fugleberg et al (1993) used recirculated cobalt cement to catalyze his reactions whereas Yamashita et al (1997) and Tozawa et al (1992) did not. The relatively high apparent rate constants measured for the Zincor base case is attributed to the high zinc dust addition used.

Fugleberg's numbers were derived for a constant reaction surface area of 750 m^2/L (A/V) and a zinc dust concentration of 1.5 times the stoichiometric requirement. This is the surface area for added cobalt seed only and excludes the surface area provided by zinc dust, which are orders of magnitude smaller. The measured reaction surface area for the Zincor base case test was 0.11 m^2/L (A/V) with zinc dust only and a zinc dust addition of 8.2 g/L or 7.5 times stoichiometric and zinc dust surface area of 0.0134 m^2/g.

Apparent rate constants for the second rate regime remained virtually unchanged across the indicated temperature range and did not display a temperature dependence. Comparable kinetic values for the second rate regime were not found in the studied literature.

The logarithm of the apparent rate constants for the first and second rate regimes were plotted against reciprocal absolute temperature to calculate activation energies for the base case as is displayed in Figure 17. The activation energy for the first rate regime was calculated as being 43 kJ/mol. This is comparable with, but significantly lower than the value measured by Fugleberg et al (1993) for the Kokkola process (70 kJ/mol) as well as the value generated by Yamashita et al (1997) (72 kJ/mol), but confirms that the first rate regime is under activation control.

Calculation of activation energy for the second rate regime yielded a value of negative 13 kJ/mol. This is ascribed to a lack of data in the case of the test at 60°C, assuming that the second rate regime has not yet fully developed. In addition the early transition to the second rate regime at 50°C is unexpected and it is possible that transition into the second rate regime has not yet occurred.

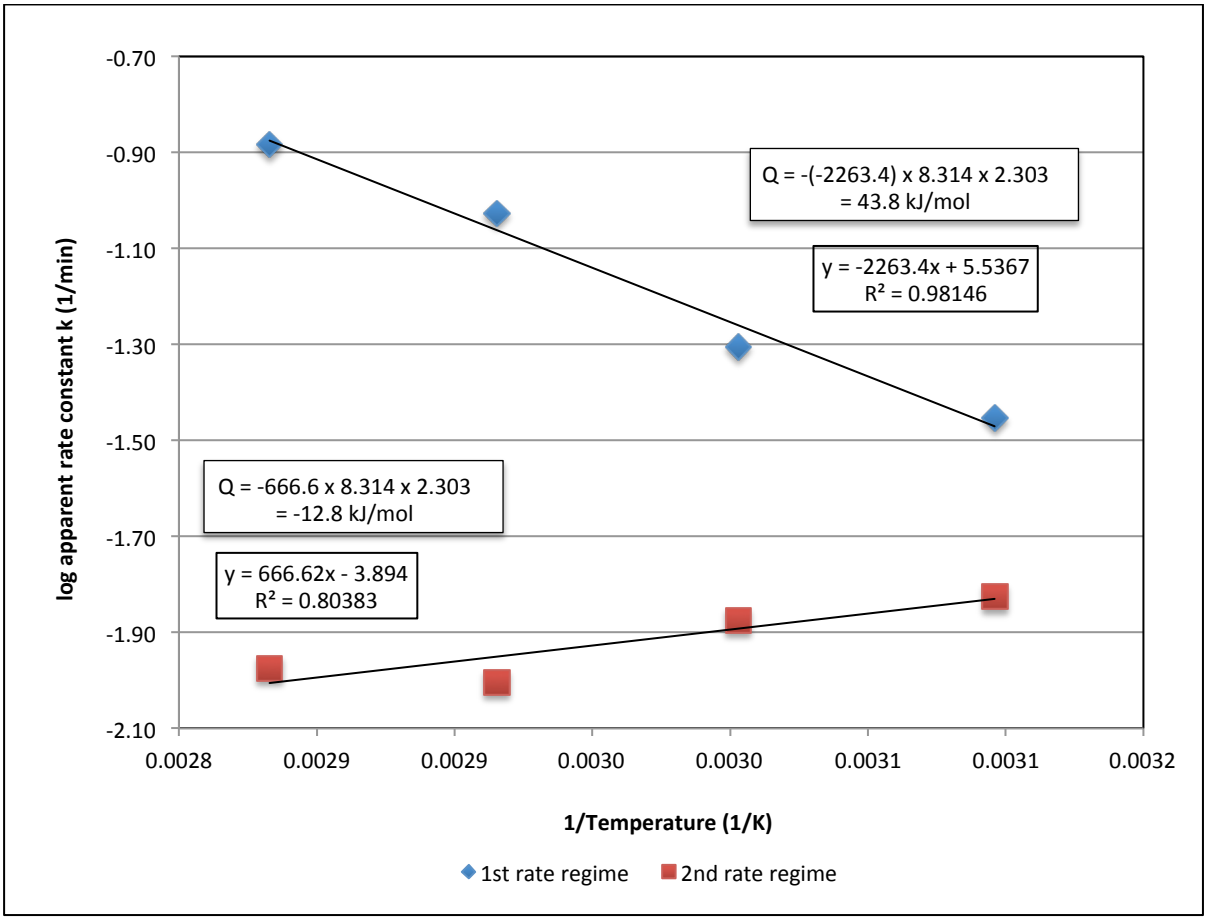

Figure 17: Arrhenius plot for cobalt batch cementation from industrial zinc sulfate for the rate constants indicated as the slopes of the lines in Figure 16.

The observed weak temperature dependence and low activation energy suggest that the rate of the cobalt cementation reaction in the second rate regime is limited by mass transfer limitations and not by the rate of the chemical reaction itself any more. This could be due to the precipitation of a basic zinc sulfate due to an increase in the pH or zinc concentration close to the surface of the precipitate or to insufficient renewal of the copper arsenide surfaces when these reagents are depleted. Further work is required to confirm this.

The pH was not controlled during batch tests and changes to pH measured during each test were the result of the reactions occurring and in particular the consumption of hydrogen. The typical change in pH over time is plotted in Figure 18. The pH increased from 5.1 to 5.4 for the particular test, representing a typical net increase of

just over 0.3. The increase in pH during the test should favour the precipitation of basic metal sulfates during the later stages of the process and could have reduced the overall rate by blocking the precipitation and/or the zinc dissolution sites.

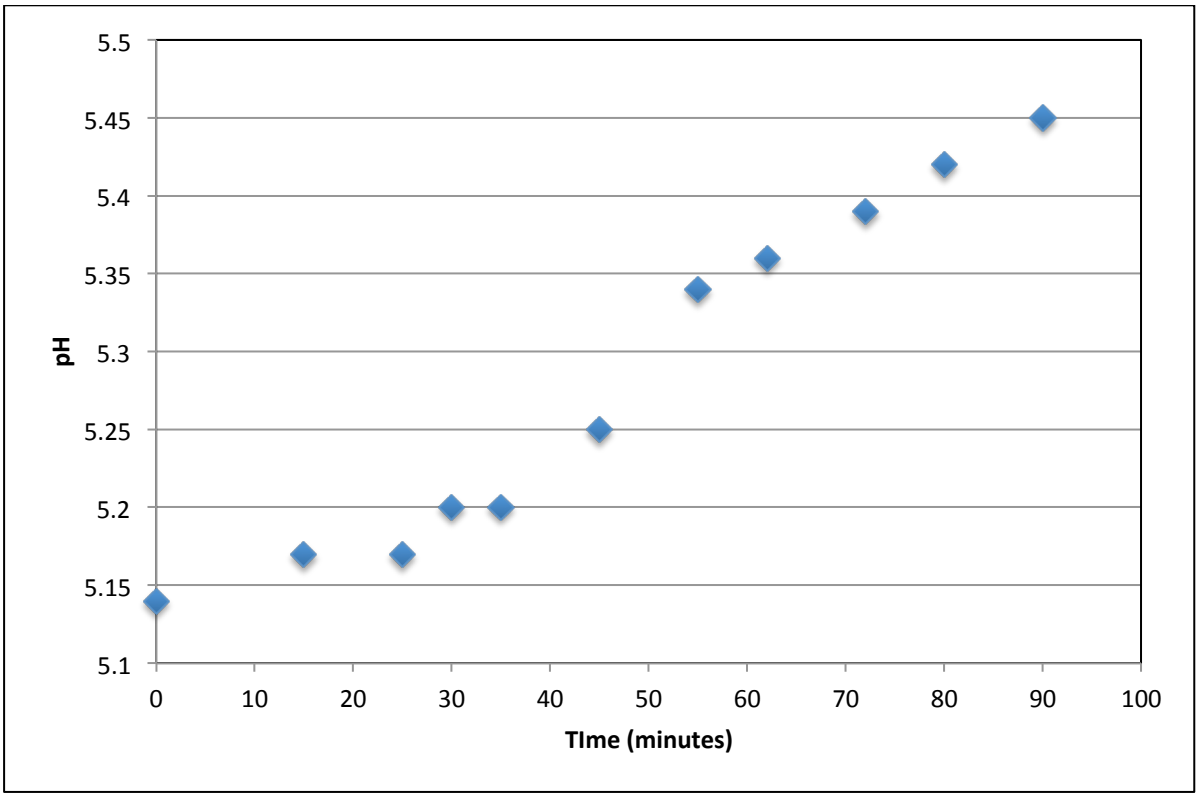

Figure 18: Typical pH increase during cobalt cementation on zinc in a stirred batch reactor as a function of time with temperature 80 °C, initial concentrations (g/L) of Zn dust: 8.2, Zn: 139, Co: 0.039, Cu: 0.880, As: 0.400, Cd: 0.266.

4.3 Optimisation of zinc dust particle size distribution

The cementation rate of cobalt should be enhanced by using finer zinc dust as the area per mass of zinc available for both the anodic and cathodic half cell reactions involved in the cementation process should increase. The use of finer zinc dust could, however, also impact negatively on the overall purification process if it significantly favours the hydrogen ion reduction reaction such that flotation of the finer zinc particles occurs, or the resultant increase in pH causes the passivation of the zinc or the formation of easily re-dissolvable basic cobalt sulfates or cobalt

hydroxides, or the galvanic interaction required for cementation is lost when the smaller zinc particles are fully consumed. Finer zinc is also more expensive and more prone to oxidation and thus loss of active zinc. There should therefore exist an optimum zinc powder size for a specific application based on these considerations.

Cobalt removal rates for zinc dust with a top size of 106, 212 and 300 µm were compared against the cobalt removal rate of industrially produced zinc dust with a top size of 500 µm. The results obtained indicate that as expected cobalt removal from the zinc leach solution is enhanced by decreasing the zinc dust particle size at a constant stoichiometric zinc addition ratio, as indicated in Figure 19.

The cobalt removal rate increases with decreasing particle size and corresponding increase in surface area per mass. The change in removal rate was significant as the target cobalt concentration was achieved after roughly 35 minutes of reaction time with a zinc dust particle top size of 106 µm compared to the 85 minutes required for the base case test with a zinc dust particle top size of 500 µm. In the cases of using zinc dust with top size of 106 µm and a top size of 300 µm the cobalt concentration is observed to increase after having reached a minimum value. This could be attributed to redissolution of cobalt. Control of the residence time in the reactor is therefore a critical to prevent redissolution of cobalt when using fine zinc dust.

The cementation kinetics were further analysed by considering the effect of zinc dust surface area on the initial stage apparent rate constant with the influence of decreasing zinc dust top size on the rate constant as summarised in Table 16 and illustrated in Figure 20. As expected the apparent rate constant is indeed directly proportional to the surface area of the zinc dust used in the cementation process as indicated by the initial apparent rate constants achieved for zinc dust particles with top sizes of 500, 212 and 106 µm. The surface area for zinc dust particles with a top size of 300 µm is an estimated value, based on the apparent rate constant achieved and the linear relationship between measured surface areas for zinc dust particles with 500, 212 and 106 µm top sizes and matching initial apparent rate constants, as the original measured value (0.0097 m^2/g) for zinc dust with a top size of 300 µm is suspect and probably too low.

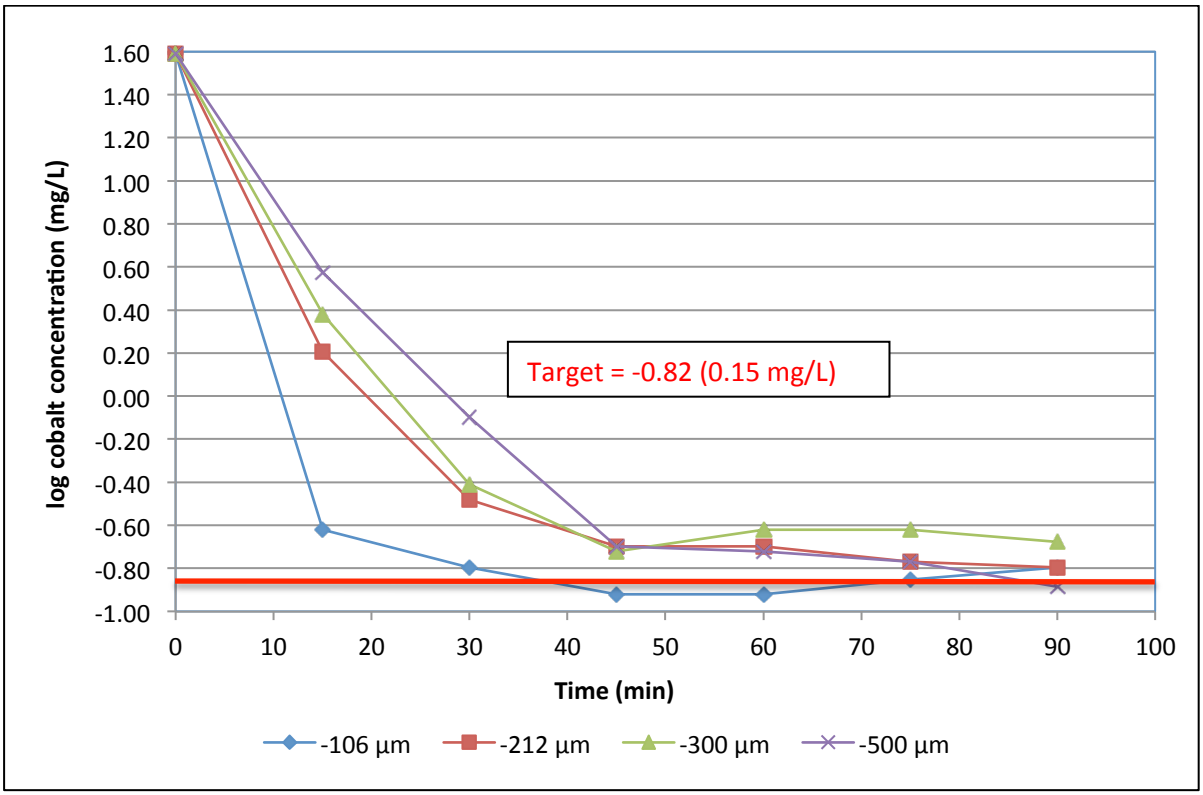

Figure 19: Logarithm of the cobalt concentration in an industrial zinc sulfate solution during cobalt cementation on zinc in a stirred batch reactor as a function of time and zinc dust size distributions with different top sizes with pH 4.9 (uncontrolled), temperature 80 °C, initial concentrations (g/L) of Zn dust: 8.2, Zn: 139, Co: 0.039, Cu: 0.880, As: 0.400, Cd: 0.266.

Table 16: Initial apparent rate constants for increasing zinc dust surface area.

Zinc dust top size	Surface area	Initial slope	Initial apparent rate constant (k)
µm	m^2/g	Δ(log C)/Δt	1/minute
500	0.0134	-0.068	0.16
300	0.0148[1]	-0.081	0.19
212	0.0161	-0.093	0.21
106	0.0238	-0.150	0.34

Note 1: Estimated value

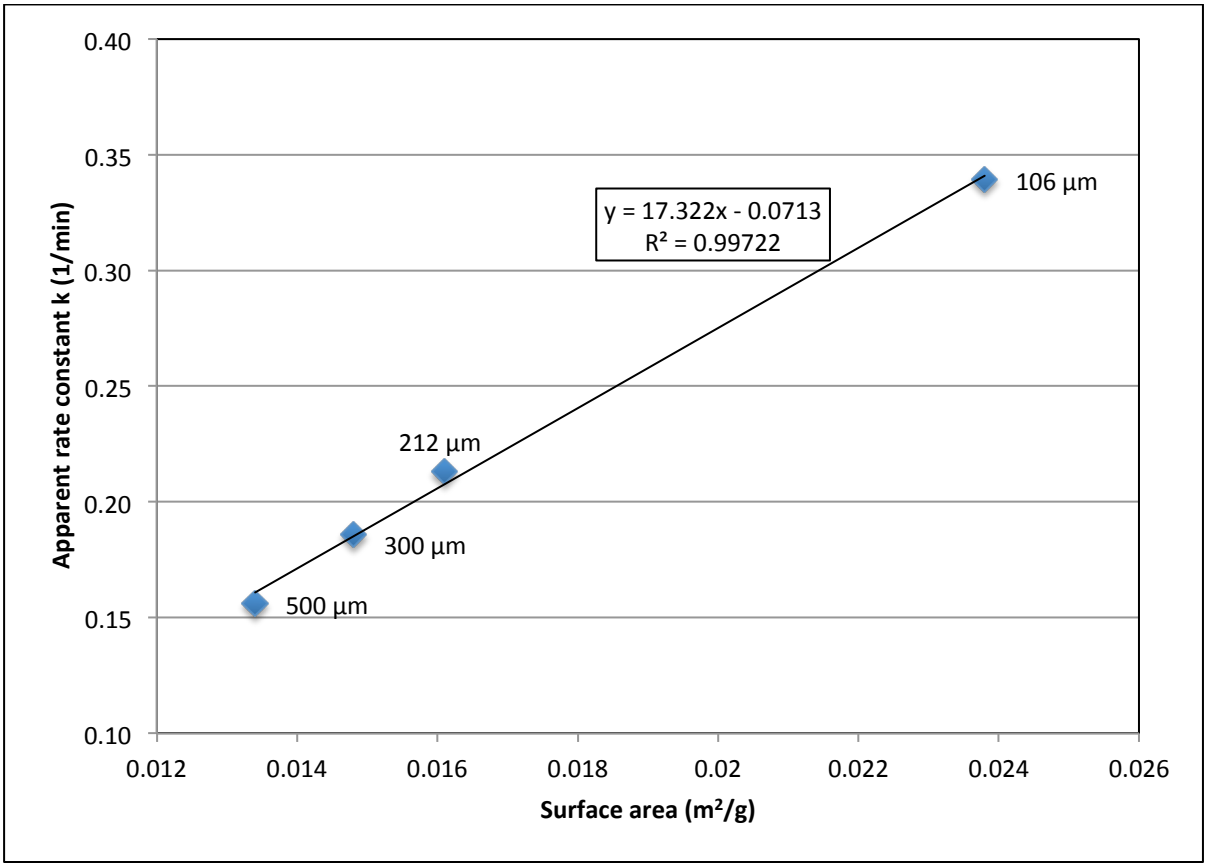

Figure 20: Initial stage apparent rate constant for cobalt cementation on zinc in a stirred batch reactor as a function of zinc dust surface area and particle top size with pH 4.9 (uncontrolled), temperature 80 °C, initial concentrations (g/L) of Zn dust: 8.2, Zn: 139, Co: 0.039, Cu: 0.880, As: 0.400, Cd: 0.266.

The zinc dust used at Zincor is significantly coarser and with a much lower surface area compared to the reported industry standard for zinc dust containing on average particle sizes of 50 µm to 75 µm with a matching surface area of 1.75 m^2/g (Nelson et al, 2000; Dreher et al, 2001). A relatively high excess zinc dust demand could therefore be expected to achieve the desired cobalt concentration at Zincor, providing an opportunity for improvement.

4.4 Optimisation of cobalt seed concentration

The rate of cobalt precipitation is significantly enhanced by addition of cobalt seed i.e. zinc with some cobalt, copper and arsenic already cemented onto it, as indicated by the results shown in Figure 21. All tests were conducted with standard zinc dust

with particle top size of 500 µm. The cobalt seed surface area was measured to be 8.3 m^2/g with ninety percent of particles smaller than 85 µm.

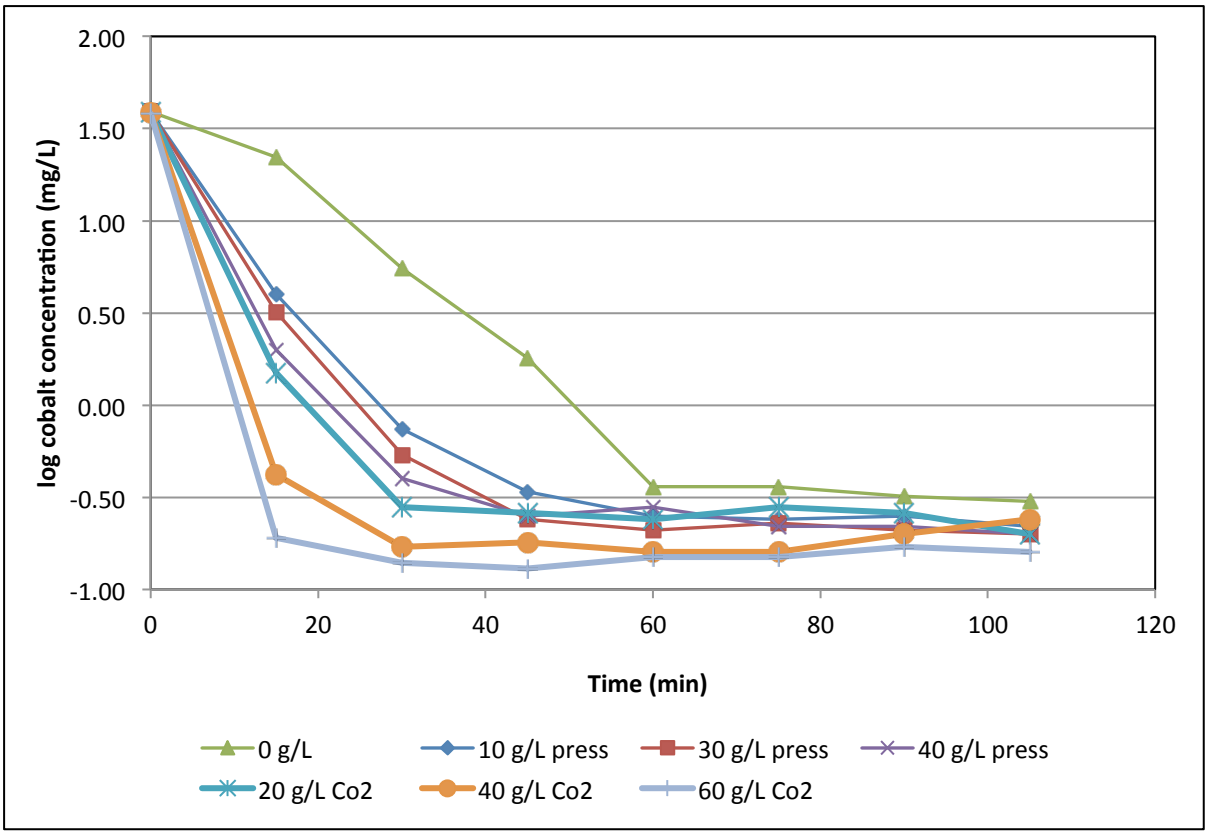

Figure 21: Logarithm of the cobalt concentration in an industrial zinc sulfate solution during cobalt cementation on zinc in a stirred batch reactor as a function of time and cobalt seed concentration with pH 4.9 (uncontrolled), temperature 80 °C. Press: seed from filter press; Co2: seed from cobalt precipitation tank 2. Initial concentrations (g/L) of Zn dust: 4.7, Zn: 139, Co: 0.039, Cu: 0.880, As: 0.400, Cd: 0.266.

Tests were conducted with cobalt precipitate harvested from the cobalt section filter presses as well as with precipitate from the No. 2 cobalt reactor. Cobalt seed from the No. 2 cobalt reactor provided improved performance compared to cobalt seed from the filter press. The required zinc dust surface area concentration for a certain rate constant may therefore be reduced substantially by partial replacement of zinc dust with recirculated cobalt seed from the No 2 cobalt reactor. The amount of zinc metal left in the cobalt seed is important in terms of the ability to substitute new zinc to supply electrons for further reactions with cobalt, copper and arsenic in solution. It

is also important from a surface area perspective, albeit less so than the precipitation products, which has a much greater reaction surface area. Unfortunately the zinc content of the cobalt seed was not measured.

The cementation kinetics were further analysed by considering the effect of cobalt seed addition on the initial stage rate constant, with the influence of varying seed addition on the initial apparent rate constant summarised in Table 17 and illustrated in Figure 22.

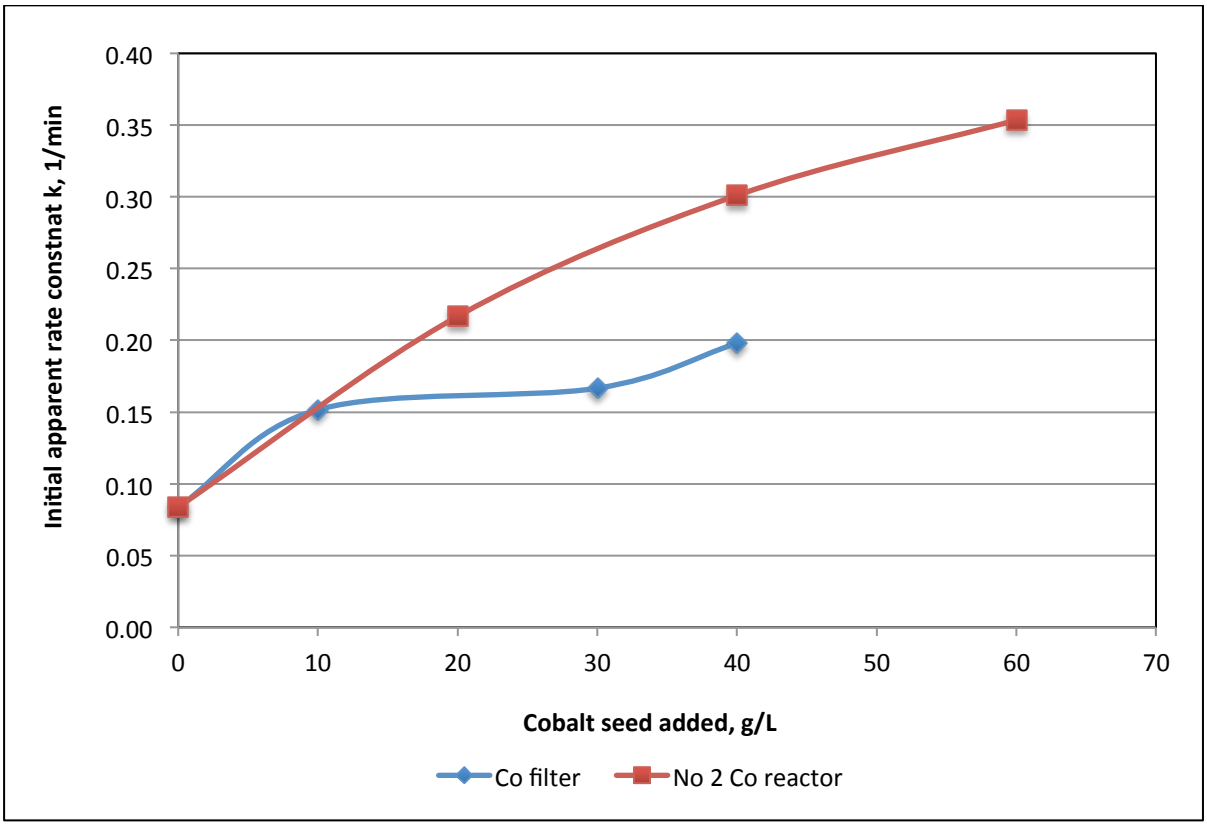

Figure 22: Initial stage apparent rate constant for the cementation of cobalt as a function of the cobalt seed addition derived from the results shown in Figure 21. Cobalt seed obtained, respectively, from filter press residue or from tank 2.

The initial rate constants indicate the advantage of using seed from earlier in the process i.e. from the No. 2 cobalt reactor of four reactors instead of using the cobalt section filter press product, and also the diminishing effect of higher seed additions on the rate of cementation. The results of the test with seed from the cobalt filter

presses are in agreement with that of Fugleberg et al (1976) who suggested that a seed concentration of at least 30 g/L is required for optimal performance and that cobalt seed concentrations in excess of 50 g/L provides little additional benefit. It is noted however that seed from the No. 2 cobalt reactor continued to add to the rate of cobalt cementation up to the highest addition evaluated, i.e. 60 g/L.

Table 17: Initial apparent rate constant for changing cobalt seed concentrations using zinc dust with top size of 500 µm.

Cobalt seed source	Cobalt seed concentration	Initial slope	Initial apparent rate constant (k)
	g/L	Δ(log C)/Δt	1/minute
No seed	0	0.036	0.08
Filter press	10	0.066	0.15
Filter press	30	0.072	0.17
Filter press	40	0.086	0.20
No. 2 cobalt reactor	20	0.094	0.22
No. 2 cobalt reactor	40	0.131	0.30
No. 2 cobalt reactor	60	0.154	0.35

Analyses of the cobalt seed with SEM and EDS confirmed the presence of unreacted zinc dust, which would partially explain the positive impact on reaction kinetics. It is suggested, however, that the increase in cobalt cementation rate with increasing cobalt seed concentration, as indicated by the increase in initial rate constant, is due also to the increase in reaction surface area provided by the irregular surface of the various cementation products on the zinc dust surface. Cemented copper products probably provide the bulk of the additional surface area due to the high initial concentrations used and the well-documented activation effect of copper on the cementation of cobalt in this system (Näsi, 2003; Yamashita et al, 1997; Tozawa, 1992; Fugleberg et al, 1980). The contribution of cadmium to the reaction surface area is considered to be also significant as most of the cadmium cements out during the cobalt cementation stage with similar initial concentrations to that of arsenic. Analyses with EDS of cementation products support this notion with cadmium assays

similar to that of arsenic with the exception of only a few analyses where arsenic assays in solid solution with cobalt exceed that of cadmium.

Adjustment of the solution pH is done in the No. 4 cobalt reactor down to roughly 4.66 to redissolve any basic zinc sulfate that may have formed. It is proposed that some surface smoothing of the cementation products then occurs due to the favourable leaching conditions created in the filter press section by the more acidic conditions as well as the forced flow through the filter cake. This could explain why cobalt seed from the filter presses are unable to activate cobalt cementation to the same level as does seed from the No. 2 reactor. Further evidence of the aggressive conditions in the cobalt filter presses is the redissolution of cadmium precipitate, with cadmium concentrations in the partially purified solution typically increasing from 50 mg/L in the filter press feed solution to 400 mg/L in the discharge solution. This may also be an indication of the positive effects of cadmium precipitate on cobalt cementation, which, if not present, leads to reduced activation of the cobalt cementation reactions.

4.5 Optimisation of zinc dust concentration

The results obtained indicate that it should be possible to reduce the required zinc dust concentration and still maintain efficient cobalt removal by using zinc dust with a finer particle size distribution and by adding cobalt seed as additional catalytic surface area, if a train of CSTRs are used for the cementation process.

This was further explored by studying the influence of decreasing additions of relatively fine zinc powder with a top size of 106 µm on cobalt cementation from the Zincor electrolyte in a batch reactor using cobalt seed from the No. 2 cobalt reactor. A comparative test was conducted with operating parameters similar to that of a current zinc operation i.e. using zinc dust with a top size of 500 µm and cobalt seed from the filter presses. All tests were conducted at 80 °C. The results displayed in Figure 23 indicate the typical initial and second stage kinetic behavior and also that significant savings in terms of zinc usage should be possible if finer zinc dust is used and some recirculation of cobalt seed from the No. 2 cobalt reactor is applied.

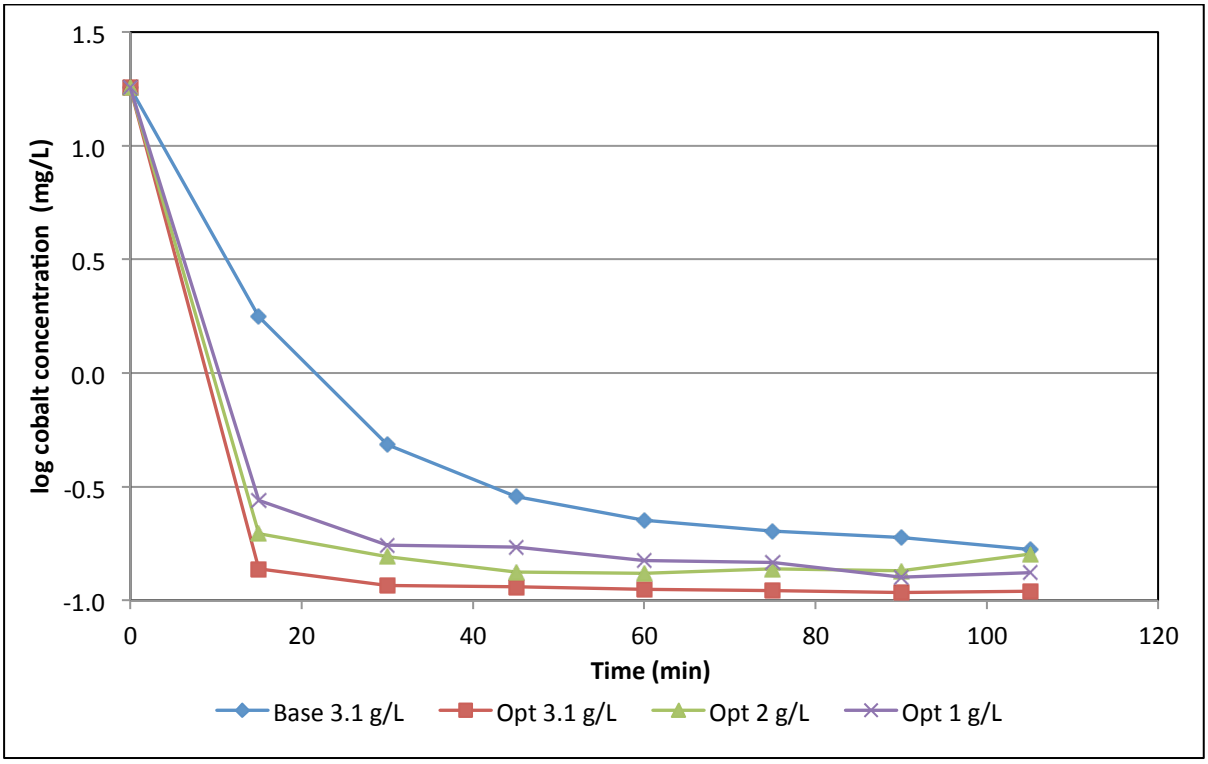

Figure 23: Logarithm of the cobalt concentration in an industrial zinc sulfate solution during cobalt cementation on zinc in a stirred batch reactor as a function of time, zinc dust concentration, zinc dust particle top size and cobalt seed concentration with pH 5.1 (uncontrolled) and temperature 80 °C. Base: 10 g/L seed from filter press and 500 µm zinc dust top size; Opt: 30 g/L seed from cobalt cementation tank 2 and 106 µm zinc dust top size. Initial concentrations (g/L) of Zn 135: Co 0.018: Cu 0.422: As 0.200: Cd 0.380.

The minimum zinc dust addition rate to be used would depend on the process configuration, i.e. for example the residence time available and the maximum allowable cobalt concentration. The present results also indicate that for the zinc particle size investigated the complete dissolution of the zinc particles and the resultant redissolution of the cobalt was unlikely within the time frame investigated.

The cementation kinetics were further analysed by considering the effect of the combined effects of zinc dust particle size and zinc dust concentration as well as cobalt seed concentration on the initial stage rate constant. The results, summarised in Table 18 and graphically presented in Figure 24 indicate that very significant savings may be achieved by using finer zinc and by re-circulating some precipitate.

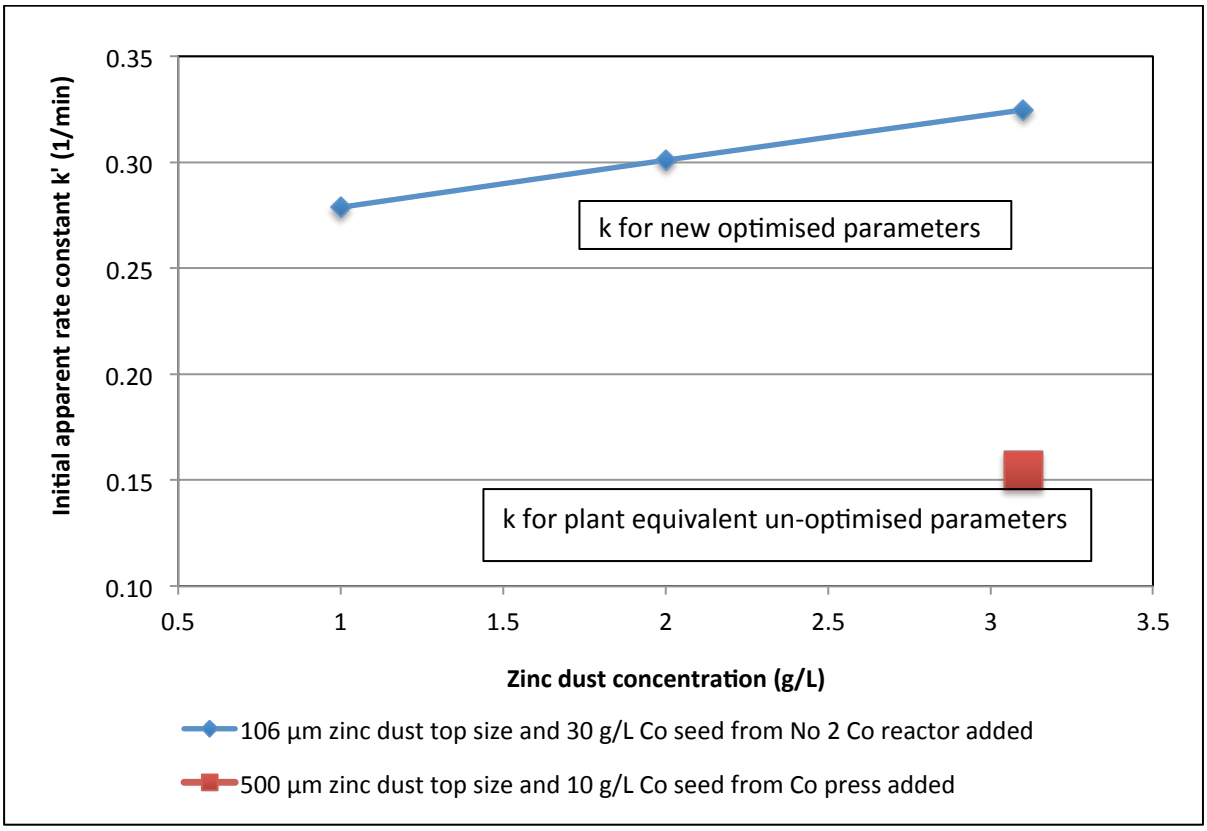

Figure 24: Initial apparent rate constant for the cementation of cobalt as a function of the zinc dust concentration, zinc dust particle size distribution and cobalt seed concentration derived from the results shown in Figure 23. Cobalt seed obtained, respectively, from filter press residue or from tank 2.

The apparent rate constant for the base case is comparable with that of previous tests under similar conditions. It is clear that the initial apparent rate constant for cobalt deposition increases significantly, even at a third of the original zinc dust concentration when adding cobalt seed concentration from the No. 2 cobalt reactor instead of from the filter press, by increasing the cobalt seed concentration and by using fine zinc dust instead of coarse zinc dust. This is attributed to the increased reaction surface area provided by using finer zinc dust, as indicated previously, as well as by unused zinc dust remaining in recirculated cobalt cement and additional catalytic surface area provided by reaction products of copper, arsenic and cadmium.

Table 18: Zinc dust concentration and initial apparent rate constants for a base case with un-optimised conditions and optimised conditions

Test	Cobalt seed concentration	Zinc dust concentration	Initial slope	Initial apparent rate constant (k)
	g/L	g/L	Δ(log C)/Δt	1/min
Base case	$10_{(press)}$	$3.1_{(500\ \mu m)}$	0.900	0.15
Optimised #1	$30_{(No.\ 2\ Co)}$	$1_{(106\ \mu m)}$	0.984	0.28
Optimised #2	$30_{(No.\ 2\ Co)}$	$2_{(106\ \mu m)}$	0.989	0.30
Optimised #3	$30_{(No.\ 2\ Co)}$	$3.1_{(106\ \mu m)}$	0.992	0.32

The zinc dust concentration may therefore be lowered even further than that used in the test to achieve the same performance as was achieved during the base case.

4.6 Deposition morphology and mechanism

The zinc dust surface and associated deposition products were studied by physical inspection using scanning electron microscopy and by analyses with electron dispersive spectroscopy to elucidate the cobalt deposition mechanism. An attempt to identify the mineralogy of deposition products through calculation of the mass ratio of respective elements yielded inconclusive results.

4.6.1 Copper and arsenic precipitation

A selected volume of purified solution was spiked with copper through addition of copper sulfate to increase the copper concentration to a level comparable with that of the impure solution. Copper was cemented out at various time intervals through reaction with arsenic and zinc dust at the stoichiometric requirement and at a temperature of 80°C in order to elucidate development of the copper and arsenic precipitate with time.

The SEM image of the precipitate, shown as Figure 25, indicates a nodular copper-arsenic precipitate, which appears lighter and clearly distinguishable around the edges of the zinc particles, which appears more greyish in the image. The form of the precipitate is significantly more irregular than the zinc substrate, indicating that the surface area of the copper-arsenic precipitate should greatly enhance the overall deposition surface area. Analyses of the precipitate in terms of mass percentage of element with increasing reaction time are displayed in Appendix C, as well as the ratio of the molar masses of copper, arsenic and oxygen, which comprised the bulk of the assay. The reaction volume depth of the EDS instrument at 20 kV is of the order of 8 µm and assaying of the zinc substrate below the copper deposit is invariably included in the sampling and could explain the decreasing zinc concentration measured at longer cementation times. The high oxygen is unexpected, but could indicate the presence of sulfate on the surface.

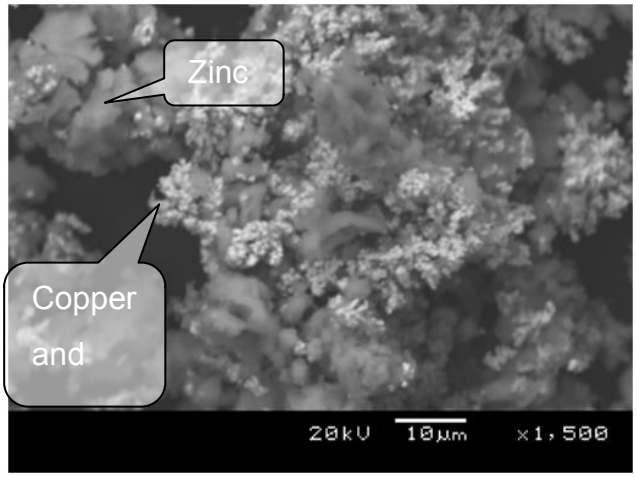

Figure 25: Zinc dust with copper and arsenic cement after 30 minutes reaction time with test conditions as per Figure 26.

The results do not allow conclusive identification of individual precipitates, due to limitations of the instrument used and the relatively small volume of deposit investigated, but do point to the presence of elemental copper rather strongly in addition to the thermodynamically predicted Cu_3As due to the high copper to arsenic ratios found. The formation of copper oxide appears unlikely due to the low measured Cu:O ratios.

The kinetics of the copper cementation with arsenic and zinc dust is illustrated in Figure 26 and indicates that the apparent rate constants, indicated by the slope of the logarithm of the copper concentration with time, are initially relatively constant and high for the first 20 minutes, and then followed by lower values up to 45 minutes. The copper in solution was only reduced from 806 mg/L to 106 mg/L during the experiment indicating that the stoichiometric quantity of zinc used was not sufficient to remove all the copper in the time frame of the experiment. The significant quantity of residual zinc observed in the sample of copper cement investigated indicates that it is probably not the decrease in zinc available for cementation that is responsible for the significant decrease in the rate of copper removal, but rather a change in the rate limiting step in the reaction sequence. However, this may not have applied to the finer zinc particles in the size distribution of the zinc dust used.

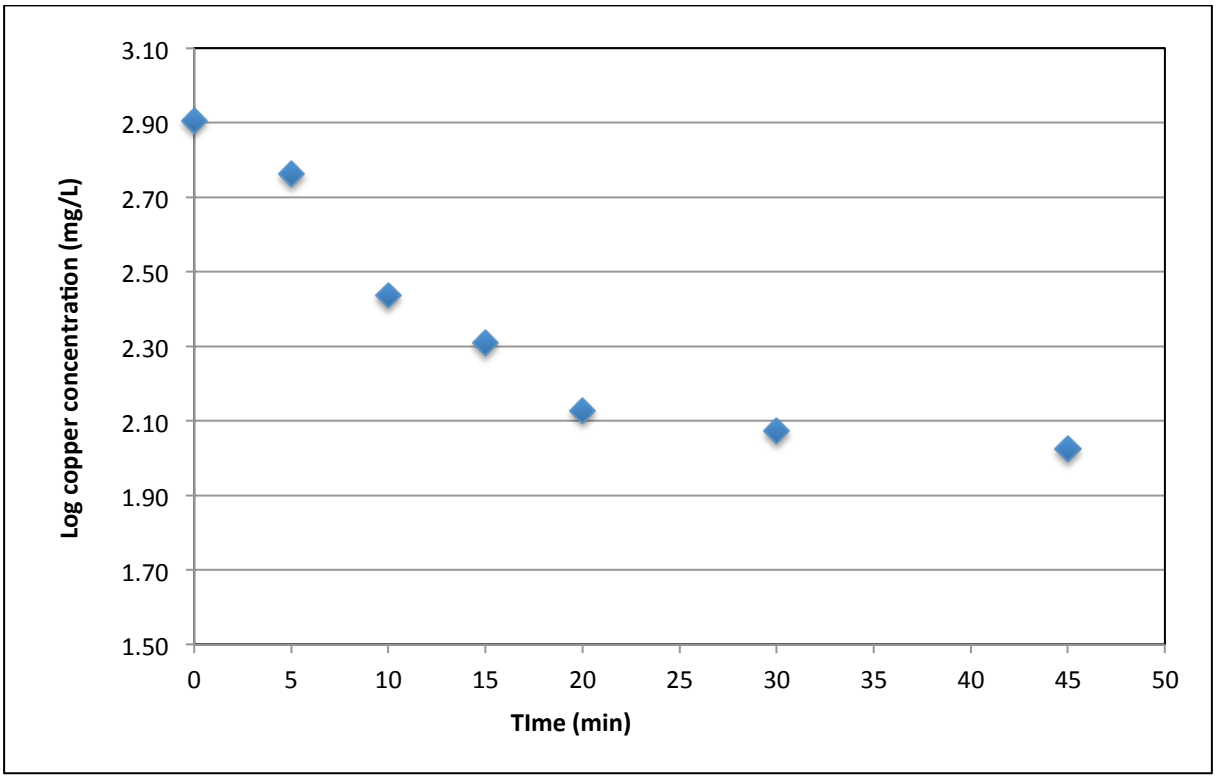

Figure 26: Logarithm of the copper concentration in an industrial zinc sulfate solution during copper cementation on zinc in a stirred batch reactor as a function of time with pH 5.1 (uncontrolled), temperature 80°C, initial concentrations (g/L) of Zn dust :1.2, Zn: 139, Cu: 0.806, As: 0.320.

4.6.2 Cobalt, arsenic and copper precipitation

The nature of the zinc dust taken from a sample with a d_{90} = 327 µm after cementation of copper, cobalt and arsenic, using only zinc dust, is illustrated in Figure 27 and in Figure 28. It is clear that the zinc dust is not spherical, but that it rather consists of vertically stacked zinc crystals assembled in arrays indicating the surface area of the zinc would be much higher than that predicted assuming a smooth surface. The copper, cobalt and arsenic cement were present as discrete clusters as indicated in more detail in Figure 29. It is also clear that the zinc platelets were still relatively intact even after the extensive time in the cementation process. This is in contrast to the surface condition of the zinc dust shown in Figure 25 for copper and arsenic precipitation only, where extensive corrosion of the zinc surface must have occurred if it is presumed that the original zinc dust morphology was the same. This is attributed to not having an excess of zinc dust available for the reaction, having used the stoichiometric zinc dust requirement, requiring a much larger physical proportion of zinc to sustain the reactions.

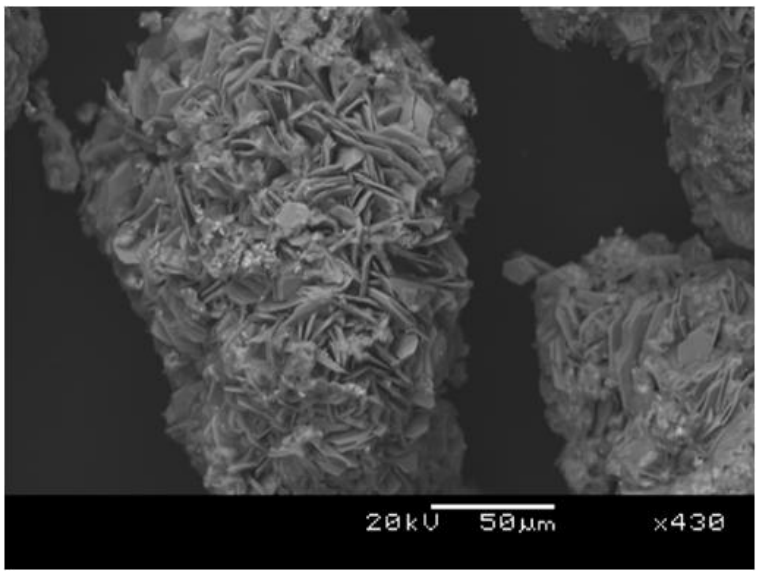

Figure 27: Zinc dust with copper, cobalt and arsenic cement after 45 minutes reaction time with test conditions as per Figure 16.

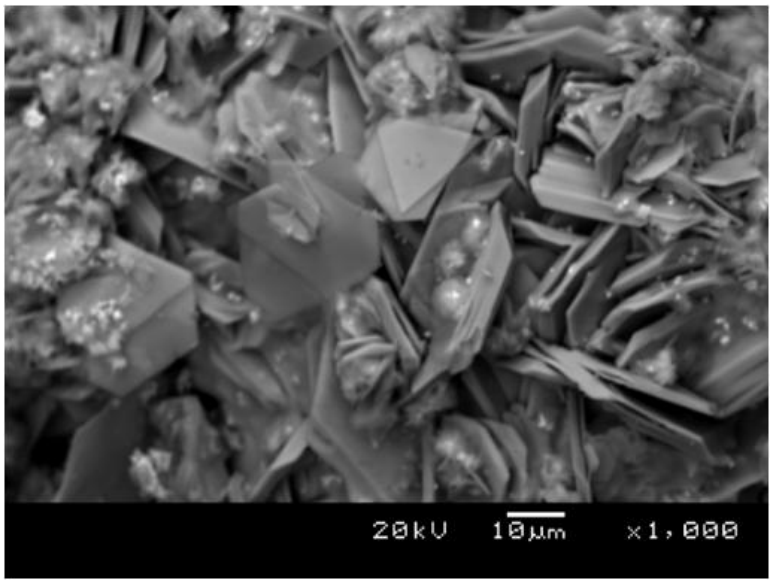

Figure 28: Zinc dust with copper, cobalt and arsenic cement after 30 minutes reaction time with test conditions as per Figure 16.

A sample of recirculated cobalt precipitate removed from the cementation circuit was also characterized and indicates that the zinc is significantly corroded in this case, as indicated in the image shown as Figure 29.

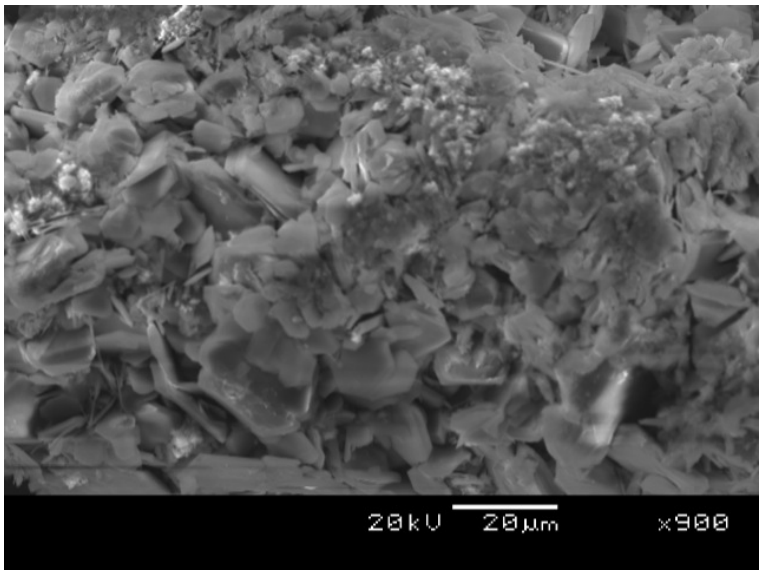

Figure 29: Cobalt filter press product with aged cobalt cement from the operation.

Corrosion of the zinc most probably occurred in the later stages of the process when the pH is lower and the precipitate is separated by filtration. This could also explain the relatively low activity of the cobalt cement obtained after the acidification and filtration.

The study of the cementation products removed from the plant also indicated that the cementation processes are subject to many variables under process conditions and that the nature of the products would not be easy to predict. For instance a study of initial cementation products yielded traces of cobalt only and with very little copper. This is an unexpected result as copper deposition has the highest driving force and as it was also found that copper deposited from early on in the copper and arsenic tests. Cobalt could be identified with arsenic, but not with copper. Copper could be identified at only a few deposition sites initially and is assumed to be present as elemental copper mostly, due to low copper to arsenic ratios and thermodynamics favoring copper deposition. Arsenic however, was identified at almost every initial deposition site, indicating that reduction of As(3+) in solution to presumably arsenic metal on zinc dust happens rather quickly. The importance of arsenic as catalyst for cobalt deposition is confirmed through the observation that cobalt deposition occurs in the presence of arsenic only, without copper being present, supporting the work done by Lawson & Nahn (1981) on the role of arsenic in cobalt deposition.

Cadmium also precipitates early on and is present in almost every deposition product assayed together with arsenic, supporting the notion that cadmium too contributes to activation of cobalt deposition. Whether cadmium aids cobalt deposition by itself and/or through some synergistic relationship with arsenic could not be ascertained from the assays alone.

The presence of copper, arsenic, cobalt and cadmium grouped together in all deposition products assayed in the final test sample suggest that some co-deposition mechanism exists between the cobalt deposition catalysts, while the bulk of the surface of new zinc dust particles remained uncovered and without deposition products.

The cobalt cement sample taken from the cobalt filter presses in the purification plant is characterized by a high zinc content, emphasizing the potential for re-use as reducing agent instead of new zinc. The cadmium concentration is low, in agreement with previous observations that cadmium re-leaches in the cobalt filter presses. Cobalt, copper and arsenic concentrations in the deposition products are high.

In summary it is proposed that copper, arsenic and cadmium precipitate first as pure metals, in addition to copper precipitating as Cu_3As. Cobalt precipitation occurred with arsenic in the initial sample, without the presence of copper, indicating that arsenic metal too acts as an important catalytic substrate for precipitation of cobalt arsenide. Cobalt precipitation occurred in the presence of copper in the following sample, emphasizing the activating effect of elemental copper as well as of copper arsenide. Arsenic and cadmium typically occurred together on most deposition sites indicating that the deposition of the one is possibly favouring that of the other, or that both are preferentially deposited at certain sites.

Cobalt deposition was limited to reaction sites occupied by activator cementation products. A co-deposition mechanism of sorts appears possible through observations that copper, arsenic and cadmium deposits occurred grouped together at all deposition sites in the last timed test sample with the bulk of the zinc dust surface remaining clear of cementation products.

4.7 Effect of optimised parameters on an industrial process

Näsi's (2004) equation for calculating the apparent rate constant or deposition efficiency for reactions in backmix reactors with continuous flow discussed in Section 2.3.1 on the rate equation was used to evaluate the apparent rate constants achieved through optimisation of particle size distribution and cobalt seed recirculation.

Initial rate constants with matching operating parameters including inlet and outlet cobalt concentrations, zinc dust concentrations and retention times are summarised in Table 19 for the un-optimised plant condition described in Section 3.5 and for the initial rate constants calculated for the first and third optimisation options in Table 19

in Section 4.5. The value of the initial apparent rate constant of 0.16 per minute calculated for the No. 1 Zincor cobalt reactor for un-optimised conditions compares well with the initial apparent rate constant of 0.15 per minute prepared in the laboratory base case as displayed in Table 19.

Table 19: Initial rate constants with matching operating parameters for various optimisation options and an un-optimised plant scenario to achieve a final cobalt concentration of 0.15 mg/L

Optimisation option	Reactor number	C_{x-1}	C_x	C_{eff} (k)	Time	Zn dust
		mg/L	mg/L	1/min	min	g/L
Un-optimised plant	Co 1	28	1.9	0.16	88	3.1
	Co 2	1.9	0.3	0.061	88	
	Co 3	0.3	0.17	0.009	88	
	Co 4	0.17	0.11	0.006	88	
Option 3	Co 1	28	0.96	0.32	88	3.1
	Co 2	0.96	0.15	0.061	88	
Option 1	Co 1	28	1.09	0.28	88	1
	Co 2	1.10	0.17	0.061	88	
	Co 3	0.17	0.15	0.009	16	

An initial apparent rate constant of 0.32 per minute, as displayed in Option 3 above, allows the required retention time to be reduced from 351 minutes to 175 minutes, while maintaining the zinc dust concentration used during the un-optimised plant condition to achieve a final cobalt concentration of 0.15 mg/L. This was achieved by increasing the cobalt seed concentration from 10 g/L to 30 g/L, by using cobalt seed from the No. 2 cobalt reactor instead of from the cobalt filter presses and by using zinc dust with a top size of 106 µm instead of using zinc dust with a top size of 500 µm.

The retention time may be reduced from 351 minutes to approximately 200 minutes using the initial apparent rate constants for the number 2 and number 3 reactors to calculate the inlet and outlet concentrations to achieve a final concentration of 0.15

mg/L, while decreasing the zinc dust concentration potentially to 1 g/L as indicated in Option 1. This would put the performance of the Zincor plant on par with that achieved by Fugleberg et al (1976) at the Kokkola plant.

It is assumed that the apparent initial rate constant achieved in the No. 2 reactor will also benefit from the increase in recirculated cobalt seed, potentially reducing the zinc dust consumption even further.

5. CONCLUSIONS

Purification of the zinc sulfate solution prior to electrowinning of zinc in the now mothballed Zincor zinc refinery in Springs, South Africa, was characterized by high zinc dust consumption to remove cobalt as well as occasional cobalt spikes in the purified solution. This study was conducted to investigate the possibility to reduce zinc dust consumption, while maintaining a sufficiently low final cobalt concentration in the purified solution, through development of an understanding of the processes and limitations that govern cobalt deposition in a zinc sulfate solution with a high zinc ion concentration. This was done by studying the thermodynamics, kinetics and deposition morphology of cobalt cementation by zinc dust in a zinc sulfate solution through activation with copper, arsenic, cadmium and elevated temperature.

The investigation of cementation products with SEM and EDS suggested that elemental copper, arsenic and cadmium precipitate early on in the process after addition of zinc dust, followed by cementation of cobalt. Further likely reaction products according to thermodynamic predictions are cobalt arsenide and copper arsenide. These cementation products, i.e. metallic copper, arsenic, cadmium and copper arsenide, increase the cobalt deposition surface area by virtue of the observed irregular shape of the precipitate. The increase in surface area was quantified by measuring the surface area of the cementation products and remaining zinc dust and by comparing this number to the surface area of new, unused zinc dust. Cobalt's contribution is assumed to be small due to low initial concentrations. The surface area per unit mass of cementation product is more than a hundred times that of new zinc dust. The surface area for the finest zinc dust used in this study was 0.0238 m^2/g as determined through BET measurements, while the surface area of the cobalt section precipitate was 8.3 m^2/g.

It should be possible to substitute a large proportion of copper in the feed solution by recirculated cobalt precipitate, while still maintaining a sufficiently high cobalt cementation rate. Moreover, initial cobalt deposition always occurred in the presence of arsenic and cadmium, even without the presence of copper, although the bulk of cobalt precipitates are associated with copper later in the cementation process. It appears that a type of association exists between arsenic and cadmium with the net

effect of improving cobalt deposition kinetics. The fact that copper is always detected with cobalt in the later stages of cementation may be due to the high initial copper concentration rather than to better activation by the copper compared to that of cadmium.

The role of arsenic is to move the potential required for cobalt precipitation to more positive values compared to that required for cobalt metal precipitation by favouring the deposition of cobalt arsenide as displayed in Figure 4. The more positive potential as well as the inhibition of hydrogen ion reduction by arsenic species also limits the alkalization of the solution at the surface of the zinc which could passify the anodic dissolution of the zinc by the formation of hydroxides and basic sulfates. Moreover, arsenic appears to stabilize the cobalt cementation product, preventing redissolution when deposition conditions deteriorate, in contrast to cadmium that readily redissolves in the cobalt reactor train and in the cobalt filter presses after cementing almost completely in the No. 1 reactor.

The role of cadmium is assumed to be similar to that of copper in terms of creating additional reaction surface area, although some of the cadmium may be leached with relative ease at the end of the process. It is observed that cobalt seed with cadmium from the No. 2 cobalt reactor catalyses cobalt precipitation far more than cobalt seed without cadmium from the cobalt filter presses.

Testwork results confirmed that the rate of cobalt removal displays a first order dependence on cobalt concentration with an apparent rate constant that incorporates the effects of temperature, zinc dust and activator surface areas. The temperature dependence of the rate constant typically follows an Arrhenius type relationship with the relatively high activation energy of 43 kJ/mol indicating that the process is under activation control, at least during the initial stages of the process. The rate of cobalt cementation becomes insensitive to temperature during the later stages of the process indicating that some form of mass transfer limitation or passivation then determines the rate. The transition from the initial fast and activation controlled stage to the slower mass transfer controlled stage always occurred at cobalt in solution concentrations below 1 mg/L, although that may be incidental rather than determining the transition.

The retention time required to reduce the cobalt concentration sufficiently is determined by the rate of reaction in both the first stage, when under activation control, and the second stage when under mass transfer control. The bulk of the cobalt is removed during the first stage and is favoured by a high, activated surface area and high temperatures. It was shown that it is possible to achieve the target cobalt concentration during the activation-controlled stage, by providing sufficient reaction surface area for precipitation to take place.

The rate of cobalt deposition is also influenced by pH, mixed potential and activator concentration as observed during plant operation. Adequate control of these parameters minimizes formation of and prevents adsorption of zinc hydroxide and precipitation of basic zinc sulfate, which in turn prevents passivation of the zinc dust surface for cobalt deposition. As with pH and potential, a window of opportunity exists within which temperature and concentrations of zinc dust and recirculated cobalt precipitate with copper, arsenic and cadmium can be optimised to bring about improved cobalt deposition kinetics.

The observed pH increase during cobalt precipitation is due to consumption of hydrogen ions by the various reactions. At the zinc refinery the pH can increase from pH 5.1 to pH 5.5 under normal operating conditions representing a typical increase of 0.4 pH units during the process. Localized increases of pH are probably higher leading to formation of basic zinc sulfates $ZnSO_4.3Zn(OH)_2.4H_2O$ and $ZnSO_4.6Zn(OH)_2$ as well as zinc hydroxide $Zn(OH)_2$. This could lead to passivation of the zinc dust surface for cobalt deposition by occupying the already limited number of deposition sites. Also, cobalt hydroxide forms at elevated pH, which contributes to solution purification, but is unstable though and is easily redissolved when the pH is decreased later in the process.

It was found with this work that the zinc dust concentration could be reduced from the 3.1 g/L used on average to less than 1 g/L, while still maintaining a cobalt concentration of 0.15 mg/L in the purified solution through increasing the effective reaction surface area by the following means:

- Increasing cobalt seed concentration to at least 30 g/L in the first reactor;

- Using cobalt seed from the No. 2 cobalt reactor taken from the No. 2 reactor overflow to the No. 3 reactor instead of from the cobalt filter press product to enhance cementation in the No. 1 cobalt reactor;

- Reducing the zinc dust particle size distribution by decreasing the zinc dust top size from 500 µm to 106 µm.

Using finer zinc dust increases the risk of redissolution of cobalt due to the total consumption of the fine zinc dust particles, which would lead to a decrease in cathodic protection of the cobalt cement. It was found, however, that recirculation of cobalt seed in excess of 30 g/L from the No. 2 cobalt reactor minimizes redissolution of cobalt when using fine zinc dust. This is ascribed to increased cathodic protection offered by the remaining zinc and cementation products.

The production of finer zinc will probably be more costly and may require an inert atmosphere to limit surface oxidation. The use of nitrogen for example for cooling of molten zinc to produce smaller zinc dust particles will be more expensive than the air that has been used at Zincor. Screening will also be required to separate coarse from fine zinc dust particles requiring labor and power. It is further assumed that all zinc dust produced can be used with fine zinc dust used in the cobalt section and the coarse zinc dust used in the copper and cadmium cementation sections.

The recirculation of cobalt seed would require additional pumping and power, for example to process the slurry containing cobalt seed from the No 2 reactor through a settler to remove excess partially purified solution, representing capital for new equipment and increased operating costs.

Although the best results were obtained at a temperature of 80 °C it is suggested that a reduction in temperature may possibly be possible due to the enhanced kinetics offered by the recirculated cobalt seed as well as by the observed temperature independence of the second rate regime. The obvious benefit of a decrease in temperature would be to reduce the cooling requirements of the feed to the electrowinning circuit with resultant cost savings as well as requiring less steam to

generate the heat in the first place, making the steam available elsewhere on the plant or even for power generation. However, the benefits of a decrease in temperature (power saving, steam generation) will have to be offset against a penalty in zinc dust concentration.

The savings to produce a smaller recirculating stream of zinc comprises the cost to electrowin and smelt the zinc that would have been used for production of zinc dust. The zinc that would have been used to produce zinc dust, that is now saved, will probably still rather be produced to be sold at an added profit. In addition to potentially requiring new equipment, the operating cost will increase, resulting in a trade-off between cost and financial benefit. The cost parameters of interest for further investigation, if required, include the following:

- Cost to produce zinc dust with finer particle size distribution
- Cost to recirculate cobalt seed
- Proceeds of decreasing the solution temperature i.e. using less steam before and requiring less cooling later
- Cost of increased zinc dust consumption due to lower solution temperature.

Alternatively the reaction time can potentially be halved, while still saving on zinc dust to achieve the required final cobalt concentration. The benefit of potentially releasing almost two thirds of zinc dust used for cobalt cementation at Zincor for sale would have been substantial considering that Zincor was a marginal operation at the time that this investigation commenced. It is a pity and rather tragic that the plant stopped producing zinc altogether shortly after this investigation was started after more than 40 years of first producing gold and then zinc.

REFERENCES

Ahmad, Z., Principles of corrosion engineering and corrosion control, Elsevier Science & Technology Books, 2006, p. 570.

Bøckman, O. and Østvold, T., Products formed during cobalt cementation on zinc in zinc sulfate electrolytes, Hydrometallurgy (54), 2000, pp. 65 – 78.

Boyanov, B.S., Konareva, V.V. and Kolev, N.K., Purification of zinc sulfate solutions from cobalt and nickel through activated cementation, Hydrometallurgy (73), 2004, pp. 163 – 168.

Dreher, T.M., Nelson, A., Demopoulos, G.P. and Filippou, D., The kinetics of cobalt removal by cementation from an industrial zinc electrolyte in the presence of Cu, Cd, Pb, Sb, and Sn additives, Hydrometallurgy (60), 2001, pp. 105 – 116.

Fugleberg, S., Järvinen, A. and Sipilä, V., Solution purification at the Kokkola zinc plant, In: JM Cigan, TS Mackey and TJ O'Keefe (Editors), Lead and Zinc '80, Metall. Soc. AIME. Warrendale, Pa (1980), pp. 157 – 171.

Fugleberg, S., Järvinen, A. and Yllö, E., Recent development in solution purification at Outokumpu Zinc plant, Kokkola, International symposium - World Zinc, 1993, pp. 241 – 247.

Fugleberg, S., Rantanen, R., Sipilä, V., Järvinen, A., Solution purification process at the Outokumpu Kokkola Zinc Plant, 113th AIME Annual Meeting, Los Angeles, USA, 1984, pp. 1 – 8.

Fugleberg, S. and Rastas, J.K., Process for purifying aqueous solutions of metal ions precipitating as arsenides, antimonides, tellurides and selenides, United States Patent description, Sept, 7, 1976.

Heukelman, S., Cadmium reversion and increase zinc dust consumption in second stage purification December 2006, Zincor internal correspondence, 2006.

Lawson, L. and Nhan, L.T., Kinetics of removal of cobalt from zinc sulfate electrolytes by cementation, Hydrometallurgy (81), Proceedings of Science, 1981, pp. G4/1 – G4/10.

Näsi, J., Statistical analyses of cobalt removal from zinc electrolyte using the arsenic activated process, Hydrometallurgy (73), 2004, pp. 123 – 132.

Nelson, A., Demopoulos, G.P. and Houlachi, G., The effect of solution constitutions and novel activators on cobalt cementation, Canadian Metallurgical Quarterly (2000), Vol. 39, No. 2, pp. 175 – 186.

Oghai, T., Heguri, S. and Fukushima, H., Mechanism of the high removal rate of cobalt in conventional cementation by zinc dust with arsenic oxide in the presence of cupric ions, 1998, pp. 79 – 86.

Pourbaix, M., Atlas of Electrochemical Equilibria in Aqueous Solutions, NACE International, 1974, p. 520.

Raghavan, R., Mohanan, P.K. and Verma, S.K., Modified zinc sulphate purification technique to obtain low levels of cobalt for the zinc electrowinning process, Hydrometallurgy (51), 1999, pp. 187 – 206.

Sinclair, R.J., The Extractive Metallurgy of Zinc, Australasian Institute of Mining and Metallurgy, Australian institute of mining and metallurgy, Spectrum series volume No. 13, 2005, pp. 93 – 111.

Singh, V., Technological innovation in the zinc electrolyte purification process of a hydrometallurgical zinc plant through reduction in zinc dust consumption, Hydrometallurgy (40), 1996, pp. 247 – 262.

Tozawa, K., Nishimura, T., Akahori, M. and Malaga, A., Comparison between purification processes for zinc leach solutions with arsenic and antimony trioxides, Hydrometallurgy (30), 1992, pp. 445 – 461.

Van der Pas, V., and Dreisinger, D.B., A fundamental study of cobalt cementation by zinc dust in the presence of copper and antimony additives, Hydrometallurgy (43), 1996, pp. 187 – 205.

Wiart, R., Cachet, C., Bozhkov, C.H.R. and Rashkov, S.T., On the nature of the "induction period" during the electrowinning of zinc from nickel containing sulphate electrolytes, Journal of Applied Electrochemistry (20), 1990, pp. 381 – 389.

Xiong, J. and Richie, I.M., An electrochemical study of the inhibition of the Co(II)/ Zn cementation reaction, In: Y Zheng and J Xu (Editors), Proceedings of the First International Conference on Hydrometallurgy (ICHM '88), 1988, pp. 632 – 636.

Yamashita, S., Okubo, M., Goto, S. and Hata, K., Purification of zinc leaching solution – Mechanism of removal of cobalt by zinc dust with arsenious oxide and copper ion, Metallurgical Review of MMIJ, Vol 14, No1, 1997, pp. 37 – 52.

Yamashita, S., Okubo, M., Goto, S. and Hata, K., Mechanism of removal of cobalt from zinc sulfate solution for electrowinning, Chiba Institute of Technology, Japan, 1989, pp. 83 – 90.

Yamashita, S., Hata, K. and Goto, S., Electropurification of zinc leaching solution, Aqueous Electrotechnologies: Progress in Theory and Practice, The minerals, Metals & Materials Society, 1997, pp. 163 – 175.

Yang, D., Xie, G., Zeng, G., Wang, J. and Li, R., Mechanism of cobalt removal from zinc sulfate solutions in the presence of cadmium, Hydrometallurgy (81), 2006, pp. 62 – 66.

Zeng, G., Xie, G, Yang, D, Wang, J., Li, X. and Li, R., The effect of cadmium ion on cobalt removal from zinc sulfate solution, Minerals Engineering (19), 2006, pp. 197 – 200.

APPENDICES

Appendix A: Procedure for calculating the Kokkola rate constant

Some effort has gone into extracting comparative kinetic data for the Kokkola process from the literature, because it is similar to the Zincor process. It is therefore assumed that the published data could provide a baseline in terms of the performance that should be aspired to. In addition, comparative kinetic data for the hot arsenic process is not readily available in literature. Fugleberg et al (1993) plotted the logarithms of decreasing cobalt concentration against time during batch cementation tests and the slope of the linear parts were used for determination of a comparative kinetic rate constant as in the example in Figure 30 for the test at 70 °C.

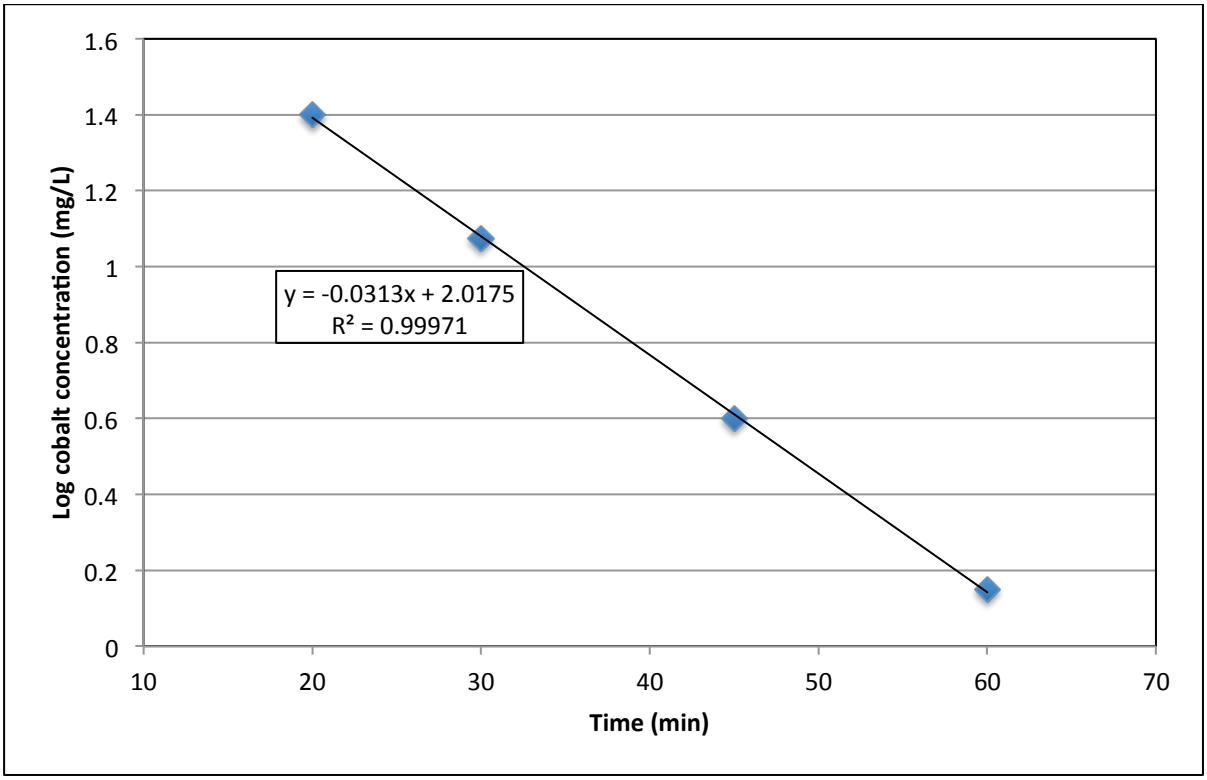

Figure 30: Logarithm of the cobalt concentration in an industrial zinc sulfate solution during cobalt cementation on zinc in a stirred batch reactor as a function of time with temperature 70 °C, recirculated cobalt seed surface area concentration 750 m^2/L and other parameters not specified (after Fugleberg et al, 1993).

The rate constant, k, for cobalt was calculated below to be 9.6 x 10^{-5} $m^{-2}.min^{-1}$ at 70°C, using Equation 41 discussed in Section 2.3.1 on the rate equation. The period (Δt) was conveniently selected as 40 minutes, i.e. from 20 minutes to 60 minutes with matching concentrations. The various meanings of parameters k", A, V and C are as per the discussion in Section 2.3.1 on the rate equation.

$$- dC/dt = k" . A/V . C \quad \ldots\ldots (41)$$

$$- dC/C = k" . A/V . dt \quad \ldots\ldots (47)$$

$$- \ln C \, I_{C_1}^{C_2} = k" . A/V . t \, I_0^t \quad \ldots\ldots (48)$$

$$- \ln C_2/C_1 = k" . A/V . \Delta t \quad \ldots\ldots (49)$$

$$- 2.303 \log C_2/C_1 = k" . A/V . \Delta t \quad \ldots\ldots (50)$$

$$- (\text{Log } C_2 - \log C_{1)} = {}^{1}\!/_{2.303} . k" . A/V . \Delta t \quad \ldots\ldots (51)$$

$$- (0.15 - 1.4) = {}^{1}\!/_{2.303} . k" . (750) . (40) \quad \ldots\ldots (52)$$

$$k" = \frac{(1.25) . (2.303)}{(750) . (40)} \quad \ldots\ldots (53)$$

$$k" = 9.6 \times 10^{-5} \; m^{-2}.min^{-1} \quad \ldots\ldots (54)$$

The apparent rate constant k takes into consideration the effects of surface area and is calculated following integration of equation 39, as follows:

$$- dC/C = k.dt \quad \ldots\ldots (55)$$

$$k = \frac{(1.25)\,.\,(2.303)}{40} \quad \ldots\ldots\ldots\ldots\ldots\ldots\ldots\ldots \quad (56)$$

$$k_{70°C} = 0.072\ \text{min}^{-1} \quad \ldots\ldots\ldots\ldots\ldots\ldots\ldots\ldots \quad (57)$$

The contribution to surface area by zinc dust is small compared to that of the recirculated cobalt precipitate and including that value in the calculation is assumed to make a small difference only.

Appendix B: Procedure for determining zinc dust dosage

Zincor's standard calculation was used to determine the required mass of zinc dust. The chemistry displayed in Table 20 was used as bases for calculating the total mass of zinc dust required for all the reactions occurring with associated stoichiometry.

Table 20: Zinc dust consumption calculation summary

No	Reaction	N^+	$m(N^+)$	m(Zn)
			g per 4.5 L	
1	$Cu^{2+} + Zn^0 = Cu^0 + Zn^{2+}$	Cu^{2+}	3.06	3.148
2	$3Cu^{2+} + As^{3+} + 4.5Zn^0 = Cu_3As + 4.5Zn^{2+}$	Cu^{2+}	0.9	1.389
3	$Cu_3As + Co^{2+} + Zn^0 = 3Cu^0 + CoAs + Zn^{2+}$	Co^{2+}	0.088	0.195
4	$Co^{2+} + As^{3+} + 2.5Zn^0 = CoAs + 2.5Zn^{2+}$	Co^{2+}	0.088	0.487
5	$Ni^{2+} + As^{3+} + 2.5Zn^0 = NiAs + 2.5Zn^{2+}$	Ni^{2+}	0.018	0.049
6	$2H^+ + Zn^0 = H_2 + Zn^{2+}$	H^+	0.000024	0.0031
Total zinc dust consumption (Stoichiometric factor of 1)				5.3

Only a small fraction of the copper was removed in the preceding copper removal stage and the bulk of the copper remained in solution. For the calculation's sake it is assumed that 200 mg/L of the copper react with arsenic while the remainder of the copper (680 mg) is free to react with elemental zinc.

The calculation to determine the mass of zinc dust associated with copper (reaction 3 and reaction 16) is as follows:

$$m(Zn) = \frac{m\,(Cu)}{M(Cu)} * \frac{M(Zn)}{1} * \frac{n\,(Cu)}{n\,(Zn)} \quad \ldots\ldots\ldots\ldots\ldots\ldots\ldots\ldots\ldots\ldots \quad (58)$$

Where m(metal) is the physical mass of the metal in grams per litre of slurry, M(metal) is the molar mass in grams per mol and n(metal) is the number of mols.

The zinc dust required to react with cobalt is determined in the same way with a fraction of the zinc apportioned to reaction 18 and the remainder to reaction 21 as follows:

$$m(Zn) = \frac{m\,(Co)}{M(Co)} * \frac{M(Zn)}{1} * \frac{n\,(Co)}{n\,(Zn)} \quad \text{.....} \quad (59)$$

Hydrogen is consumed by the following reactions in addition to being consumed by other reactions discussed in the section on chemistry.

$$2H_2O + Zn^0 = H_2 + Zn(OH)_2 \quad \text{.....} \quad (60)$$

$$Zn(OH)_2 + H_2SO_4 = ZnSO_4 + 2H_2O \quad \text{.....} \quad (61)$$

$$Zn^0 + H_2SO_4 = ZnSO_4 + H_2 \quad \text{.....} \quad (62)$$

All of these are summarised by reaction 10. The zinc dust required to react with acid (H^+) for reaction 10 is calculated by determining how much hydrogen was consumed during the cementation process on account of the change in pH. The pH changes from an average pH 5 into the cobalt section to pH 5.5 out of the No. 3 reactor (before pH control is done).

$$m(Zn) = \frac{m\,(H^+)}{M(H^+)} * \frac{M(Zn)}{1} * \frac{n\,(H^+)}{n\,(Zn)} \quad \text{.....} \quad (63)$$

The total required mass of zinc dust is calculated by adding the individual masses of zinc dust calculated previously and by applying a stoichiometric factor to that mass.

Appendix C: Raw data from EDS analyses of precipitates

All assays are presented on a weight percentage basis.

Table 21: Timed sample assays for copper and arsenic cementation

Time	Sample	Unit	Zn	O	S	Cu	As	Cu:As	Cu:O
5 min	Assay 1	%	30	34	10	18	4	4.0	1.9
	Assay 2	%	25	36	11	21	5	4.3	1.7
10 min	Assay 1	%	10	17	3	44	16	2.8	0.4
	Assay 2	%	21	32	4	18	5	3.4	1.7
	Assay 3	%	14	20	3	46	2	27.1	0.4
15 min	Assay 1	%	5	14	3	68	6	12.1	0.2
	Assay 2	%	27	41	12	14	2	6.0	2.9
	Assay 3	%	22	45	8	15	5	3.3	3.0
30 min	Assay 1	%	8	11	3	63	10	6.1	0.2
	Assay 2	%	41	25	15	15	2	7.2	1.6
	Assay 3	%	16	22	8	40	10	3.9	0.6
	Assay 4	%	30	18	10	32	8	4.2	0.5
105 min	Assay 1	%	13	20	5	31	12	2.6	0.7
	Assay 2	%	4	13	3	53	21	2.6	0.2
	Assay 3	%	25	40	11	16	2	9.9	2.5
	Assay 4	%	35	25	11	14	3	5.0	1.8
	Assay 5	%	29	43	11	7	1	5.0	6.1
	Assay 6	%	21	25	11	35	5	7.6	0.7
	Assay 7	%	26	35	12	18	4	5.0	2.0

Table 22: 5 Minute sample assays for cobalt cementation – base case

Sample ID	Unit	Zn	O	S	Co	Cu	As	Cd	Co:As	Cu:As
Co1(2)_1	%	37.1	36.2	6.1		9.1	5.8	1.9		1.6
Co1(2)_2	%	72.6	17.2	4	0.3		3	1.5	0.1	
Co1(2)_3	%	54.8	34.3	6.9			1.9	1.3		
Co1(2)_4	%	62.1	23.7	7.2			2.7	3.3		
Co1-2(1)_1	%	49.4	31	6			1.7	2.7		
Co1-2(1)_2	%	29.2	41.3	4.7		8.9	4.7			1.9
Co1-2(1)_3	%	52.8	18.9	4.7	0.3		2.9	7		

Table 23: 10 Minute sample assays for cobalt cementation – base case

Sample ID	Unit	Zn	O	S	Co	Cu	As	Cd	Co:As	Cu:As
Co2(1)_1	%	76.5	13.7	3.5			4	1.6		
Co2(1)_2	%	41.6	37.6	7	0.4		6.2	5.9	0.1	
Co2(1)_3	%	37.5	16	4.5		12.9	18.2	9.1		0.7
Co2(1)_4	%	35	14.6	4.1	0.4	15.8	18.7	9.3		0.8

Table 24: 15 Minute sample assays for cobalt cementation – base case

Sample ID	Unit	Zn	O	S	Co	Cu	As	Cd	Co:As	Cu:As
Co3(1)_1	%	53.3	35.2	5.6	0.3		1.9	2.3	0.2	
Co3(2)_1	%	70.7	19.5	5.5	0.4		0.8	2.1	0.5	
Co3(2)_2	%	47.9	34.7	6.7	0.2		3.3	6.5	0.1	
Co3(2)_3	%	55.9	34.2	7.4	0.3		0.8	0.8	0.4	
Co3-1(1)_1	%	48.2	28	4.1			1.4	2.1	0.0	
Co3-2(1)_1	%	35.8	25.5	3.7	0.6	13.9	4.2	1.8	0.1	3.3

Table 25: 30 Minute sample assays for cobalt cementation – base case

Sample ID	Unit	Zn	O	S	Co	Cu	As	Cd	Co:As	Cu:As
Co6(1)_1	%	66.9	24.9	6.2				0.8		
Co6(1)_2	%	32.6	19.4	4.7	0.9	25.9	12.9		0.1	2.0
Co6(2)_1	%	30.8	33.6	7		13.5	7.1	2.4		1.9
Co6(2)_2	%	25.9	21.8	4	1.4	26.5	16.3	2.1	0.1	1.6

Table 26: 45 Minute sample assays for cobalt cementation – base case

Sample ID	Unit	Zn	O	S	Co	Cu	As	Cd	Co:As	Cu:As
Co5(1)_1	%	62.1	24.6	7.2				0.5		
Co5(1)_2	%	56.5	29.8	6.7				0.6		
Co5(1)_3	%	41.8	35.9	6.4	0.2		3.7	6	0.1	
Co5(1)_4	%	42.2	37	7.4			2.2	2.9		
Co5(1)_5	%	46.3	36.5	6			0.7	1.5		
Co5(1)_6	%	40.2	36.9	7.4			2.8	5.5		
Co5(2)_1	%	34.1	40.8	5.6			3.6	9.4		
Co5(2)_2	%	29	35	5.7		8.1	6	9.1		1.4

Table 27: 120 Minute sample assays for cobalt cementation – base case

Sample ID	Unit	O	S	Co	Cu	Zn	As	Cd	Co:As	Cu:As
Co7(3)_1	%	51.9	9.1	1.1	15.6	14.7	3.6	4.0	0.3	4.3
Co7(3)_2	%	20.4	4.5	1.8	47.3	10.2	9.8	5.9	0.2	4.8
Co7(3)_3	%	29.6	6.4	2.2	35.5	11.7	9.2	5.5	0.2	3.9
Co7(3)_4	%	10.0	5.1	1.9	55.0	14.0	7.3	6.7	0.3	7.5
Co7(3)_5	%	31.1	6.8	1.3	26.0	24.1	5.1	5.5	0.3	5.1
Co7(4)_1	%	30.5	2.7	1.4	42.1	9.0	10.3	4.1	0.1	4.1
Co7(4)_2	%	28.1	2.6	2.1	41.6	10.4	11.5	3.7	0.2	3.6
Co7(4)_3	%	18.4	2.4	1.7	46.9	14.1	12.2	4.3	0.1	3.8
Co7(4)_4	%	28.7	1.1	1.1	48.5	5.1	12.7	2.8	0.1	3.8
Co7(4)_5	%	37.7	5.0	0.0	8.9	45.6	1.8	1.1		5.0
Co7(5)_1	%	38.0	1.0	0.8	42.1	6.3	9.9	1.8	0.1	4.2
Cob7(5)_2	%	61.4	3.1	1.0	17.6	10.0	4.5	2.4	0.2	3.9
Co7(6)_1	%	37.4	2.4	2.0	33.2	11.3	11.4	2.4	0.2	2.9
Co7(6)_2	%	68.9	1.1	0.8	18.9	3.8	5.3	1.1	0.1	3.6
Co7(6)_3	%	37.3	4.3	1.5	30.3	15.3	6.7	4.5	0.2	4.6
Co7(6)_4	%	45.2	1.7	1.7	27.2	12.9	8.2	3.1	0.2	3.3

Table 28: Old cobalt cement sample assay

Sample ID	Unit	Zn	O	S	Co	Cu	As	Cd	Co:As	Cu:As
Co2-2(1)_1	%	24.9	24	3.1	2.9	26.5	9.3	1.2	0.3	2.8
Co2-2(1)_2	%	21.3	21.2	2.4	2.6	26.9	9	0.7	0.3	3.0
Co2-2(1)_3	%	37.9	27.4	4.6	0.9	7.6	2.6		0.3	2.9
Co2-3(1)_1	%	44.1	32.1	6.3			2.1	0.3		
Co2-3(1)_2	%	51.4	15.2	3.8	1.2		4.3	0.6	0.3	
Co2-3(2)_1	%	75	9.6	2.2				2.8		
Co2-3(2)_2	%	39.4	27	4.6			3.3	10.9		
Co2-4(3)t1	%	61.3	13.6	3.5		10.9	4.1	0.5		2.7
Co2-4(4)_1	%	41.1	13.5	1.9	1.1	27.3	10.7	0.6	0.1	2.6
Co2-7(1)_1	%	42.1	14.1	1.9		18.1	6.5	0.7		2.8

Appendix D: Raw data for kinetic tests

The raw data for all kinetic tests are displayed in Appendix D with the concentration of cobalt remaining in solution against the time in table format, starting from the time that the test started to the time that the test ended.

Table 29: Cobalt concentration (mg/L) against time for tests to determine the effect of temperature on cobalt cementation rate

Time	Temperature			
Minutes	**50°C**	**60°C**	**70°C**	**80°C**
0	39	39	39	39
15	23.3	17.3	8.4	3.69
30	13.6	8.6	2.3	0.78
45	10.5	4.1	0.54	0.19
60	8.1	2	0.22	0.18
75	6.4	0.9	0.18	0.16
90	5.1	0.44	0.16	0.12
105	4.3	0.36	0.14	

Graphs in Figure 14, Figure 15, Figure 16 and Figure 17 were constructed with manipulation of the raw data presented in Table 29.

Table 30: Cobalt concentration (mg/L) against time for tests to determine the effect of zinc dust particle size distribution on cobalt cementation rate

Time	Zinc dust top size			
Minutes	**106 µm**	**212 µm**	**300 µm**	**500 µm**
0	39	39	39	39
15	0.24	1.6	2.4	3.75
30	0.16	0.33	0.39	0.8
45	0.12	0.2	0.19	0.2
60	0.12	0.2	0.24	0.19
75	0.14	0.17	0.24	0.17
90	0.16	0.16	0.21	0.13

Graphs in Figure 19 and Figure 20 were constructed with manipulation of the raw data presented in Table 30.

Table 31: Cobalt concentration (mg/L) against time for tests to determine the effect of cobalt seed concentration on cobalt cementation rate

Time	Cobalt seed concentration						
	Base case	Cobalt filter press (source)			No 2 cobalt reactor (source)		
Minutes	0 g/L	10 g/L	30 g/L	40 g/L	20 g/L	40 g/L	60 g/L
0	39	39	39	39	38.7	38.4	38.1
15	22.1	4	3.2	2	1.5	0.42	0.19
30	5.5	0.74	0.54	0.4	0.28	0.17	0.14
45	1.8	0.34	0.24	0.25	0.26	0.18	0.13
60	0.36	0.25	0.21	0.28	0.24	0.16	0.15
75	0.36	0.24	0.23	0.22	0.28	0.16	0.15
90	0.32	0.25	0.21	0.22	0.26	0.2	0.17
105	0.30	0.22	0.20	0.20	0.2	0.24	0.16

Graphs in Figure 21 and Figure 22 were constructed with manipulation of the raw data presented in Table 31.

Table 32: Cobalt concentration (mg/L) against time for tests to determine the effect of zinc dust concentration on cobalt cementation rate for optimized conditions

Time	Zinc dust concentration			
	Base case	Optimised conditions		
Minutes	3.1 g/L	3.1 g/L	2 g/L	1 g/L
0	18	18	18	18
15	1.80	0.14	0.2	0.28
30	0.50	0.12	0.18	0.16
45	0.30	NA	0.18	0.14
60	0.24	0.14	0.16	0.14
75	0.22	0.12	0.16	0.15
90	0.21	0.12	0.14	0.15
105	0.19	0.18	0.15	0.12

Graphs in Figure 23 and Figure 24 were constructed with manipulation of the raw data presented in Table 32. The tests conducted under optimized conditions used zinc dust with top size equal to 106 µm and a cobalt seed concentration of 30 g/L of solution with cobalt seed from the No 2 cobalt reactor. The base case test used zinc dust with top size of 500 µm and a cobalt seed concentration of 10 g/L of solution with cobalt seed from the cobalt filter presses.